A CONTINUUM APPROACH TO THE STUDY AND DETERMINATION OF FIELD LONGITUDINAL DISPERSION COEFFICIENTS

by

Richard L. Naff

Submitted in Partial Fulfillment

of the Requirements for the Degree of

Doctor of Philosophy

NEW MEXICO INSTITUTE OF MINING AND TECHNOLOGY

Socorro, New Mexico

June, 1978

ACKNOWLEDGEMENTS

The author is indebted to the professional staff at New Mexico Institute of Mining and Technology for the many fine instructional courses which made this dissertation possible. In particular, the continual guidance of his advisor, Dr. Lynn Gelhar, through the difficult intricacies of the dispersion process in porous media was invaluable. Through the effort of Dr. Allan Gutjahr, the author gained an understanding of stochastic processes which enabled him to accomplish the analyses in the following pages. Other members of the mathematics department were also helpful in the solution of many of the integrals contained herein.

The continued financial support of the United States Geological Survey during the two years when the author completed the major portion of his work was extremely helpful. Dr. Rufus Getzen of the U.S.G.S. read the first draft with an especially preceptive eye, and many of his comments have been incorporated into this draft. The author's colleague and friend, Dr. Yuksel Birsoy, helped with preparation of the initial and final drafts. Mrs. Patricia Valentine valiantly undertook the task of typing both drafts.

Finally, the author wishes to express his gratitude to his many friends and colleagues who offered their continual moral support. In particular, Dr. Steven Hook of the New Mexico Bureau of Mines and Mineral Resources and Mr. George Hoffman, an independent consultant, were available to humor the author during the darker periods of this study. The author's parents, Theodore and Mary Naff, gave additional moral and financial support to this endeavor.

ABSTRACT

It has become increasingly apparent to investigators in the field that there exists a large disparity between longitudinal dispersion coefficients determined in the laboratory and those determined from field experiments. This disparity is generally attributed to variability in hydraulic conductivity of the aquifer, allowing variable convection to mask dispersion at a local, or microscopic, scale. This study utilizes a first-order analysis and properties of random stationary fields to analyze the global, or macroscopic, dispersion for unstratified and stratified media. The method necessitates that the investigator aribitrarily select a particular spectral form. Because of the first-order analysis, results are limited to media in which the variance in hydraulic conductivity is small.

The results of the analysis generally indicates that a) given sufficient travel time, global dispersion is Fickian; b) the global longitudinal dispersion coefficient is a simple product of a global dispersivity and the mean specific discharge; and c) this dispersivity is proportional to the variance in hydraulic conductivity and the square of a correlation length scale, and inversely proportional to a local transverse dispersivity. Additionally, global dispersivities for the unstratified case are found to be continuous functions of the ratio of local transverse to local longitudinal dispersivities, and of the ratio of horizontal to vertical correlation length scales. Comparisons are made between global dispersivities resulting from stratified and unstratified medium conditions and an attempt is made to determine the sensitivity of the results to the local dispersivity ratio and to the length-scale ratio. Additionally, aspects of possible application of the results to field situations are discussed.

TABLE OF CONTENTS

	Page
ACKNOWLEDGEMENTS	ii
ABSTRACT	iii
TABLE OF CONTENTS	iv
LIST OF FIGURES AND TABLES	vi
LIST OF SYMBOLS	vii
INTRODUCTION	
Definition of Problem	1
Length Scales in Sedimentary Aquifers	6
Review of Literature	9
Approach	17
DERIVATION OF MODEL EQUATION	
Prototype	21
Perturbed Quantities	31
Global Longitudinal Dispersive Flux	36
First-Order Analysis	38
Local Dispersive Flux	42
SOLUTION OF MODEL EQUATION	
Development of Global Dispersive Flux Equation	46
Transfer Functions	49
One-Dimensional Flow Case	60
Three-Dimensional Flow Case	66
Note to Derivation of Global Longitudinal Dispersivity Equation	79
EVALUATION AND APPLICATION	
Limitations of First-Order Analysis	83
Qualification of Long-Term Process	94
Comparisons between Results	99
Sensitivity of Results	104
Application of Results	110
HYDRAULIC HEAD VARIANCE IN GLOBALLY ANISOTROPIC MEDIA	
Background	120
Derivation and Choice of Spectrum	120
Solution of Head Variance Equation and Discussion	125
CONCLUSIONS AND RECOMMENDATIONS	
Conclusions	128
Recommendations	130
REFERENCES	132
Appendix 1: SOME PROPERTIES OF RANDOM STATIONARY FIELDS	139
Appendix 2: GEOMETRIC MEAN AND LOGNORMAL DISTRIBUTION	144
Appendix 3: CONVECTIVE-DISPERSION EQUATION	146

		Page
Appendix 4:	MOVING COORDINATES	148
Appendix 5:	NEGATIVE-EXPONENTIAL AUTOCOVARIANCE FUNCTION	150
Appendix 6:	MODIFIED NEGATIVE-EXPONENTIAL AUTOCOVARIANCE FUNCTION	153
Appendix 7:	EVALUATION OF INTEGRALS WITH SPECTRUM OF SIMPLE NEGATIVE-EXPONENTIAL AUTOCOVARIANCE FUNCTION	158
Appendix 8:	EVALUATION OF INTEGRALS WITH SPECTRUM OF MODIFIED NEGATIVE-EXPONENTIAL AUTOCOVARIANCE FUNCTION	166
Appendix 9:	SOLUTION OF VARIANCE EQUATION FOR HYDRAULIC HEAD	173

LIST OF FIGURES AND TABLES

Figure		Page
2.1	A "visualized" porous medium.	22
3.1	Autocorrelation functions and spectra for one-dimensional flow case.	64
3.2	Isopleth contour of modified negative-exponential autocorrelation function in vertical plane.	71
3.3	Hydraulic conductivity factor for spectrum (3.64).	74
3.4	Porosity factor for spectrum (3.64).	75
3.5	Hydraulic conductivity factor for spectrum (3.66).	77
3.6	Porosity factor for spectrum (3.66).	78
4.1	Comparison of hydraulic conductivity factors for three-dimensional flow case.	103
4.2	Hydraulic conductivity factor as function of local dispersivity ratio.	108
4.3	Comparison between one-dimensional and three-dimensional results.	109

Table		Page
4.5	Sample Calculation Comparison Between Various Dispersivity Equations.	105

LIST OF SYMBOLS

Symbols listed here pertain to the body of the report: symbols used in the appendices are arbitrary and, in most instances, independent of those in the body.

Symbol	Explanation
a	Correlation length scale [L], equation (3.57).
A	Constant $[(TL)^{-1}]$, equation (4.58).
b	Length scale factor $[L^2]$, equation (3.59).
B	Constant $[(TL)^{\frac{1}{2}}]$, equation (3.45).
B_1	Dimensionless constant, equation (4.57).
B_2	Constant [L], equation (4.62).
B_3	Constant $[(TL)^{\frac{1}{2}}]$, equation (4.63).
c	Concentration [M].
dZ_c	Complex Fourier amplitude, c' process.
dZ_{E_ℓ}	Complex Fourier amplitude, $E_\ell{}'$ process.
$dZ_{E_{ij}}$	Complex Fourier amplitude, $E_{ij}{}'$ process.
dZ_f	Complex Fourier amplitude, f' process.
dZ_K	Complex Fourier amplitude, K' process.
dZ_n	Complex Fourier amplitude, f' process.
dZ_{q_i}	Complex Fourier amplitude, $q_i{}'$ process.
dZ_w	Complex Fourier amplitude, w' process.
dZ_{α_I}	Complex Fourier amplitude, $\alpha_I{}'$ process.
dZ_ϕ	Complex Fourier amplitude, ϕ' process.
d_{50}	Median grain size [L].
D_ℓ	Effective global longitudinal dispersion coefficient $[L^2/T]$.
E_{ij}	Local bulk dispersion coefficient $[L^2/T]$.

Symbol	Explanation
E_ℓ	Local bulk longitudinal dispersion coefficient $[L^2/T]$.
E_t	Local bulk transverse dispersion coefficient $[L^2/T]$.
f	Logarithm of hydraulic conductivity.
F	Hydraulic conductivity factor, equation (3.67).
F°	Hydraulic conductivity factor, equation (3.68).
G	Porosity factor, equation (3.67).
G°	Porosity factor, equation (3.68).
H	Head variance factor, equation (5.14).
J	Mean hydraulic gradient, equation (3.10).
k_i	Wave number, i^{th} direction [1/L].
K	Hydraulic conductivity [L/T].
K_ℓ	Effective hydraulic conductivity.
ℓ	Correlation length scale [L], equation (3.55).
ℓ_i	Correlation length scale [L], equation (3.65).
M	Slope, Archie's equation (3.25).
n	Porosity.
$\underset{\sim}{N}$	Local dispersive flux vector [M/T].
η	Porosity term, one-dimensional flow case, equation (3.37).
P	Porosity term, three-dimensional flow case, equation (3.60).
q_i	Element of specific discharge vector [L/T].
$\underset{\sim}{q}$	Specific discharge vector [L/T].
R	Ratio of horizontal to vertical length scales, equation (3.67).
R°	Ratio of horizontal to vertical length scales, equation (3.68).
R_{KK}	Autocovariance function, K' process.
R_{ff}	Autocovariance function, f' process.

Symbol	Explanation
R_1	Length scale ratio, head variance equation (5.10).
R_3	Length scale ratio, head variance equation (5.10).
R_1°	Length scale ratio, head variance equation (5.14).
R_3°	Length scale ratio, head variance equation (5.14).
s_i	Lag number, i^{th} direction [L].
S	Constant [$MT^{\frac{1}{2}}$], equation (4.42).
t	Time variable [T].
w	Derivative of concentration [M/L], equation (4.1).
x_i	Space variable, i^{th} direction [L].
α_ℓ	Effective local longitudinal dispersivity [L].
α_t	Effective local transverse dispersivity [L].
α_I	Local longitudinal dispersivity [L].
α_{II}	Local transverse dispersivity [L].
β	Local dispersivity difference [L], equation (3.71).
γ_i	Correlation length scale [L], equation (5.7).
δ_{ij}	Kronecker delta.
λ_i	Integral scale [L], equation (3.63).
μ	Uniformity coefficient.
ξ	Moving coordinate [L].
ρ	Effective local dispersivity ratio, equation (3.67).
ρ_{KK}	Autocorrelation function, K' process.
ρ_{ff}	Autocorrelation function, f' process.
σ_c^2	Variance, c' process
σ_f^2	Variance, f' process
$\sigma_{q_1}^2$	Variance, q_1' process.
$\sigma_{q_3}^2$	Variance, q_3' process.

Symbol	Explanation
σ_w^2	Variance, w' process.
σ_ϕ^2	Variance, ϕ' process.
τ	Derivative c' process [M/T], equation (4.39).
ϕ	Hydraulic head [L].
Φ_{cc}	Spectrum, c' process.
Φ_{ff}	Spectrum, f' process.
Φ_{KK}	Spectrum, K' process.
Φ_{nn}	Spectrum, n' process.
$\Phi_{q_1q_1}$	Spectrum, q_1' process.
Φ_{q_1c}	Cross spectrum, q ' and c' processes.
$\Phi_{q_1E_\ell}$	Cross spectrum, q_1' and E_ℓ' processes.
$\Phi_{q_1E_{ij}}$	Cross spectrum, q_1' and E_{ji}' processes.
Φ_{q_1n}	Cross spectrum, q_1' and n' processes.
$\Phi_{q_1\alpha_I}$	Cross spectrum, q_1' and α_I' processes.
Φ_{q_3w}	Cross spectrum, q_3' and w' processes.
ψ	Effective local dispersivity ratio, equation (4.14).

INTRODUCTION

> The success of attempts to solve problems in turbulence depends strongly on the inspiration in making crucial assumptions.
> —Tennekes and Lumley, 1974, p. 4.

Definition of Problem

In recent years, investigators have become increasingly concerned with the effect of variation of aquifer properties on flow phenomena within aquifers (e.g., Warren and Price, 1961; Warren and Skiba, 1964; Freeze, 1975; Bakr, 1976; Gelhar, 1976). This concern is, in part, attributable to the lack of conformity between the results of laboratory tests and field experiments for similar phenomena, which indicates that aquifer properties at the scale of the representative elementary volume (Bear, 1972) cannot necessarily be extrapolated to represent the aquifer itself. It is generally conceded that aquifer properties used in computer simulations of flow phenomena, as well as those obtained from *in situ* field testing, are particular averages of point properties of the aquifer. The validity and representation of these averages have been examined by the above investigators; this report is largely concerned with the effect of medium variability on dispersion in porous media.

Considering that dispersion is, in the case of groundwater flow systems, a medium-dependent phenomenon, it is to be expected that it will vary in intensity from location to location in the aquifer. Indeed since both hydraulic conductivity and dispersivity can be related to grain size (Harleman and Melhorn, 1963), one can postulate a relationship between dispersivity and hydraulic conductivity at the scale of the representative elementary volume. Thus, if the large variances in hydraulic conductivity noted by investigators (e.g., Law, 1944) are veritable, then it is only reasonable to expect that dispersivity, and therefore dispersion, is also subject to similar variations.

Simplistically, one might ask if it is not possible to average in some way these local dispersivities. However, if aquifer properties vary as stated in the previous paragraph, then another problem can immediately be discerned when attempting to describe dispersion in natural porous media. In particular, as a consequence of variable convective transport, hydraulic conductivity variations from point to point in an aquifer will cause a random fingering of the tracer to appear along the mean flow direction of the fluid. That is, the tracer will be displaced varying distances with respect to a common front in response to variation in seepage velocity along the front. Thus, the concentration of a composite sample of a tracer taken over the entire aquifer thickness, as by a fully penetrating well in which the fluid within the bore is well mixed, will be dominated by these random convective effects rather than by dispersion at the local level. Indeed, if the flow has three-dimensional random components, then sampling at any point in the aquifer will result in a more elongated breakthrough curve than could be produced without a random convective effect. That this phenomenon is indeed operative is exhibited by the fact that dispersivities calculated from field tests over large areal distances will generally be larger than dispersivities calculated from laboratory tests on cores (e.g., Fried, 1972), prompting some invesitgators to refer to the former dispersion as "phenomenological" (Heller, 1972).

This type of phenomena has been studies rather intensively in the petroleum industry, where attempts are made to sweep oil from a reservoir by injection of a miscible solvent. The process of sweeping out the oil is frequently hampered by the formation of fingers, leading to an early breakthrough of the solvent and an extended period during which both solvent and oil are produced (Koval, 1963). Finger formation is generally considered to be closely associated with variations in hydraulic conductivity within the aquifer, but may be obliterated if transverse dispersion between fingers is sufficiently operative in comparison to convective transport (Claridge, 1972). Fingering has also been noted in supposedly homogeneous models, where it has been attributed to unfavorable mobility ratios (Slobod and Thomas, 1963). Even in these cases, however, transverse spreading has been observed to obliterate individual fingers. Similar phenomena have been observed in soil columns, where fluid density contrasts are the primary driving force (Starr and Parlange, 1976). Oakes and Edworthy (1976), investigating recharge in the Bunter Sandstone, postulate the occurrence of a similar process to account for the larger dispersivity values obtained when considering the entire aquifer thickness as compared to smaller values for discrete layers. In particular, the presence of "large scale stratiform heterogeneities" is suggested, along with mixing between layers by local transverse dispersion, to account for this discrepancy. It may be concluded, then, that there exists a growing body of evidence which advances variations in hydraulic conductivity as the principal mechanism promoting large scale dispersion in natural sedimentary aquifers.

If one were to model the transport of a tracer through an extensive volume of an aquifer, it would be desirable to have a single parameter which would describe the spreading of the tracer throughout the aquifer. If it could be assumed that the spreading process were Fickian in nature (that is, the solute flux is proportional to the concentration gradient) then it would be possible to use the standard convective-dispersion equation (see Appendix 3) in the modelling effort. Thus one of the questions we must ask ourselves is whether the afore-described phenomena are, in some average manner, Fickian in nature (see Zilliox and Muntzer, 1975). Assuming that the Fickian Model is suitable, it remains to be seen whether, given the appropriate aquifer properties, some vehicle exists for the determination of an effective dispersion coefficient which would be applicable in conjunction with mean components of flow and concentration in the medium. If both of these questions can be answered positively, one should be able to model the transfer of pollutants, in a mean sense, through an aquifer. These questions will be examined in detail throughout the remainder of this report but, before leaving this section, a portion of the literature supporting this concept for the spreading of a tracer in natural aquifers will be examined in more detail.

Stratified aquifer systems, that is aquifers which are composed of continuous layers of contrasting hydraulic conductivity, have been the preoccupation of a number of investigators studying dispersion in porous media. Mercado (1967) developed a model to estimate the longitudinal spreading of a tracer in such aquifers, subject to several assumptions, perhaps the most important of which is that mixing between layers is negligible. Expanding on the work of Marle *et al.* (1967), Renault *et al.* (1975) performed laboratory tests on scaled examples of stratified porous media, in which longitudinal dispersion coefficients were calculated from breakthrough curves as the fluid left the model. They found that transverse mixing was an important aspect of the process, and that dispersion coefficients for layered aquifers, with large contrasts in hydraulic conductivity between layers, could be several orders of magnitude greater than coefficients for individual layers. These results have been verified to some extent by the aforementioned in situ field work of Oakes and Edworthy (1976).

Attempts to examine the effect of multidimensional variations in hydraulic conductivity on dispersion have, in large part, been studied through computer simulation. Heller (1972), working with computer simulations of the movement of a fluid through a two dimensional system of cells in which hydraulic conductivities were assigned on a random basis, also found finger-like frontal movements. His simulations did not consider dispersion at a local scale which might attenuate the over-all effect of convective transport. Simulation of flow through three-dimensional random hydraulic conductivity arrays were executed by Warren and Skiba (1964), where dispersion coefficients were determined by tracking particles through the flow system. Local dispersion was again neglected but, significantly, the authors were able to conclude that "macroscopic" dispersion, or the over-all dispersive effect, is related to variations in hydraulic conductivity and scale of the heterogeneity. These latter investigators also suggest that, within limits, the dispersion process is Fickian in nature. Both groups of investigators assigned hydraulic conductivities randomly from lognormal distributions, using Monte Carlo schemes.

Skibitzke and Robinson (1964) endeavored to model the passage of a tracer through isolated heterogeneities in otherwise homogeneous media by carefully constructing laboratory experiments. These experiments demonstrated the magnification of spreading of a tracer upon entering regions of contrasting hydraulic conductivity. Transverse spreading of the tracer away from channels of higher hydraulic conductivity was also observed. Zilliox and Muntzer (1975) conducted similar experiments, in which a heterogeneity consisting of a higher hydraulic conductivity was positioned perpendicular to the direction of flow. A marked increase in lateral spreading was noted as the tracer passed through the more conductive zone. Thus, again the importance of conductivity variations together with the secondary effect of local dispersion of the entire spreading phenomenon has been documented. This report will primarily be concerned with the first-order analysis of a model with these features, which will be described in more detail in a later section.

Length Scales in Sedimentary Aquifers

In the preceding discussion a scale over which dispersion phenomena operate was implied. Before proceeding further, it will be helpful to discuss scales and their application to the problem at hand. A number of investigators have devised classification schemes for scales of flow and transport pehnomena in porous media, usually basing their scheme on the size of heterogeneities to be expected (e.g., Groult et al., 1966; Alpay, 1972; Claridge, 1972; Fried, 1975; Freeze, 1975). For the purpose of this report, a synthesis of the various schemes shall be attempted, incorporating features as needed for the following discussion.

The smallest scale of interest to this discussion is the intrapore size. At this scale, molecular diffusion is the dominant factor contributing to the dispersion of a tracer in most flow systems (Fried and Combarnous, 1971). Beyond the dimensions of the pore channels themselves, we become interested in how particles move between pores. In particular, as a particle passes through a medium, it can be visualized as traveling a certain average distance between intersections of the various pore channels (e.g., Scheidegger, 1954). This average distance will be referred to as the interpore scale. If sufficient pore space is taken in union, then aquifer properties tend to become constant, at least with regard to that volume of pore space. The quantity of pore space necessary to reach this condition is called the representative elementary volume (Bear, 1972), and represents the smallest scale at which aquifer properties can be quantified and the aquifer itself construed as a continuum. For reasons discussed in the following paragraph, this scale will be referred to as the local scale. Beyond this dimension, a scale can be conceived at which variations in aquifer properties, as defined at the local scale, can be measured. That is, in accord with introductory discussion, it is not to be expected that aquifer properties at a local scale will be spatially constant in natural aquifers. We will refer, then, to the average distance necessary for these variations in aquifer properties at a local scale to become evident as the aquifer correlation scale (see Appendix 1). This scale, as noted later, can be multidimensional and is a fundamental method of representing heterogeneities in aquifers (Bakr, 1976). Realizing that aquifer properties are rather variable, we may ask ourselves what travel distance would be necessary for us to obtain the average value of some flow or transport parameter. For instance, if one were to attempt to determine the average seepage velocity through a particular aquifer, then it would be desirable to locate observation wells at a distance from each other equivalent to several correlation lengths in order to allow for sufficient averaging to occur along the flow path (e.g., Corompt et al., 1974). This distance will be referred to as the global scale in this thesis, and is significant in that it is the scale over which most "effective" aquifer properties operate. Yet another scale can be defined from the average distance over which statistical moments of aquifer properties, as defined from the local scale, remain constant (or stationary). Over extensive regions, it is only reasonable to expect that aquifer property moments themselves will be subject to change (e.g., Alpay, 1976). The average distance over which moments can be considered to be stationary will be referred to as the regional scale.

The above classification scheme is based on the relative statistical and flow properties of an aquifer. As with all classification schemes it is lacking in some areas and will not be universally satisfactory. For instance, it may be quite possible that the probability moments, defined at the local scale, are a continuous function of space, preventing definition of a region where they are approximately stationary. In such a case, the correlation scale would be a function of spatial variables and the regional scale would cease to be defined. Such possible models will be excluded from this study. Also, flow and transport phenomena at less than the local scale will not be of concern to us. With regard to the term "local" as used in the previous paragraph, Zilliox and Muntzer (1975) noted that while simple homogeneous and isotropic models of transport phenomena preserve the natural structure of the interconnection of pores, they also represent "local" configurations in more complex models. This is also the sense of the term as used herein. Renault et al. (1975) used the term "global" to connote dispersion influenced by variations in hydraulic conductivity. In a similar sense, "global" is used herein to define a length scale over which averages in flow and transport parameters are obtained from variations in aquifer properties. Because of the method of analysis used, results from this research are only applicable within that portion of the medium encompassed by the regional scale.

The preceding discussion forms a basic framework for the development of a model equation to describe dispersion resulting from variations in aquifer properties. These introductory statements indicate that dispersion in porous media occurs at two different scales in response to differing mechanisms. In the remainder of this report, dispersion phenomena which results from the intricate geometry of the pore system will be referred to as local, while that attributed to variation in medium properties themselves will be called global. Thus, dispersion coefficients will be referred to as either local or global; the effective dispersion coefficient which quantifies spreading in natural aquifers is equivalent to the global coefficient.

Review of Literature

Various approaches or methods have been proposed in the literature to represent and analyze the dispersion process in porous media. These models are generally constructed from a stochastic representation of the medium at one scale, and are applicable at another, larger scale. It is of interest to review these models with an eye toward application to the problem at hand.

In the last two decades, considerable effort has been expended on a group of models generally classified as random-tube models. Reviews of these models are available in Greenkorn and Kessler (1969), Bear (1972), Wilson and Gelhar (1974), and Fried (1975). Since it is impossible to describe exactly the passage of a tracer through porous media at an intrapore level because of the irregularity of disposition of boundary conditions, investigators have generally turned to models wherein the pore openings are simulated by a network of randomly oriented tubes. This approach enables investigators to treat the porous medium, at an interpore scale, as a statistical quantity with associated probability density functions. The earliest of these models, and perhaps the most edifying in terms of understanding their probabilistic basis, was proposed by Scheidegger (1954). He recognized that the sample space for the probability density of the displacement of a particle was actually an "ensemble" of porous media, and considered that this density could be related to the physical density of the tracer concentration by "ergodicity" (Appendix 1). By assuming that particle motion can be represented by a Markov process, a probability density function was developed and subsequently shown to be a solution of the convective-dispersion equation (applicable at the local scale), which allowed Scheidegger to conclude that local dispersion coefficients are related to the variance in particle displacement. By averaging Newton's equation for particle motion, a form for the variance was derived. The same basic procedure has been used by other investigators in the field, except that more emphasis has been placed on the derivation of the variance term for particle displacement. Scheidegger concluded from this analysis that dispersion at a local level was Fickian in nature and could be quantified by an isotropic medium constant called a "dispersivity." Later investigators have found, however, that dispersivities should be tensor quantities, even in otherwise isotropic media, as longitudinal dispersion is significantly greater than transverse dispersion. This disparity created further interest in this type of stochastic approach at an interpore scale.

Later investigators have mainly concentrated on predicting the displacement variance from the random-walk scheme inherent to these models. De Josselin de Jong (1958) devised a model with uniform capillary tube length and diameter, but having tubes oriented randomly. Radial diffusion within tubes was assumed to cause a particle to travel at the mean velocity of the fluid in tubes, which varies with respect to the mean flow direction in the medium. With the aid of Markov's method, de Josselin de Jong developed a three-dimensional density function for particle displacements, from which both longitudinal and transverse dispersivities are calculated. Saffman (1959) independently derived de Josselin de Jong's results, and also considered the case where radial diffusion is small, allowing for the occurrence of velocity variations over the tube radius. Haring and Greenkorn (1970) extended this latter case to include random variations in tube radius and length, as described by beta distributions. They were able to conclude that for unconsolidated sedimentary materials the ratio of longitudinal to transverse dispersivity should range from three to ten, but might be greater for consolidated sediments.

In general, random tube models give us insight into the dispersion phenomenon at the local level and, as in the case of Haring and Greenkorn's (1970) model, may be useful in predicting local dispersivities. However, it would be difficult if not impossible to scale these models up to the global level of interest in this study. The problem is similar to that of attempting to model local dispersion with an intrapore-scale model; the complex boundary conditions caused by random variations in hydraulic conductivity would have to be taken into account when applying these random-walk probability models. It is suggested, then, that our time may be more profitably spent looking at models constructed at the local scale.

Another possible approach to study the dispersion phenomenon at a global scale employs Monte Carlo schemes similar to those constructed by Heller (1972), Schwartz (1977), and Warren and Skiba (1964). As noted previously, these models attempt to represent natural media by compartmentalizing a medium into equidimensional blocks in which the model hydraulic conductivity is assigned randomly. In the case of Warren and Skiba's investigation (which is somewhat enhanced over the work of the other investigators in that their model was three dimensional) hydraulic conductivities were assigned from a lognormal distribution and porosities from a normal distribution. Global longitudinal dispersion coefficients were determined from the variance of reference particles tracked through the medium under a steady flow regime. The effect of porosity on the global dispersion process was found to be second order and was consequently neglected. In the modelling effort, the effects of block size and variance in hydraulic conductivity were investigated (block size is roughly equivalent to the correlation length scale which characterizes the size of heterogeneities in natural media). Monte Carlo simulations of this nature have been criticized for lacking an autocovariance function for medium parameters (Gelhar et al., 1977) which causes them to be incompatible with real-world aquifers. Additionally, these modelling efforts have neglected dispersion at the local scale which, in the sense of Taylor's (1953) work (see section entitled "Approach"), may not allow the particle variance to become independent of travel time. The effect of varying travel times on dispersion coefficients has not been studied by any of the above investigators. These defects could probably be rectified and further research employing these schemes is encouraged. For example, Boreli et al. (1977) have incorporated the convective-dispersion equation into their scheme, thus allowing for local dispersion. The results from this study, however, are rather inconclusive. In general, while lending themselves well to the study of dispersion at a global scale, an analytical form for the process does not evolve readily from such schemes.

Global dispersion in stratified aquifers, because of the inherent simplicity of randomness in hydraulic conductivity involved, is more amenable to a mathematical treatment. By assuming a local transport model which is entirely convective, Mercado (1967) proposed a method of analysis for stratified aquifers in which the hydraulic conductivity at any point in a vertical cross section is normally distributed. A constant porosity was assumed for the model and, plainly, local dispersion has been neglected. As might be expected, a normal distribution was found to represent the depth-averaged tracer concentration and the standard deviation from this distribution was used to characterize global longitudinal dispersion. If one postulates that the standard deviation of the tracer concentration is directly related to the global coefficient in much the same way as Scheidegger (1954) has done, then it can be demonstrated that the resulting longitudinal coefficient is time dependent. Time dependence of dispersion coefficients in these models is probably closely related to assumptions concerning lateral spreading at a local level (see Renault, et al., 1975; Fried, 1972). If no lateral mixing is assumed, which is probably a reasonable supposition for early time or small distance from the injection site, then time dependence of the dispersion coefficient is to be expected. For large time, as will be noted in the next paragraph, lateral mixing becomes significant and the dispersion coefficient is independent of time. Thus, Mercado's results are probably valid only in a small area surrounding the injection site.

Marle et al. (1967) developed a method of predicting longitudinal dispersion coefficients in stratified aquifers, provided that aquifer parameters (porosity, permeability and dispersivities) for each layer are known. Utilizing a method of moments developed by Aris (1956), whereby the moments of longitudinal displacement are calculated from the relative tracer concentration distribution, Marle et al. derived an expression for the global longitudinal dispersion coefficient. Their analysis consists of solving the moment equations inductively, neglecting certain higher order, time-dependent terms by assuming a long-duration process, and results in a solution consisting of integrals where local porosities and dispersion coefficients form the arguments. The integrals must be evaluated over the entire aquifer thickness in order to obtain the global coefficient. The results are significant in that they are valid only for large time, indicating that lateral mixing between layers is fully operative and that time dependence has been lost. Additionally, the method of solution suggests that global dispersion in natural aquifers is a Fickian process.

The results of the work of Marle et al. (1967) have been verified to some extent by Renault et al. (1975) in laboratory experiments with stratified models. The significance of the work, however, is largely found in its applications toward the better understanding of the dispersion process at a global scale, since it would be difficult to apply these results to field situations consisting of multiple strata because of formidable data requirements involved.

For media in which aquifer properties are randomly distributed in all directions (or, for that matter, in one direction as would be the case for stratified aquifers), the approach of Buyevich et al. (1969)

to the problem of analyzing global dispersion holds promise. Using the Navier-Stokes equation of motion, the continuity equation, and the convective-dispersion equation, all at a local scale, these invesitgators considered the effect of three-dimensional porosity variations on mass transport in statistically homogeneous, isotropic porous media. Corresponding to the porosity variations, linear perturbations were assumed for seepage velocity, pressure, and tracer concentration which, when properly considered in a nondimensional form in the previous equations, allowed for their transformation, in terms of perturbed quantities, into a set of linear equations. With the aid of the well-developed theory of stationary random processes (Appendix 1), these equations can be solved simultaneously in terms of spectra and cross spectra. Correlation functions can then be derived by taking the Fourier transform of the spectral equations (or transfer functions) and these functions, in turn, can be related to global dispersion coefficients for both long and short time durations.

Approaches utilizing properties of second-order stationary processes have the advantage that they treat the medium as a continuum in which variations in aquifer properties are represented by statistical moments and length scales. In turn, fluid and transport phenomena can also be conceived of as continuous processes which contain variations represented by statistical parameters. With regard to the work of Buyevich et al. (1969), porosity variations are associated with a correlation length scale which is approximately equivalent to the distance over which porosity can be considered constant. If, as in the case of their large-time results, the global dispersion coefficient is found to be proportional to a correlation length scale and velocity standard deviation, then one only need estimate these statistical parameters to obtain an order-of-magnitude approximation of the dispersion coefficient. In general, if a porous medium can be considered to be a spatially stationary random-field process, then an approach of this kind may be a practical method of analyzing dispersion in porous media. The approach is not without pitfalls, however, as it necessitates that partial differential equations governing flow and transport be linearized before application can be made.

While making an impressive contribution to the subject, the specific approach used by Buyevich et al. (1969) is lacking in some respects. It has been previously noted that variations in hydraulic conductivity are considered to be the primary cause of global dispersion. Thus, their analysis depends on the degree of relationship between hydraulic conductivity and porosity. The quality of the result in this type of analysis is dependent to a large degree on the nature of linearizing assumptions used. In the case of Buyevich et al., it was assumed that the perturbation was much smaller than the mean; a rather restrictive assumption for most porous media. For simplicity, the investigators used an isotropic porosity spectrum; yet most natural aquifers are stratified to some degree which would preclude this type of spectrum. Finally, their long-term result, which we consider to be more significant, is rather unprecisely reported as a simple proportionality. Thus, we consider that these investigators have not exhausted the possibilities of the approach.

Before passing on to a more detailed description of the approach to be taken in this paper, it should be noted that the theory of spatially stationary random-field processes has been applied previously to the analysis of groundwater flow in natural aquifers (Gelhar, 1976 and 1976a; Bakr, 1976). The principal objective of these investigators has been the analysis of variance in hydraulic head caused by variations in medium parameters. Application of the theory has been achieved for one-, two-, and three-dimensional flow schemes. Thus, considerable precedent exists for its application to problems in flow through porous media.

Approach

The analysis followed in this thesis owes its spirit, to no small degree, to an earlier work by G. I. Taylor (1953). While analyzing the dispersion of a pulse of tracer injected into capillary tubes in which laminar flow is occurring, Taylor considered the transfer of mass across a plane which moves with the mean flow velocity and is oriented perpendicular to the flow direction. Taylor reasoned that, with sufficient time lapse, convection of mass across the plane, as caused by the true parabolic velocity distribution, would equal the amount of radial diffusion occurring perpendicular to the direction of flow. That is, with regard to the moving plane, radial mass transfer and mass transport in the direction of flow at any point in the tube could be regarded as being in equilibrium. Taylor obtained a solution to the differential equation describing this model and whence, given sufficient time lapse, found an expression describing the distribution of a tracer at any point in the tube. By integrating this distribution over the tube cross section, an expression for the amount of tracer flux transferred across the moving plane was obtained, and thereby an expression for the longitudinal dispersion coefficient for the mean tracer concentration. The assumptions leading up to this coefficient were verified by Taylor through laboratory experimentation.

If one considers an "average" stream tube within a natural medium in which a pulse of tracer material has been injected over its width, then certain analogies exist between this model and Taylor's (1953) tube model. For instance, if a moving coordinate for average motion of a fluid through the stream tube is considered then, with respect to this coordinate, an equilibrium may exist (under certain conditions) between longitudinal and lateral transfer of mass. The parabolic velocity distribution causing longitudinal transfer in the capillary tube could be replaced, in the natural aquifer, by a random velocity distribution about a mean which, with regard to the dispersive process, has the same function but is caused by random variations in hydraulic conductivity rather than by boundary effects. Similarly, rather than depend upon diffusion for lateral spreading, dispersion at a local level could serve this purpose. However, it is to be expected that tracer concentration at any point within the stream tube will contain random as well as deterministic components because of the random nature of the medium. With the existence of many analogies with Taylor's work, one could possibly proceed immediately to write a partial differential equation which would properly describe the dispersion process at a local scale and then evaluate this expression. Nevertheless, we shall proceed more formally in the following chapter to derive a model equation which, in moving coordinates and for sufficient time duration, will describe a balance between longitudinal transfer and dispersive lateral mixing in terms of zero-mean random variables.

Once derived, the model equation must be solved and the amount of tracer flux transferred through the moving plane found. As most of the variables in the problem are random, it would be difficult to proceed in the same manner as Taylor (1953). Indeed, it will be shown that the desired tracer flux is an expected value of the product of specific discharge and concentration random variables. Thus, it would appear to be necessary to know the probability density functions of the variables involved. These densities could be identified from an ensemble of realizations of our experiment; that is, by investigating a very large number of pulse injections of a tracer over the width of an average stream tube in probabilistically similar porous media. Clearly, such an ensemble of observations, while representing the real probabilistic basis of the random variables involved in the problem, would be difficult to obtain.

By taking advantage of the properties of stationary random processes in much the same way as Buyevich et al. (1969), certain simplifications result in the over-all problem. In our case, this will imply that we assume the medium to be spatially second-order stationary or, in other terms, statistically homogeneous over a regional scale. Simply stated, second-order stationarity implies that all second moments of the joint probability density functions of random variables are independent of absolute spatial location (a relative spatial dependence is considered, however). This assumption plus the properties of the process will allow us to find expected values of products of random variables and in essence solve the model equation, to a first-order approximation, for a tracer flux through the moving plane. The method of solution involves assuming a reasonable form for certain autocovariance functions of medium properties which will allow for the calculation of other second moments via the representation theorem (Appendix 1). Additionally, it is assumed that boundaries of the medium are at sufficient distance to be inconsequential to autocovariance functions.

In summary, the prototype proposed herein is one in which tracer concentration, specific discharge, dispersion coefficients, porosity and hydraulic conductivity are statistically homogeneous random variables at the local level. This probabilistic description is based on the concept of the ensemble, and should not be confused with the results of a single realization of the experiment. Utilization of the local scale for definition of variables will allow, as noted previously, a continuum treatment of flow and transport phenomena. It will be necessary to assume that hydraulic conductivity of the medium is physically isotropic at a local level. This assumption is not restrictive, however, since statistical anisotropy can be introduced at the aquifer correlation scale. These and other assumptions will be treated in more detail in the following section.

With the approach outlined in this section, we will attempt to obtain from the model equation an expression for the global dispersive flux. If this expression has a Fickian form, we will then be able to say that the convective-dispersion equation applies at the global scale. Additionally, we may also obtain information concerning the applicability of this expression which may have some impact on design of field experiments for testing for global coefficients. Finally, the form of the expression itself may suggest some method of approximating global longitudinal dispersion coefficients without extensive field testing.

DERIVATION OF MODEL EQUATION

Prototype

In introductory statements to this point, the problem of attempting to apply dispersion coefficients determined from laboratory tests to actual modelling of the transport of a tracer mass in natural aquifers was discussed. Specifically, variations in medium properties (as measured at the local level) will augment the spreading of a tracer beyond that which would otherwise be expected. Additionally, a few statements were made regarding the method of solution and its ramifications on assumptions concerning the porous medium. We will now formally state the nature of the prototype experiment, the equations for which will be developed and solved in subsequent sections.

We design a theoretical experiment with the expectation that, as in the case of Taylor (1953), we derive information from it which is not dependent on the experiment itself. In particular, we envision a considerable "lump" of granular material, which has the minimum approximate dimension of the global scale (Figure 2.1). Within the medium, steady state flow is occurring such that its mean component is unidirectional in the sense of the positive x_1 coordinate (this implies a mean hydraulic gradient in the same direction). A tracer has been injected over a large area perpendicular to the mean direction of flow at a distance equivalent to several global dispersivities upstream from our present observation point. For convenience, we may think of the injection as having occurred instantaneously in time. The tracer is ideal and conservative in that it travels identically as the transporting agent, unaffected by density contrasts, and does not lose mass along its path of travel.

Medium properties, which shall be considered to possess a random

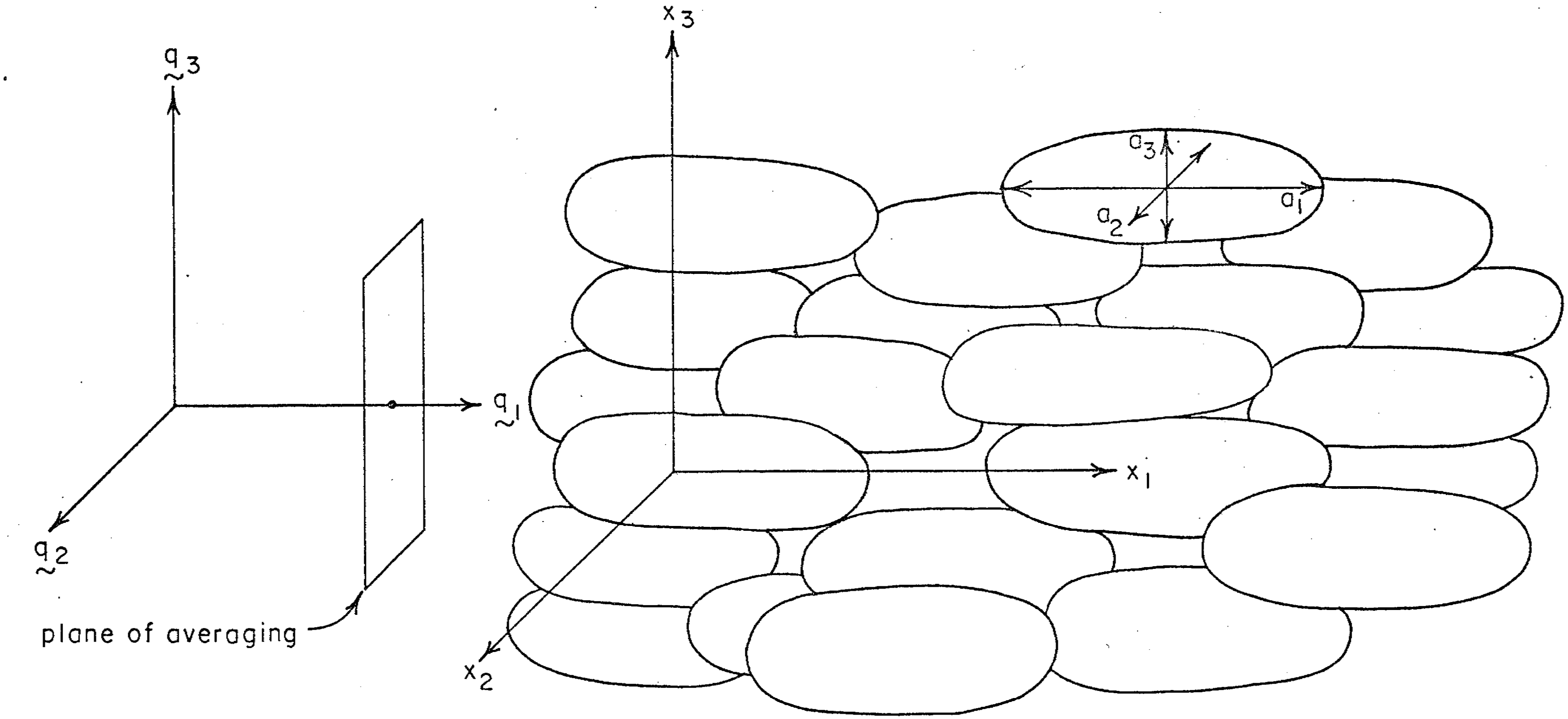

Figure 2.1. A "visualized" porous medium. x_1, x_2, and x_3 – reference axes. $\underset{\sim}{q}_1$, $\underset{\sim}{q}_2$, and $\underset{\sim}{q}_3$ – specific discharge vectors along principal axes. a_1, a_2, and a_3 – correlation length scales.

component, can be characterized from a statistical description of the medium, using the local scale as the sample space. For instance, the prototype medium will be considered to be nonuniform, meaning that its properties possess a finite variance (Greenkorn and Kessler, 1969). We note that this statistical description has its basis in probability density functions founded on an ensemble of realizations of the medium. There is no reason that these density functions (and therefore moments of medium properties), in addition to having an underlying sample space, could not also be dependent on their location in the medium. For simplicity and reasons noted previously we restrict joint density functions of medium properties by allowing them to depend only on the separation of points in space and not on the absolute location of the points; a restriction known as stationarity. However, we normally depend on a weaker condition that requires only the second moment to be independent of spatial location. That is, if the autocovariance function, which can be thought of as the covariance of a property with itself at two different locations, is dependent only on the separation vector between two points and not on their actual locations, we characterize the medium as being spatially second-order stationary or, as more frequently used in this report, statistically homogeneous (Bakr et al., 1977). This weaker requirement is not unreasonable as we shall work principally with first and second moments in the subsequent analysis. By making this assumption of the prototype medium properties, we implicitly extend statistical homogeneity to the fluid regime itself, since medium properties govern motion and transport in the fluid. Thus, statistical homogeneity is not only an important property of the medium, but also of fluid flow.

The autocovariance function will enable us to add anisotropy to the prototype at a global scale. At the local scale, as noted previously, we make the simplifying assumption that the medium is essentially isotropic. This assumption is not precisely true for most sediments, but does not appear to be extreme, especially for coarser grain sizes (Pettijohn et al., 1973, p. 529). However, because there is correlation between properties at different locations in the medium, and as this correlation is less than perfect, it follows that local isotropy may not be perpetrated throughout the medium. We examine this concept with the correlation length scale, which can be thought of as the average distance, along the three cardinal directions of the prototype medium, over which medium properties are correlated (see section entitled "Length Scales in Sedimentary Aquifers"). The correlation length scales can formally be defined as integral scales of an autocorrelation function, or simply that distance over which a property is positively correlated (Appendix 1). In either case, correlation length scales are medium constants associated with every autocorrelation function. In summary, the prototype medium is also characterized by correlation length scales a_1, a_2, and a_3 which we assume to be oriented with the principal axes (Figure 2.1). (This assumption is necessary in order to maintain colinearity of the hydraulic gradient and flow.) Although somewhat unprecise, these length scales can be thought of as defining an ellipsoidal region throughout which a particular medium property is approximately constant. If we allow the horizontal length scales to become very large with respect to the vertical one, a stratified aquifer is obtained. Indeed, in this case the autocorrelation function reduces to one dependent only on the vertical separation vector. In essence, if a length scale is rather limited in any one direction, then we assume that the sedimentary structure is changing rather rapidly in that direction. On the other hand, if the length scale is large, then we assume that few changes occur.

At this point, we may opportunely discuss the physical significance of statistical homogeneity. Does it, in fact, imply physical homogeneity in some mean sense? Let us consider the case where correlation length scales are equal in all directions (the case of unequal length scales is a simple extension of this case): If the medium is statistically homogeneous, will this isotropy be perpetuated throughout the aquifer? From an ensemble point of view, and in agreement with the preceding paragraph, statistical parameters such as the mean, variance, covariance and length scales will be the same at every point in a stationary medium; therefore, we would reply affirmatively that, in a mean sense, physical homogeneity is implied. We may question, however, the applicability of this result to a single realization of the medium. To investigate statistical homogeneity as applied to a single realization, we must resort to the principal of ergodicity (Appendix 1). By this principle, we should be able to sample one realization sufficiently to reproduce whatever statistical parameter we desire. Thus, we can imagine sampling over a large volume of the aquifer at two different localities in the medium and, using the appropriate estimators, calculate the statistical parameters in question and assign them to these localities. However, it is obvious that, by ergodicity, these parameters will asymptotically approach the ensemble parameters. Whence, we again conclude that, in a mean sense, the same expectations apply to the single realization as to the ensemble, and we would consider the single realization to be globally isotropic. This result is not unexpected from the point of view of fluid motion, as there is obviously no preferential medium direction; only a random distribution of heterogenities which have some over-all average.

As indicated in the section entitled "Length Scales in Sedimentary Aquifers," the distance over which moments of medium properties remain spatially stationary is referred to in this report as the regional scale. Beyond this distance, the medium ceases to be statistically homogeneous and, in a mean sense, it would be referred to as effectively heterogeneous. This heterogeneity is rather like that used by numerical modelers when they divide two-dimensional horizontal models into regions of equal effective hydraulic conductivity. In any one region the aquifer is considered to be homogeneous (even though the real aquifer probably contains numerous heterogeneities of a correlation-scale size in each of these regions) but, over-all, the aquifer must be considered to be heterogeneous. The prototype medium considered herein should be considered to be of a dimension somewhere between the global scale and the regional scale.

With respect to motion and transport in the fluid regime, we note that the prototype medium is characterized by three types of parameters: porosity, hydraulic conductivity and dispersion coefficients. It is of interest to define these quantities at a local scale, since this is the scale around which equations of transport and motion are formulated. In particular, we are especially concerned with the effect of variations in hydraulic conductivity on tracer transport at a global scale. Analysis of multiple core samples from the same aquifer indicates that hydraulic conductivities at this scale are frequently lognormally distributed (Law, 1944; Freeze, 1975). To the extent that these results can be taken to represent the local scale, we expect that hydraulic conductivities will frequently possess a lognormal density function.

. The question arises, then, of what consists the "average" hydraulic conductivity which governs the aforementioned mean flow component in the x_1 direction. This is a rather necessary question since, as a means of simplification, we will subsequently assume that the quantity K_ℓ, defined as

$$K_\ell = \exp [\overline{\ln K}] \qquad (2.1)$$

where K is the local hydraulic conductivity and the bar indicates expectation (the taking of an expected value), represents the effective hydraulic conductivity of other than stratified aquifers. The quantity K_ℓ is the population equivalent of the geometric mean which is equivalent to the median of the lognormal distribution (Appendix 2). Three-dimensional Monte Carlo simulations have indicated that the geometric mean is the best estimator of the effective hydraulic conductivity (Warren and Price, 1961). However, Gutjähr et al., (in press), using properties of a stationary random-field process to analyze three-dimensional flow, recently concluded that the best first-order estimate of effective hydraulic conductivity is $K_\ell[6 + \overline{(\ln K)^2} - (\overline{\ln K})^2]/6$. That is, K_ℓ underestimates the effective hydraulic conductivity by a factor of one-sixth the variance of lnK. This underestimate is about 14% for a variance of lnK equal to one. Thus, another characteristic of our prototype is that we shall assume that K_ℓ is the effective hydraulic conductivity of unstratified media, even though K_ℓ may not be the best estimator of this quantity in all cases.

For stratified aquifers, the arithmetic mean (or its population equivalent, the first moment) is a superior estimator of the effective hydraulic conductivity for flow parallel to bedding (Bear, 1972). This difference in estimators is the result of suppression of flow in other than the x_1 direction, resulting in a model where flow has vector components only in that direction. Indeed, we shall treat the stratified aquifer as a separate case because of this single dimensionality of flow. It is this same phenomenon which makes it difficult to compare results of analyses from stratified and unstratified aquifers, even though, in a limiting sense, we can extend correlation length scales to cause the results of three-dimensional flow analyses to approach the one-dimensional or stratified case. Thus, in deference to this problem, we relinquish the use of K_ℓ for one-dimensional flow through stratified aquifers and simply use the expectation of hydraulic conductivity for this case.

Bulk dispersion coefficients will be used in the prototype to represent the dispersive process at the local level. In this case, the term "bulk" means that, in addition to being a function of seepage velocity and a dispersivity, we also include a porosity dependence. Following Bear (1972, p. 612), we express these local bulk dispersion coefficients E_{ij} for an isotropic medium as

$$E_{ij} = \alpha_{II} q \delta_{ij} + (\alpha_I - \alpha_{II}) q_i q_j / q \qquad (2.2)$$

where

α_I	local longitudinal dispersivity;
α_{II}	local transverse dispersivity;
q_i	element of specific discharge vector, $\underset{\sim}{q}$;
q	magnitude of $\underset{\sim}{q}$;
and δ_{ij}	Kronecker delta.

The dependence of the local bulk dispersion tensor on the specific discharge is significant in that it could force us to deal with nine different tensor components in our analysis. For, although we admit to a mean flow component of the x_1 direction, the three-dimensional nature of variations in hydraulic conductivity in most natural media will cause flow at any point to have a three-dimensional aspect. Thus, we may represent the specific discharge vector as

$$\begin{aligned} \underset{\sim}{q}(\underset{\sim}{x}) &= q_1(\underset{\sim}{x})\underset{\sim}{i} + q_2(\underset{\sim}{x})\underset{\sim}{j} + q_3(\underset{\sim}{x})\underset{\sim}{k} \\ &= (\bar{q}_1 + q_1'(\underset{\sim}{x}))\underset{\sim}{i} + q_2'(\underset{\sim}{x})\underset{\sim}{j} + q_3'(\underset{\sim}{x})\underset{\sim}{k}\ , \quad \underset{\sim}{x} = (x_1, x_2, x_3) \end{aligned} \tag{2.3}$$

where the primed quantities are zero-mean perturbation of the vector components (Figure 2.1). We assign no restrictions on the size of the perturbations at present, leaving that until a later section. However, it should be noted that the variability in specific discharge is expected to be proportional to that in hydraulic conductivity, and greatest in the direction of mean flow (x_1). As all vector components of specific discharge are present in the prototype model, the local dispersion tensor could be quite complicated.

An immediate question arising from equation (2.3) is whether equation (2.2) must be used for the principal diagonal of the local dispersion tensor, or whether the simpler form, utilizing only the specific discharge component in the direction of mean flow, is not sufficient. We may analyze the significance of the perturbed quantities on the dispersion tensor by first approximating the magnitude of the specific discharge vector with the binomial expansions

$$q = (q_1^2 + q_2^2 + q_3^2)^{1/2} = q_1\left[1 + 1/2\,(q_2/q_1)^2 + 1/2\,(q_3/q_1)^2 + \cdots\right]$$

and $$q^{-1} = (q_1^2 + q_2^2 + q_3^2)^{-1/2} = q_1^{-1}\left[1 - 1/2\,(q_2/q_1)^2 - 1/2\,(q_3/q_1)^2 + \cdots\right] \tag{2.4}$$

Upon truncating these expansions and substituting them into equation (2.2), we obtain for the local longitudinal dispersion coefficient

$$E_{11} \approx \alpha_I q_1\left[1 - 1/2\,(q_2/q_1)^2 - 1/2\,(q_3/q_1)^2\right] + \alpha_{II} q_1\left[(q_2/q_1)^2 + (q_3/q_1)^2\right]. \quad (2.5a)$$

Similarly, for the transverse coefficient,

$$E_{22} \approx \alpha_{II} q_1\left[1 + (\alpha_I/\alpha_{II} - 1/2)(q_2/q_1)^2 + 1/2\,(q_3/q_1)^2\right] \quad . \quad (2.5b)$$

In both cases, it is apparent that the largest second order terms are $(q_2/q_1)^2$ and $(q_3/q_1)^2$ and, in accord with the previous paragraph, they probably contribute little to either coefficient. However, in the case of E_{22}, it may be possible that (α_{II}/α_I) is of the same order magnitude as (q_2/q_1), making it difficult to neglect the product $(\alpha_I/\alpha_{II})(q_2/q_1)^2$. Except in the case of global isotropy, this possibility seems remote to us, and therefore will be ignored. For the main diagonal of the tensor, we assume that the local dispersion coefficients take the form

$$E_{11} = E_\ell = \alpha_I q_1 \quad (2.6a)$$

and $E_{22} = E_{33} = E_t = \alpha_{II} q_1 \, .$ (2.6b)

We note that this analysis does not mean that α_I and α_{II} are constant throughout the medium; as with all local medium parameters, they are subject to random variations.

In a manner similar to the previous paragraph, the off-diagonal terms $E_{23} = E_{32}$ are also negligible. However, if we proceed as before for the terms $E_{12} = E_{21}$ and $E_{13} = E_{31}$, we find that

$$E_{12} \approx q_2' (\alpha_I + \alpha_{II}) \tag{2.7a}$$

and $$E_{13} \approx q_3' (\alpha_I + \alpha_{II}), \tag{2.7b}$$

which indicates, to the accuracy of the first-order analysis developed subsequently, that these terms may be significant. However, for aquifers which are even moderately stratified, we expect that q_2' and q_3' will be exceedingly small, thus causing E_{12} and E_{13} to contribute little to dispersion at the local scale. In any case, because of the Fourier-Stieltje's integral method with which the model equation is solved, we need only consider that equation (2.6) represents the principal elements of the dispersion tensor. This will be demonstrated ex post facto at a later point in this report. For the present, we conclude that local dispersion in the prototype can be characterized by the elements of the main diagonal of the dispersion tensor, and that these elements have a simple linear relationship with specific discharge in the mean flow direction.

Perturbed Quantities

As noted in previous discussion, we may conceive of medium properties as having a mean value which, because of stationarity, is constant throughout the medium. However, rather than thinking of the mean as being embedded in a continuum of randomness, we will consider that the mean is a property common to the medium and that randomness has been superimposed upon it. For example, porosity n can be written as

$$n(\underset{\sim}{x}) = \bar{n} + n'(\underset{\sim}{x}), \quad \underset{\sim}{x} = (x_1, x_2, x_3) \tag{2.8}$$

where $\bar{n}$ is the mean of the property and $n'(\underset{\sim}{x})$ is a random perturbation. The perturbation will always be considered to be a zero-mean, spatial stochastic process which is statistically homogeneous. Generally, it is preferable to work with perturbations which are small since linearizing implies products of perturbations are small and can be neglected. However, it is not always possible to proceed in this manner because variations in some properties, such as hydraulic conductivity, can be large.

When analyzing three-dimensional flow models, we will use the logarithm of hydraulic conductivity rather than hydraulic conductivity itself. Formally, we express this quantity as

$$f(\underset{\sim}{x}) = \ln\left[K(\underset{\sim}{x})\right] \tag{2.9}$$

and its perturbation as

$$f(\underset{\sim}{x}) = \bar{f} + f'(\underset{\sim}{x}) \quad . \tag{2.10}$$

Equation (2.1), the effective hydraulic conductivity K_ℓ, then becomes

$$K_\ell = \exp\left[\bar{f}\right] \quad . \tag{2.11}$$

It is of interest to note that, by considering the logarithm of the process, we numerically reduce the amount of variability involved. However, the variance of the logarithm of the process, in the case of hydraulic conductivity, can itself be large (Freeze, 1975). When we must work with $K(\underset{\sim}{x})$ itself, we can obtain an expression from equation (2.10) which, in the form of a truncated Maclaurin series, gives us the linear approximation

$$K(\underset{\sim}{x}) = K_\ell \exp\left[f'(\underset{\sim}{x})\right] \approx K_\ell\left[1 + f'(\underset{\sim}{x})\right] \quad . \tag{2.12}$$

This approximation is severely limited if f' is large, possessing an error on the order of one-half the variance of the f process. However, it has approximately the same order-of-magnitude significance as the model equation, which results from a similar kind of first-order analysis.

In order to utilize an equivalent of the arithmetic mean of hydraulic conductivity for the stratified, unidirectional flow case, we shall simply perturb hydraulic conductivity itself. That is,

$$K(x_3) = \bar{K} + K'(x_3) \tag{2.13}$$

where $\bar{K}$ is the first moment of the $K(x_3)$ process. It is of interest to note that, while the perturbed quantity in this case can be extremely large -- much larger than the mean -- the size of the perturbation, because of the one-dimensional nature of the problem, will not directly restrict the first-order approximation. If the equations with which we are working are nearly linear, as in this case, then the size of the perturbation becomes less significant; only for those equations which are initially nonlinear, as the three-dimensional flow case presented herein, does the size of the perturbation become important.

A similar perturbation scheme is used for the local bulk dispersion coefficients. Expressing equation (2.6) in tensor form, we obtain

$$E_{ij}(\underset{\sim}{x}) = \left[\bar{E}_{ij} + E'_{ij}(\underset{\sim}{x})\right]\delta_{ij} \quad . \tag{2.14}$$

In this form, the local dispersion coefficients are functions of three types of medium properties: porosity, seepage velocity, and local dispersivities. Equation (2.14) is adopted for the first-order analysis rather than sorting out all the contributing factors to these coefficients, which would only further complicate an already complex analysis. At a later point, it will be necessary to define what $\bar{E}_{ij}$ represents in terms of a local effective dispersivity.

Since the medium is considered to contain random variations in both hydraulic conductivity and porosity, flow of a fluid through the medium will have similar variations. Thus, for the unstratified case, we re-express equation (2.3) as

$$\underset{\sim}{q}(\underset{\sim}{x}) = \bar{\underset{\sim}{q}} + \underset{\sim}{q}'(\underset{\sim}{x}) = (\bar{q}_1 + q_1'(\underset{\sim}{x}))\underset{\sim}{i} + q_2'(\underset{\sim}{x})\underset{\sim}{j} + q_3'(\underset{\sim}{x})\underset{\sim}{k} \quad . \qquad (2.15)$$

As the medium becomes more stratified, the q_2 and q_3 vector components lose significance until, for a completely stratified aquifer, we may express specific discharge as

$$\underset{\sim}{q}(x_3) = (\bar{q}_1 + q_1'(x_3))\underset{\sim}{i} \qquad (2.16)$$

where the x_3 dependence is the result of the total stratification (note that the flow in this case is uniform). A similar conclusion can be reached with regard to hydraulic head: for three-dimensional flow, the perturbed head relationship is

$$\phi(\underset{\sim}{x}) = \bar{\phi}(x_1) + \phi'(\underset{\sim}{x}) \qquad (2.17)$$

while for one-dimensional flow, we obtain

$$\phi(x_1) = \bar{\phi}(x_1) \quad . \tag{2.18}$$

That is, under completely stratified conditions, flow is unidirectional (variations in specific discharge are the result of variations in hydraulic conductivity in the x_3 direction). Conversely without benefit of stratification, three-dimensional variations in flow must be accompanied by equivalent variations in head.

Finally, we must consider a perturbation scheme for concentration of the tracer flux. As noted in the discussion of the prototype, we will consider only the case where the tracer has been injected instantaneously over a large area of the medium, perpendicular to the direction of flow. If observations are made as the tracer passes another point in the medium down gradient from the injection site, it will be found that, from an ensemble viewpoint, the mean or first moment of concentration will be invariant with respect to the x_2 and x_3 directions, varying only with the mean flow direction. For the three-dimensional case, fluctuations in concentration remain three dimensional, resulting in the perturbation expression

$$c(\underset{\sim}{x}, t) = \bar{c}(x_1, t) + c'(\underset{\sim}{x}, t) \tag{2.19}$$

where $\bar{c}(x_1,t)$ represents the ensemble mean. For the stratified case, dependence of the perturbation on the x_1 and x_2 directions are suppressed, resulting in

$$c(x_1, x_3, t) = \bar{c}(x_1, t) + c'(x_3, t) \tag{2.20}$$

where the reasoning behind this form parallels that of equation (2.16). That is, spatial variations in concentration will be associated with spatial variations in specific discharge and hydraulic conductivity. (With regard to the spatial dependence of the perturbation c', expression (2.20) is only approximate, as c' will also be subject to longitudinal spreading at the local level; however, we consider that for large time this dependence is not substantial.) Note that the concentration mean is not statistically homogeneous as it is dependent on the x_1 direction. However, the perturbation in concentration, after an initial start-up time, is considered to be statistically homogeneous. The start-up period is necessary to establish a stationary autocovariance function. That is, at the time of injection perfect correlation exists in the plane perpendicular to flow and none in the x_1 direction. It is necessary, from a spatial or ensemble viewpoint, to allow sufficient travel distance (which can be considered equivalent to the global scale) to take place before the process becomes stationary, with an associated autocovariance function.

Equations (2.8) through (2.19) represent the working variables for the subsequent first-order analysis. Again, we note that the perturbations are considered to be zero-mean, stationary random-field processes, amendable to representation by Fourier-Stieltjes integrals.

Global Longitudinal Dispersive Flux

The primary objective of this report is the definition of longitudinal dispersion in a medium which is randomly heterogeneous at the correlation length scale. The vehicle that we will use to accomplish this objective is a probabilistic dispersive flux in the direction of mean flow. Specifically, we can define the total flux in the x_1 direction as the expectation of the product of the component of specific discharge in this direction and concentration, $\overline{q_1 c}$. However, the mean convective flux in that direction is the product of expectations, $\overline{q_1}\ \overline{c}$. The difference between these two products must represent, then, the global longitudinal dispersive flux at any point in the aquifer. This difference can be easily shown to be

$$\overline{q_1' c'} = \overline{q_1 c} - \overline{q}_1 \overline{c} \quad . \tag{2.21}$$

(This result applies equally to stratified and unstratified aquifers.) Thus, it is the expectation of the product of perturbations in specific discharge and concentration which must be analyzed for in subsequent sections. If this product is subsequently shown to be Fickian in nature, we will expect it to have a form

$$\overline{q_1' c'} = - \overline{q}_1 A_\ell \frac{\partial \overline{c}}{\partial x_1} \tag{2.22}$$

where A_ℓ is the global longitudinal dispersivity. Hence, our final objective will be the definition of A_ℓ in terms of statistics of aquifer parameters.

We must qualify the result of equation (2.21) by noting that it is based on ensemble probabilities; that is, many realizations of the same experiment in probabilistically similar porous media. How, then, does the result apply to a single realization? Here, we must use the rationale of Scheidegger (1954) and state that ergodicity will allow the results of equation (2.22) to be applied to any single realization. However, if our observation point is not distant from the injection site, tracer particles may not sample a sufficient portion of the medium to be representative of all possible paths in order for the concentration autocovariance to become stationary. Thus, implicit in this usage of ergodicity is the concept of the global scale - the distance over which ensemble averages of flow and transport parameters become valid when applied to a single realization.

There also exists a question as to what constitutes the proper sampling interval to obtain representative tracer concentrations from a single realization of the experiment at some distance from the injection site. For example, in a single realization of a stratified aquifer, sampling at a single point would not be representative of the global dispersive process occurring in the aquifer. We leave this question until a later section of this thesis, where it can be answered more appropriately.

First-Order Analysis

We proceed to develop the model equation in its most general form in this section, and then modify it for analysis of both one-dimensional and three-dimensional flow schemes. Specifically, we use the convective-dispersion equation for three-dimensional flow at the local level, which can be written (Appendix 3)

$$\frac{\partial}{\partial t}\left[n(\underset{\sim}{x})\, c(x,t)\right] + \nabla.\left[c(\underset{\sim}{x},t)\, \underset{\sim}{q}(\underset{\sim}{x})\right] + \nabla.\underset{\sim}{N} = 0 \tag{2.23}$$

where $\underset{\sim}{N}$ is the local dispersive flux vector. As the flow regime is steady state with a unidirectional mean in the x_1 direction, we will implement the following moving coordinate scheme (Appendix 4):

$$\xi(x_1,t) = x_1 - t\,\bar{q}_1/\bar{n} \quad , \tag{2.24a}$$

$$\left.\frac{\partial}{\partial t}\right|_{x_1} = \left.\frac{\partial}{\partial t}\right|_{\xi} - \frac{\overline{q}_1}{\overline{n}} \left.\frac{\partial}{\partial \xi}\right|_{t} , \tag{2.24b}$$

and $$\nabla = \nabla_{\xi} = \left(\frac{\partial}{\partial \xi} \underset{\sim}{i} + \frac{\partial}{\partial x_2} \underset{\sim}{j} + \frac{\partial}{\partial x_3} \underset{\sim}{k} \right) . \tag{2.24c}$$

In addition we note that the steady flow assumption implies (all density contrasts have been neglected)

$$\nabla . \underset{\sim}{q} = 0 . \tag{2.25}$$

Then writing the convective-dispersion equation (2.23) in terms of moving coordinates, and making use of equation (2.25), perturbation expressions are substituted for porosity (equation (2.8)), specific discharge (equation (2.15)), and concentration (equation (2.19)) to obtain

$$\frac{\partial}{\partial t}\left[(\overline{c}+c')(\overline{n}+n')\right] - \frac{\overline{q}_1}{\overline{n}} \frac{\partial}{\partial \xi}\left[(\overline{c}+c')(\overline{n}+n')\right]$$

$$+ (\underset{\sim}{\overline{q}} + \underset{\sim}{q'}) . \nabla_{\xi} (\overline{c} + c') + \nabla . \underset{\sim}{N} = 0 . \tag{2.26}$$

Since, by analogy with Taylor's (1953) work, we desire an equation for the amount of flux transferred across a moving plane, and as the component of flux is a random quantity, we find the expected value of equation (2.26) and then subtract this mean equation from equation (2.26). The mean equation is

$$\frac{\partial}{\partial t}\left[\overline{c}\,\overline{n} + \overline{c'n'}\right] - \frac{\overline{q}_1}{\overline{n}} \frac{\partial}{\partial \xi}\left[\overline{c'n'}\right] + \overline{\underset{\sim}{q'} . \nabla_{\xi} c'} + \overline{\nabla . \underset{\sim}{N}} = 0 . \tag{2.27}$$

Although we may have suspected that the mean equation would contain only mean quantities, it must be remembered that both the mean and the perturbation are governed by the same physical process. Hence, it is not surprising to find covariances of perturbations of different parameters occurring in this expression. Subtracting equation (2.27) from equation (2.26), we obtain

$$\frac{\partial}{\partial t}\left[\bar{c}\,n' + c'\bar{n}\right] - \frac{\bar{q}_1}{\bar{n}}\frac{\partial}{\partial \xi}\left[\bar{c}\,n' + c'\bar{n}\right] + \bar{\underset{\sim}{q}}\cdot\nabla_\xi c'$$

$$+ \underset{\sim}{q}'\cdot\nabla_\xi \bar{c} + \nabla\cdot\underset{\sim}{N} - \overline{\nabla\cdot\underset{\sim}{N}} \approx 0 \qquad (2.28)$$

where the second-order terms

$$\frac{\partial}{\partial t}\left[c'n' - \overline{c'n'}\right] \quad , \qquad (2.29a)$$

$$\frac{\partial}{\partial \xi}\left[c'n' - \overline{c'n'}\right] \quad , \qquad (2.29b)$$

and $\underset{\sim}{q}'\cdot\nabla_\xi c' - \overline{\underset{\sim}{q}'\cdot\nabla_\xi c'}$ (2.29c)

have been neglected. It is unfortunate that we must neglect these terms but, as mentioned in earlier sections, the solution method used to solve the model equation does not permit their retention. In particular, term (2.29c) models convective transport due to randomness in the medium which, in the sense of Taylor's analysis, probably permits more rapid lateral mixing of the tracer. This lateral mixing is responsible for the attainment of equilibrium between longitudinal and lateral mass transfer, which allows us to neglect the time dependence in the mean-removed equation (2.28). The result of neglecting this term will be discussed in a later section of this report, although we may mention now that the magnitude of the term is dependent on the degree of randomness of the medium.

Following Taylor (1953), then, we neglect the time derivative, assuming that

$$\frac{\partial}{\partial t}\left(\bar{c}\, n' + c'\bar{n}\right) \approx 0 \ . \tag{2.30}$$

Since expected values of medium properties and fluid parameters are independent of position (otherwise statistical homogeneity would not apply) and time, we note that

$$\frac{\partial \bar{n}}{\partial \xi} = 0 \ . \tag{2.31}$$

With regard to concentration, the taking of derivatives is not so simple, since the mean of tracer concentration is dependent upon the x_1 direction (see discussion associated with equation (2.19)). Thus, the gradient of the mean of tracer concentration is

$$\nabla_{\xi}\bar{c} = \frac{\partial \bar{c}}{\partial \xi}\,\underset{\sim}{i} \ . \tag{2.32}$$

Using simplifications (2.30), (2.31), and (2.32), we rewrite the mean-removed equation (2.28) as

$$q_1'\frac{\partial \bar{c}}{\partial \xi} - \frac{\bar{q}_1}{\bar{n}}\frac{\partial}{\partial \xi}\left[\bar{c}\, n'\right] = -\left[\nabla . \underset{\sim}{N} - \overline{\nabla . \underset{\sim}{N}}\right] \ . \tag{2.33}$$

This result constitutes the most general form of the model equation for subsequent analysis. The first term on the left-hand side represents the influence of variations in hydraulic conductivity (via the specific discharge perturbation), while the second represents the influence of porosity variations. If we neglect the porosity term, then the equation takes on a form much like Taylor's, where random convection across a moving plane is balanced by lateral mixing.

A similar analysis for the stratified or one-dimensional flow case will give precisely the same expression as equation (2.33), the only difference being in the second-order terms neglected. Since perturbations in porosity and concentration are dependent only on the x_3 direction, and the specific discharge vector contains only a q_1 component (see equation (2.16)), only term (2.29a) would be of significance to us. This term, however, would be negligible for a slowly varying process, so that, with regard to the stratified case, equation (2.33) is linear in perturbed quantities without the need to neglect any terms. It remains, then only for us to analyze the local dispersive flux term on the right-hand side of equation (2.33) before the final form of the model equation can be obtained.

<u>Local Dispersive Flux</u>

If a Fickian model can be assumed at the local level -- and this model does appear to be generally acceptable (see Fried, 1975) -- then we may write the local dispersive flux as

$$-\nabla \cdot \underset{\sim}{N} = \frac{\partial}{\partial x_i} E_{ij} \frac{\partial c}{\partial x_j} \qquad (2.34)$$

where E_{ij} is the local bulk dispersion coefficient. Proceeding as before, we introduce perturbation expressions (2.14) and (2.19) into equation (2.34), obtaining

$$-\nabla \cdot \underset{\sim}{N} = \frac{\partial}{\partial x_i}\left[\left(\bar{E}_{ij} + E'_{ij}\right)\frac{\partial}{\partial x_j}\left(\bar{c} + c'\right)\right] \tag{2.35}$$

and then take expected values;

$$-\overline{\nabla \cdot \underset{\sim}{N}} = \frac{\partial}{\partial x_1}\bar{E}_{11}\frac{\partial \bar{c}}{\partial x_1} + \frac{\partial}{\partial x_i}\left[\overline{E'_{ij}\frac{\partial c'}{\partial x_j}}\right] \quad . \tag{2.36}$$

Subtracting equation (2.36) from equation (2.35), we obtain

$$-\left[\nabla \cdot \underset{\sim}{N} - \overline{\nabla \cdot \underset{\sim}{N}}\right] \approx E'_{11}\frac{\partial^2 \bar{c}}{\partial x_1^2} + \frac{\partial E'_{11}}{\partial x_1}\frac{\partial \bar{c}}{\partial x_{11}} + \bar{E}_{ij}\frac{\partial^2 c}{\partial x_i \partial x_j} \quad . \tag{2.37}$$

where the term

$$\frac{\partial}{\partial x_i}\left[E'_{ij}\frac{\partial c'}{\partial x_j} - \overline{E'_{ij}\frac{\partial c'}{\partial x_j}}\right] \tag{2.38}$$

has been neglected. Neglecting this term is rather like neglecting term (2.29b), but is not considered to be as important as term (2.29c), since convective transport is generally considered more significant than dispersive transport.

The first term on the right-hand side of equation (2.37) is taken to be zero for a slowly varying process. That is, for large time, we may consider

$$\frac{\partial \bar{c}}{\partial x_1} \approx \text{constant} \tag{2.39}$$

because the mean tracer concentration changes slowly in the x_1 direction. This result is implicit in the process of neglecting the time derivative in equation (2.33), for we are assuming that convective transport in the mean flow direction -- and therefore $\partial\bar{c}/\partial\xi$ -- is constant. Whence, we can rewrite equation (2.37) as

$$-\left[\nabla.\underset{\sim}{N} - \overline{\nabla.\underset{\sim}{N}}\right] = \frac{\partial E_\ell'}{\partial x_1}\frac{\partial \bar{c}}{\partial x_1} + \bar{E}_\ell \frac{\partial^2 c'}{\partial x_1^2} + \bar{E}_t\left[\frac{\partial^2 c'}{\partial x_2^2} + \frac{\partial^2 c'}{\partial x_3^2}\right] \tag{2.40}$$

where E_ℓ equals E_{11}, and E_t equals E_{22} and E_{33}. The unstratified model equation, describing the random transfer of mass at any point in the aquifer, can then be written

$$q_1' \frac{\partial \bar{c}}{\partial \xi} - \frac{\bar{q}_1}{\bar{n}}\frac{\partial}{\partial \xi}\left[\bar{c}\, n'\right]$$
$$= \frac{\partial E_\ell'}{\partial x_1}\frac{\partial \bar{c}}{\partial x_1} + \bar{E}_\ell \frac{\partial^2 c'}{\partial x_1^2} + \bar{E}_t\left[\frac{\partial^2 c'}{\partial x_2^2} + \frac{\partial^2 c'}{\partial x_3^2}\right] \quad . \tag{2.41}$$

With regard to the stratified case, a term similar to equation (2.38), but containing only an x_3 dependence, must also be neglected. Hence, some approximation is introduced into the mean-removed, local dispersive flux equation for this case. Since the concentration perturbation is only dependent on the x_3 direction (see equation (2.20)), derivatives with other than this variable are zero for the stratified equivalent of equation (2.40). This equivalent can be written simply as

$$-\left[\nabla.\underset{\sim}{N} - \overline{\nabla.\underset{\sim}{N}}\right] = \bar{E}_t \frac{\partial^2 c'}{\partial x_3^2} \tag{2.42}$$

where, because of stratification, the derivative of E_ℓ' with respect to x_1 has also been dropped. The model equation for the stratified case can therefore be written

$$\left[q_1' - n' \frac{\bar{q}_1}{\bar{n}}\right] \frac{\partial \bar{c}}{\partial \xi} = \bar{E}_t \frac{\partial^2 c'}{\partial x_3^2} \quad . \tag{2.43}$$

Equations (2.41) and (2.43) represent the final form for the model equations to be used in the subsequent analysis. In the next chapter we proceed to use properties of stationary random-field processes to evaluate these equations.

SOLUTION OF MODEL EQUATION

Development of Global Dispersive Flux Equation

We proceed in this section to analyze the model equation and to find an interim form for the global dispersive flux equation. This will be accomplished by means of the representation theorem (Appendix 1), of which we shall assume that the reader has a working knowledge. Recalling first the three-dimensional model equation (2.41),

$$q_1' \frac{\partial \bar{c}}{\partial \xi} - \frac{\bar{q}_1}{\bar{n}} \frac{\partial}{\partial \xi}\left[\bar{c}\, n'\right]$$

$$= \frac{\partial E_\ell'}{\partial x_1} \frac{\partial \bar{c}}{\partial x_1} + \bar{E}_\ell \frac{\partial^2 c'}{\partial x_1} + \bar{E}_t \left[\frac{\partial^2 c'}{\partial x_2^2} + \frac{\partial^2 c'}{\partial x_3^2}\right] \quad ,$$

we proceed to replace random quantities by Fourier-Stieltjes integrals. In this case, we will consider that the Fourier-Stieltjes integrals possess a slightly different form than that indicated in Appendix 1. In particular, using c' as an example, we let

$$c'(\xi, x_2, x_3) = \iiint_{-\infty}^{\infty} e^{i(k_1\xi + k_2 x_2 + k_3 x_3)}\, dZ_c(\underset{\sim}{k}) \quad .$$

Similar Fourier-Stieltjes integrals can be written for other random quantities with a three-dimensional spatial dependence. By replacing the x_1 dependence with the moving coordinate ξ, we maintain the probabilistic description of the random variable in the general region of the tracer front. In context of the discussion in the section entitled "Perturbed Quantities" this transfer of dependence is necessary in order for the perturbation in concentration to establish, for the unstratified case, a stationary field. Then dropping all pretenses of integration, equation (2.41) can be written with primed quantities appropriately replaced by complex Fourier amplitudes:

$$\left[dZ_{q_1}(\underset{\sim}{k}) - \frac{\bar{q}_1}{\bar{n}}\, dZ_n(\underset{\sim}{k})\right]\frac{\partial \bar{c}}{\partial \xi} = i k_1 \frac{\bar{q}_1}{\bar{n}}\, \bar{c}\, dZ_n(\underset{\sim}{k})$$

$$+ i k_1 dZ_{E_\ell}(\underset{\sim}{k})\frac{\partial \bar{c}}{\partial x_1} - \left[\bar{E}_\ell k_1^2 + \bar{E}_t(k_2^2 + k_3^2)\right] dZ_c(\underset{\sim}{k}) \quad ,$$

$$\underset{\sim}{k} = (k_1, k_2, k_3) \quad . \tag{3.1}$$

Taking the complex conjugate of equation (3.1) and multiplying by dZ_{q_1}, one obtains

$$\left[dZ_{q_1} dZ^*_{q_1} - \frac{\bar{q}_1}{\bar{n}}\, dZ_{q_1} dZ^*_n\right]\frac{\partial \bar{c}}{\partial \xi} = i k_1\left[\frac{\bar{q}_1}{\bar{n}}\, \bar{c}\, dZ_{q_1} dZ^*_n\right.$$

$$\left. + \frac{\partial \bar{c}}{\partial x_1} dZ_{q_1} dZ^*_{E_\ell}\right] - \left[\bar{E}_\ell k_1^2 + \bar{E}_t(k_2^2 + k_3^2)\right] dZ_{q_1} dZ^*_c \quad . \tag{3.2}$$

We proceed to take expected values and apply the representation theorem to obtain

$$\Phi_{q_1 c}(\underset{\sim}{k}) = \frac{-1}{\left[\bar{E}_\ell k_1^2 + \bar{E}_t(k_2^2+k_3^2)\right]}\left\{\frac{\partial \bar{c}}{\partial \xi}\left[\Phi_{q_1 q_1}(\underset{\sim}{k}) - \frac{\bar{q}_1}{\bar{n}}\,\Phi_{q_1 n}(\underset{\sim}{k})\right]\right.$$

$$\left. + i k_1\left[\frac{\bar{q}_1}{\bar{n}}\, \bar{c}\, \Phi_{q_1 n}(\underset{\sim}{k}) + \frac{\partial \bar{c}}{\partial x_1}\Phi_{q_1 E_\ell}(\underset{\sim}{k})\right]\right\} \quad . \tag{3.3}$$

At this point, we note that the inverse Fourier transform of the cross spectrum $\Phi_{q_1 c}$ evaluated at zero lag will give us the covariance of the q_1' and c' processes $(\overline{q_1' c'})$. This is precisely the quantity we need in order to evaluate the global dispersive flux (2.21) and find the global longitudinal dispersivity A_ℓ. However, before we can proceed with this operation, it is necessary to develop a set of equations, known as transfer functions, which will allow us to relate spectra and cross spectra of flow parameters to spectra of medium properties. This shall be done in the subsequent section.

The adequacy of representation of processes in moving coordinates (as opposed to stationary coordinates) within the Fourier-Stieltjes integrals may be subject to dispute. Although this investigator has assumed that, for reasons cited previously, this representation is proper, other investigators might prefer the stationary coordinate representation. However, use of stationary coordinates will, if properly considered, cause the inclusion of a time-derivative term in the three-dimensional spectral form of the model equation, and place the use of a Taylor (1953) model for the three-dimensional flow case in doubt. It appears, at the present time, that use of a stationary coordinate representation would cause the three-dimensional analysis presented herein to be restricted to the cases where the aquifer is highly stratified.

Before leaving this section, we briefly develop a similar result for the one-dimensional flow case. In particular, recalling equation (2.43),

$$\left[q_1' - n' \frac{\bar{q}_1}{\bar{n}}\right] \frac{\partial \bar{c}}{\partial \xi} = \bar{E}_T \frac{\partial^2 c'}{\partial x_3^2} \quad ,$$

we can, as a consequence of the development in the previous paragraph, immediately write a spectral form for the global dispersive flux equation:

$$\Phi_{q_1 c}(k_3) = \frac{-1}{\bar{E}_t k_3^2}\left[\Phi_{q_1 q_1}(k_3) - \frac{\bar{q}_1}{\bar{n}} \Phi_{q_1 n}(k_3)\right] \frac{\partial \bar{c}}{\partial \xi} \quad . \tag{3.4}$$

This equation must also be rewritten in terms of spectra of media properties. (Since the spatial dependence of the one-dimensional case is entirely in the x_3 direction, the Taylor (1953) model should be applicable without qualification.) However, note that the right-hand side is presently a function of the mean concentration gradient; thus, the appearance of a Fickian process is already present in the equation. This subject will be dealt with in more detail in subsequent analyses of the one-dimensional and three-dimensional cases.

Transfer Functions

As mentioned in the introductory chapter, it is generally believed that global dispersion is the result of variations in hydraulic conductivity. Hence, we will strive to relate all spectra and cross spectra of flow parameters to the spectrum of hydraulic conductivity. This will necessitate, in the case of some cross spectra, the use of certain empirical relationships which may be questionable; however, because of the strong dependence on hydraulic conductivity, this is considered to be a preferable approach than attempting to develop and justify forms for all the spectra in equations (3.3) and (3.4) individually.

For the three-dimensional flow case, a transfer function relating the specific discharge spectrum $\Phi_{q_1 q_1}$ to the hydraulic conductivity spectrum Φ_{ff} ($f = \ln K$) can be developed from the local flow equation for steady state, saturated flow of an incompressible fluid through a rigid, isotropic porous medium:

$$\nabla . K \nabla \phi = 0 \quad . \tag{3.5}$$

Because of the steady state flow conditions, equation (3.5) can be rewritten

$$\nabla \phi . \nabla f + \nabla^2 \phi = 0 \quad , \quad f = \ln K \quad . \tag{3.6}$$

Additionally, we will need the Darcy relationship for unidirectional flow

$$q_1 = -K \frac{\partial \phi}{\partial x_1} \tag{3.7}$$

in order to relate head ϕ to specific discharge q_1. We proceed as earlier, finding mean-removed equations for both equations (3.6) and (3.7). In particular, by substituting perturbation expressions (2.10) and (2.17) into equation (3.6), we obtain

$$\frac{\partial}{\partial x_i}\left(\bar{\phi} + \phi'\right) \frac{\partial}{\partial x_i}\left(\bar{f} + f'\right) + \frac{\partial^2}{\partial x_i \partial x_i}\left(\bar{\phi} + \phi'\right) = 0 \quad . \tag{3.8}$$

where tensor notation has been used for simplicity. Since we are working with a statistically homogeneous medium with a mean flux oriented in the x_1 direction, we note that

$$\frac{\partial \bar{f}}{\partial x_i} = 0 \quad , \quad i = 1, 2, 3 \tag{3.9}$$

and $$\frac{\partial \bar{\phi}}{\partial x_1} = -J \quad , \quad \frac{\partial \bar{\phi}}{\partial x_2} = 0 \quad , \quad \frac{\partial \bar{\phi}}{\partial x_3} = 0 \quad . \tag{3.10}$$

Hence, upon expanding equation (3.8), we obtain

$$\frac{\partial^2 \bar{\phi}}{\partial x_i \partial x_i} + \frac{\partial^2 \phi'}{\partial x_i \partial x_i} = J \frac{\partial f'}{\partial x_1} - \frac{\partial \phi'}{\partial x_i} \frac{\partial f'}{\partial x_i} \quad . \tag{3.11}$$

The mean equation for equation (3.11) is

$$\frac{\partial^2 \bar{\phi}}{\partial x_i \partial x_i} = - \overline{\frac{\partial \phi'}{\partial x_i} \frac{\partial f'}{\partial x_i}} \quad . \tag{3.12}$$

Subtracting, we obtain the mean-removed equation

$$\frac{\partial^2 \phi'(\underset{\sim}{x})}{\partial x_i \partial x_i} \approx J \frac{\partial f'(\underset{\sim}{x})}{\partial x_1} \tag{3.13}$$

where we have neglected terms

$$\frac{\partial \phi'}{\partial x_i} \frac{\partial f'}{\partial x_i} - \overline{\frac{\partial \phi'}{\partial x_i} \frac{\partial f'}{\partial x_i}} \quad . \tag{3.14}$$

Neglecting these terms may affect our ability to approximate the specific discharge spectrum with a transfer function containing the hydraulic conductivity spectrum. In turn, as we must assume some form for the hydraulic conductivity spectrum (see section entitled "Three-Dimensional Flow Analysis") we may choose an inappropriate form due to an extreme influence of this approximation. These effects are difficult to assess and we will generally pass over them, except to say that they probably grow in importance as the degree of variability in the medium increases.

Passing to the Darcy relationship, we can similarly express it in perturbed form by making use of expressions (2.12), (2.15), and (2.17), giving us the result

$$\bar{q}_1 + q_1' = - K_\ell (1 + f') \frac{\partial}{\partial x_1} (\bar{\phi} + \phi') \quad . \tag{3.15}$$

With an approximation similar to (3.14), we arrive at the mean-removed equation

$$q_1'(\underset{\sim}{x}) \approx K_\ell \left[J f'(\underset{\sim}{x}) - \frac{\partial \phi'(\underset{\sim}{x})}{\partial x_1} \right] \quad . \tag{3.16}$$

Writing this equation in complex Fourier amplitudes, we obtain

$$dZ_{q_1}(\underset{\sim}{k}) = \bar{q}_1 dZ_f(\underset{\sim}{k}) - ik_1 K_\ell dZ_\phi(\underset{\sim}{k}) \tag{3.17}$$

and similarly expressing the mean-removed flow equation (3.13) in this form, we have

$$dZ_\phi(\underset{\sim}{k}) \left[\underset{\sim}{k} \cdot \underset{\sim}{k} \right] = -ik_1 J dZ_f(\underset{\sim}{k}) \quad . \tag{3.18}$$

Substituting equation (3.18) into equation (3.17), we find

$$dZ_{q_1}(\underset{\sim}{k}) = \bar{q}_1 \left[1 - \frac{k_1^2}{\underset{\sim}{k} \cdot \underset{\sim}{k}} \right] dZ_f(\underset{\sim}{k}) \quad . \tag{3.19}$$

Multiplying both sides of equation (3.19) by their complex conjugate and taking expected values, the representation theorem gives us

$$\Phi_{q_1 q_1}(\underset{\sim}{k}) = \bar{q}_1^2 \left[\frac{k_2^2 + k_3^2}{k_1^2 + k_2^2 + k_3^2} \right]^2 \Phi_{ff}(\underset{\sim}{k}) \quad . \tag{3.20}$$

This equation represents, for the three-dimensional flow case, the appropriate transfer function for the specific discharge spectrum. It remains for us only to find an appropriate form for the hydraulic conductivity spectrum.

The one-dimensional flow case is considerably simplified by the occurrence of medium variations only in the x_3 direction. To write the transfer function for this case, we need only consider the Darcy relationship (3.7) and perturbation expressions (2.13), (2.16), and (2.18), from which we obtain the expression

$$\bar{q}_1 + q_1' = -(\bar{K} + K')\frac{\partial \bar{\phi}}{\partial x_1} \quad . \tag{3.21}$$

It is easily seen that the mean-removed equation for this case is

$$q_1'(x_3) = -K'(x_3)\frac{\partial \bar{\phi}}{\partial x_1} = J\,K'(x_3) \tag{3.22}$$

which follows immediately from equation (3.21) without approximation. In terms of complex Fourier amplitudes, equation (3.22) can be written

$$dZ_{q_1}(k_3) = J\,dZ_K(k_3) \tag{3.23}$$

from which it follows that the appropriate transfer function for the one-dimensional case is

$$\Phi_{q_1q_1}(k_3) = J^2\,\Phi_{KK}(k_3) \quad . \tag{3.24}$$

Again, the innate linearity of the one-dimensional case is to be noted, which greatly simplifies the problem.

In order to develop transfer functions for the cross spectrum of specific discharge and porosity Φ_{q_1n}, we will need to use an empirical relationship. As an initial possibility, we suggest that the logarithmic relationship

$$n(\underset{\sim}{x}) = Mf(\underset{\sim}{x}) + I \quad , \quad f(\underset{\sim}{x}) = \ln K(\underset{\sim}{x}) \tag{3.25}$$

where M and I are the appropriate regression coefficients, may be acceptable for the three-dimensional flow case. The validity of this relationship has been investigated by Archie (1950) and more recently by Bredehoeft (1964). The mean-removed equivalent of equation (3.25) is

$$n'(\underset{\sim}{x}) = Mf'(\underset{\sim}{x}) \quad . \tag{3.26}$$

However, this is not the only possible relationship we can use.

Another possibility for the three-dimensional flow case is the Kozeny-Carmen equation, which may be written (Bear, 1972, p. 166)

$$K(\underset{\sim}{x}) = Cn(\underset{\sim}{x})^3 \big/ \left[1 - n(\underset{\sim}{x})\right]^2 \quad . \tag{3.27}$$

Taking logarithms of both sides of equation (3.27), we obtain

$$f = \ln C + 3\ln n - 2\ln(1-n) \quad . \tag{3.28}$$

The terms ln n and ln(1 - n) are expanded in Taylor's series about $\bar{n}$, at which point equation (3.28) can be written

$$\begin{aligned} \bar{f} + f' = \ln C &+ 3\left[\ln \bar{n} + \frac{n'}{\bar{n}} - \frac{1}{2}\left(\frac{n'}{\bar{n}}\right)^2 + \quad . \quad . \quad . \right] \\ &- 2\left[\ln(1-\bar{n}) - \frac{n'}{1-\bar{n}} + \frac{1}{2}\left(\frac{n'}{1-\bar{n}}\right)^2 - \quad . \quad . \quad . \right] \quad . \end{aligned} \tag{3.29}$$

By neglecting products of primed quantities we obtain the approximation from which the mean-removed equation

$$n'(\underset{\sim}{x}) \approx \frac{\bar{n}(1-\bar{n})}{3-\bar{n}} f'(\underset{\sim}{x}) \tag{3.30}$$

is derived. Note that the approximation producing the linearization is considered acceptable, as variations in porosity are generally small. Both equations (3.26) and (3.30) are simple linear forms which can be represented as

$$n'(\underset{\sim}{x}) = Pf'(\underset{\sim}{x}) \tag{3.31}$$

where P is either constant relating perturbations of the n' and f' processes. Proceeding to write equation (3.31) in complex Fourier amplitudes, one obtains

$$dZ_n(\underset{\sim}{k}) = P\,dZ_f(\underset{\sim}{k}) \quad . \tag{3.32}$$

By properly combining the complex conjugate of equation (3.32) with equation (3.19), we obtain, after taking expected values and applying the representation theorem,

$$\Phi_{q_1 n}(\underset{\sim}{k}) = P\bar{q}_1\left[\frac{k_2^2 + k_3^2}{k_1^2 + k_2^2 + k_3^2}\right]\Phi_{ff}(\underset{\sim}{k}) \quad . \tag{3.33}$$

Equation (3.33), then, gives us an appropriate form of $\Phi_{q_1 n}$ for the three-dimensional flow case.

For the one-dimensional flow case, we will again resort to an empirical relationship from which a first-order approximation must be derived. Equation (3.25) could be used for this approximation; however, it would entail expanding lnK into a Taylor's series about $\bar{K}$. This procedure generally does not produce favorable results (Bakr, 1976). Instead we will rely on the Kozeny-Carmen equation (3.27), considering only an x_3 spatial dependence. Expanding the right-hand side of this equation in a Taylor's series about $\bar{n}$, one obtains

$$\bar{K} + K' = C\bar{n}^3\left[\frac{1}{(1-\bar{n})^2} + \frac{(3-\bar{n})}{(1-\bar{n})^3}\frac{n'}{\bar{n}} + \frac{3}{(1-\bar{n})^4}\frac{n'^2}{\bar{n}^2} + \frac{1+3\bar{n}}{(1-\bar{n})^5}\frac{n'^3}{\bar{n}^3} + \cdots\right] \tag{3.34}$$

By neglecting products of primed quantities, a first order approximation is obtained, the mean-removed equation of which is

$$n'(x_3) \approx \frac{(1-\bar{n})^3}{(3-\bar{n})C\bar{n}^2} K(x_3) \tag{3.35}$$

This approximation is adequate provided that variations in porosity are not extreme -- the case with most moderately well-sorted sediments. Equation (3.35) can be further modified by first taking the expected value of equation (3.34) and substituting the result into equation (3.35). This expected value can be expressed as

$$C\bar{n}^2 = \frac{\bar{K}}{\bar{n}}\left[\frac{1}{(1-\bar{n})^2} + \frac{3}{(1-\bar{n})^4}\frac{\sigma_n^2}{\bar{n}^2}\right]^{-1} \tag{3.36}$$

where σ_n^2 is the variance of the n' process. Odd moments greater than one have been neglected because porosity is commonly normally distributed

(Law, 1944), or at least approaches a Gaussian distribution. Additionally, powers of the variance, which should appear in higher order terms, become insignificant. Thus, substituting equation (3.36) into equation (3.35), one obtains

$$n'(x_3) = \frac{\bar{n}}{\bar{K}} \eta(\bar{n}, \sigma_n) K'(x_3)$$

where (3.37)

$$\eta(\bar{n}, \sigma_n) = \frac{1}{(3-\bar{n})}\left[1 - \bar{n} + \frac{3}{(1-\bar{n})} \frac{\sigma_n^2}{\bar{n}^2}\right]$$

which, when expressed in complex Fourier amplitudes is

$$dZ_n(k_3) = \eta(\bar{n}, \sigma_n) \frac{\bar{n}}{\bar{K}} dZ_K(k_3) \quad . \tag{3.38}$$

By properly combining the complex conjugate of this expression with equation (3.23), the transfer function

$$\Phi_{q_1 n}(k_3) = J \eta(\bar{n}, \sigma_n) \frac{\bar{n}}{\bar{K}} \Phi_{KK}(k_3) \tag{3.39}$$

is obtained. Equation (3.39) constitutes the form of $\Phi_{q_1 n}$ which shall be used in the subsequent analysis of the one-dimensional flow case.

In reference to equation (3.3), there remains to be constructed a transfer function for the cross spectrum of specific discharge and bulk longitudinal dispersivity $\Phi_{q_1 E_\ell}$ for the three-dimensional flow case. Recalling equations (2.6a), the bulk longitudinal dispersion coefficient is written

$$E_\ell(\underset{\sim}{x}) = \alpha_I(\underset{\sim}{x})\, q_1(\underset{\sim}{x}) \quad . \tag{3.40}$$

From equation (2.14), the perturbation of the coefficient can be expressed as

$$E_\ell'(\underset{\sim}{x}) = E_\ell(\underset{\sim}{x}) - \overline{E}_\ell \quad . \tag{3.41}$$

By appropriately substituting equation (3.40) into equation (3.41), we obtain

$$E_\ell' \approx \overline{\alpha}_I\, q_1' + \alpha_I'\, \overline{q}_1 \tag{3.42}$$

where the term $[\alpha_I' q_1' - \overline{\alpha_I' q_1'}]$ has been neglected. Since the local longitudinal dispersivity can vary significantly (Klotz, 1973), it is difficult to assess the effect of neglecting this term, but it cannot be worse than that of neglecting earlier terms (2.29). Replacing the primed quantities in equation (3.42) by their complex Fourier amplitudes, that is

$$dZ_{E_\ell}(\underset{\sim}{k}) = \overline{\alpha}_I\, dZ_{q_1}(\underset{\sim}{k}) + \overline{q}_1\, dZ_{\alpha_I}(\underset{\sim}{k}) \quad , \tag{3.43}$$

and then taking the complex conjugate of this expression and multiplying by dZq_1, we obtain, upon taking expected values,

$$\Phi_{q_1 E_\ell}(\underset{\sim}{k}) = \overline{\alpha}_I\, \Phi_{q_1 q_1}(\underset{\sim}{k}) + \overline{q}_1\, \Phi_{q_1 \alpha_I}(\underset{\sim}{k}) \quad . \tag{3.44}$$

The spectrum $\Phi_{q_1 q_1}$ can be replaced by transfer function (3.20), but another transfer function must be developed for $\Phi_{q_1 \alpha_I}$. This may be accomplished through the empirical relationship (Harleman et al., 1963)

$$\alpha_I(\underset{\sim}{x}) = B\left[K(\underset{\sim}{x})\right]^{1/2} \tag{3.45}$$

where B is an appropriate constant. Substituting perturbation expression (2.12) and assuming an expression similar to (2.8) for α_I, we obtain

$$\bar{\alpha}_I + \alpha_I' = B(K_\ell)^{1/2} \exp\left[f'/2\right] \quad . \tag{3.46}$$

Expanding the exponential term in equation (3.46) into a Maclaurin series and truncating, the first-order linear approximation

$$\bar{\alpha}_I + \alpha_I' \approx B(K_\ell)^{1/2}(1 + f'/2) \tag{3.47}$$

is obtained. The mean-removed equivalent of this equation is

$$\alpha_I'(\underset{\sim}{x}) = \frac{B}{2}(K_\ell)^{1/2} f'(\underset{\sim}{x}) \quad . \tag{3.48}$$

Replacing the primed quantities with their complex Fourier amplitudes, equation (3.48) becomes

$$dZ_{\alpha_I}(\underset{\sim}{k}) = \frac{B}{2}(K_\ell)^{1/2} dZ_f(\underset{\sim}{k}) \quad . \tag{3.49}$$

Taking the complex conjugate of this expression and multiplying both sides, appropriately, by equation (3.19), one obtains

$$\Phi_{q_1\alpha_I}(\underset{\sim}{k}) = \frac{B}{2}(K_\ell)^{1/2}\bar{q}_1\left[\frac{k_2^2 + k_3^2}{k_1^2 + k_2^2 + k_3^2}\right]\Phi_{ff}(\underset{\sim}{k}) \tag{3.50}$$

upon taking expected values. It should be noted that, upon substitution of equations (3.50) and (3.20) into equation (3.44), the cross spectrum $\Phi_{q_1E_\ell}$ is entirely real and even valued, provided Φ_{ff} is even valued.

In the following two sections the global dispersive flux equation is solved utilizing these transfer functions for both the one-dimensional and three-dimensional cases.

<u>One-Dimensional Flow Case</u>

We now proceed with the solution of the longitudinal dispersive flux equation for the one-dimensional flow case. We note that this case applies only to completely stratified aquifers with uniform flow in the x_1 direction. Stratification, in this case, implies that medium properties are randomly distributed in the x_3 direction. Analysis to this point allows us to conclude that equation (3.4) is a close approximation of a spectral representation for the global dispersive flux equation for this case.

Allowing k to equal k_3, we rewrite equation (3.4) in terms of transfer functions (3.24) and (3.39):

$$\Phi_{q_1c}(k) = \frac{-J^2}{\bar{E}_t k^2}\left[1 - \eta(\bar{n}, \sigma_n)\right]\frac{\partial\bar{c}}{\partial\xi}\Phi_{KK}(k) \quad . \tag{3.51}$$

Taking the inverse Fourier transform evaluated at zero lag, the covariance of the $q_1{}'$ process and the c' process is obtained (Appendix 1):

$$\overline{q_1'c'} = -\frac{\partial \bar{c}}{\partial \xi}\frac{J^2}{\overline{E}_t}\left[1-\eta(\bar{n},\sigma_n)\right]\int_{-\infty}^{\infty}\frac{\Phi_{KK}(k)}{k^2}\,dk \quad . \tag{3.52}$$

This result clearly defines a Fickian process; thus, for the one-dimensional flow case, we have answered one of the questions put forth in the introduction. If we proceed to define some local effective transverse dispersivity α_t such that

$$\overline{E}_t = \alpha_t \overline{q}_1 \tag{3.53}$$

then we may rewrite equation (3.52) in terms of the global dispersivity (2.22) as

$$A_\ell = \frac{1}{\alpha_t \overline{K}^2}\left[1-\eta(\bar{n},\sigma_n)\right]\int_{-\infty}^{\infty}\frac{\Phi_{KK}(k)}{k^2}\,dk \tag{3.54}$$

where $\eta(\bar{n},\sigma_n)$ is defined in equation (3.37).

We will attempt to define α_t with more thoroughness in a subsequent section. Note that utilization of an effective local transverse dispersivity -- which is rather like the effective hydraulic conductivity in that it represents a particular average -- enables us to represent the global dispersion coefficient as a linear function of the mean specific discharge. Thus, to at least a first-order approximation, dispersion at the global scale appears to have many of the properties of dispersion at the local scale.

We add a note at this point concerning the validity of equation (3.54). If the square of the coefficient of variation $\sigma_n/\bar{n}$ is greater than approximately 0.6 then this expression borders on becoming negative and therefore invalid. However, if this is the case, then the approximation leading to equation (3.35) is also invalid. In face, it would be difficult to make this approximation if $\sigma_n/\bar{n}$ were much greater than 0.25. Thus, there is no possibility of obtaining a negative global dispersivity if this approximation is adhered to. It should also be noted that the effect of porosity variations on global dispersion are essentially already encompassed in equation (3.54), in that, if porosity perturbations had not been included in the model equation, then the term in brackets would simply equal one. As it is, A_ℓ has been reduced by approximately one-third through the inclusion of these effects.

In the remainder of this section, we shall be primarily concerned with selecting an appropriate form for the hydraulic conductivity spectrum Φ_{KK}. Note that, as perceived in equation (3.54), this spectrum in addition to accounting for medium properties, must also remove the singularity occurring at the origin in the integrand. In choosing a spectrum, it is frequently advisable to look at the form of its associated autocovariance (or autocorrelation) function. For example, it is generally desirable to select an autocovariance function which decreases in correlation with increasing lag distance, much as one would expect in natural sediments. However, any spectrum which is absolutely integrable and piecewise continuous will, as a consequence of the Riemann-Lebesque theorem (Titchmarsh, 1948, p. 11), have an autocovariance function with this property. Thus, we must concern ourselves with the shape of the function itself. The negative-exponential is a function which, because of its inherent simplicity, is frequently used to model natural phenomena. It does not, however, possess a spectrum which will remove the singularity in equation (3.54). A related autocovariance function is the function

(Bakr et al., in press)

$$R_{KK}(s) = \sigma_K^2 (1 - |s|/\ell)\, e^{-|s|/\ell} \quad , \quad s = s_3 \tag{3.55}$$

which has the spectrum

$$\Phi_{KK}(k) = \frac{2}{\pi}\, \sigma_K^2\, \frac{\ell^3 k^2}{(1 + \ell^2 k^2)^2} \tag{3.56}$$

where ℓ is the correlation scale in the x_3 direction and σ_K^2 indicates the variance of the K' process. This spectrum will adequately remove the singularity in equation (3.54); but the autocorrelation function indicates that the process is negatively correlated at distances greater than ℓ (Figure 3.1a). Bakr (1976), in estimating spectra and autocorrelation functions from core data taken from wells, found several instances where such models would be acceptable for vertical arrays of hydraulic conductivity data (whether they are generally acceptable has not yet been determined). Thus, one possible spectrum for use in determining the global longitudinal dispersivity for the one-dimensional flow case is equation (3.56).

Another possible form arises when we attempt to develop from equation (2.43) an expression for the variance in tracer concentration. As will be noted in a subsequent section, this integral expression will contain, in the integrand involving the spectrum of hydraulic conductivity, a fourth-order singularity at the origin. Thus, if we desire a spectrum which will also produce a finite concentration variance, it becomes necessary to consider a spectrum of the form

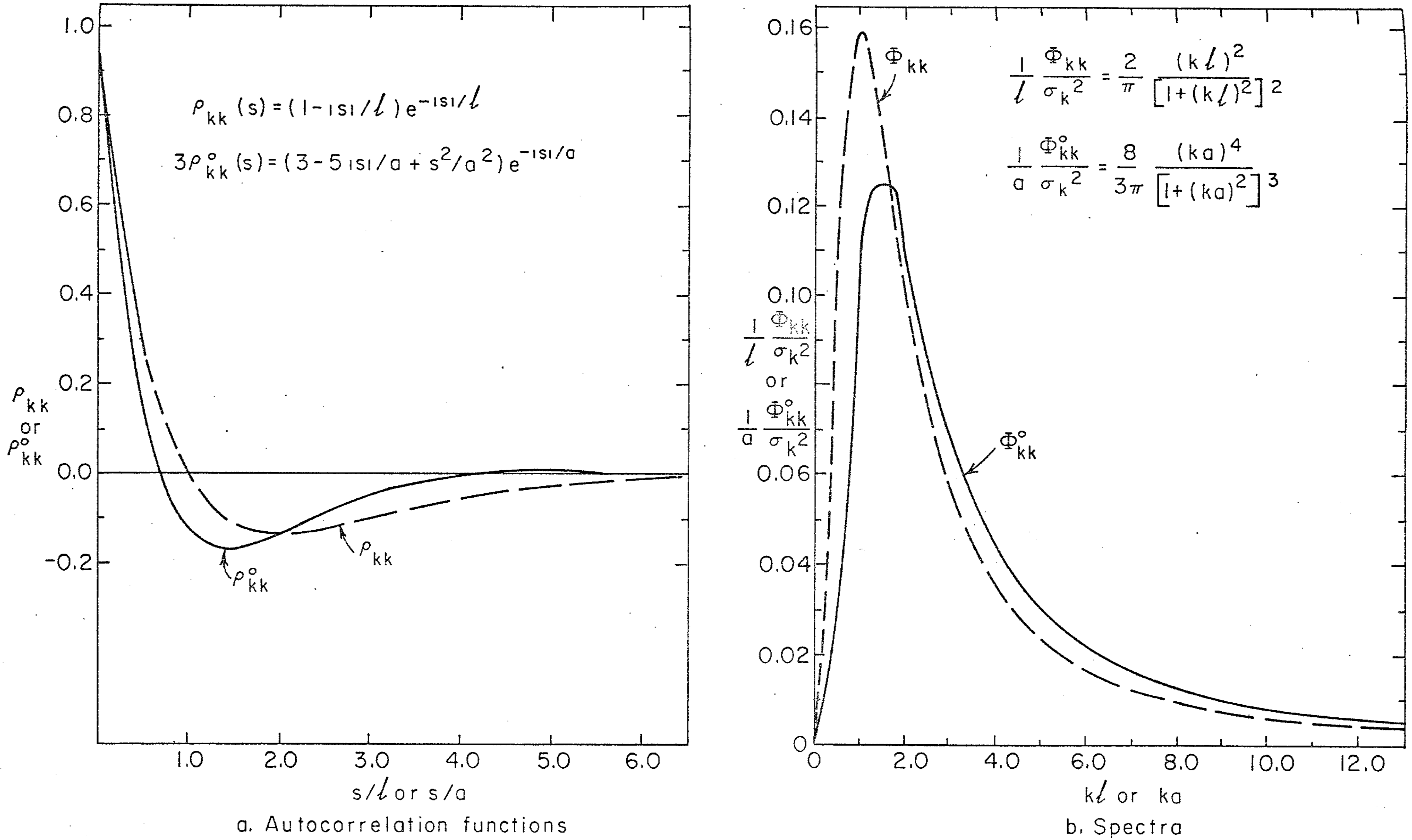

Figure 3.1. Autocorrelation functions and spectra for one-dimensional flow case.

$$\overset{o}{\Phi}_{KK}(k) = \frac{8}{3}\frac{\sigma_K^2}{\pi}\frac{a^5 k^4}{(1+a^2k^2)^3} \tag{3.57}$$

which has an autocovariance function of (Oberhettinger, 1973, p. 20, no. 33)

$$\overset{o}{R}_{KK}(s) = \frac{\sigma_K^2}{3}\left(3 - 5|s|/a + s^2/a^2\right)e^{-|s|/a} . \tag{3.58}$$

Note that this expression has an integral scale equivalent to 2a/3, while the previous autocorrelation function of equation (3.55) has a correlation scale of ℓ, but does not possess an integral scale. The autocorrelation function of equation (3.58) is rather more complex than function (3.55) and hence is not as amenable to modelling of natural processes (Figure 3.1a).

In order that the global dispersivity equation (3.54) be acceptable, it is not required that the same spectrum for hydraulic conductivity produce a finite variance for the tracer concentration, although it would be desirable. Therefore, we have solved equation (3.54) for both spectra (3.56) and (3.57). Thus, by simple integration, we obtain for the one-dimensional flow case a global longitudinal dispersivity of

$$A_\ell = \frac{b}{\alpha_t}\left(\frac{\sigma_K}{\bar{K}}\right)^2\left[1 - \eta(\bar{n}, \sigma_n)\right] \tag{3.59}$$

where

$$b = \begin{cases} \ell^2 & \text{for spectrum (3.56)} \\ a^2/3 & \text{for spectrum (3.57)} \end{cases} .$$

Equation (3.59) concludes the analysis of the one-dimensional flow case. Notable in this expression is the dependence of A_ℓ on the coefficient of variation of hydraulic conductivity $\sigma_K/\bar{K}$, a correlation length-scale parameter, and the local transversive dispersivity; two of which represent statistical parameters quantifying the variability of the medium, and the third representing mixing at the local scale. We defer further discussion of the expression until a later section. However, before leaving this chapter, we note again that, for this case, global dispersion can be regarded as Fickian, and the global longitudinal dispersion coefficient is linearly related to the mean specific discharge.

Three-Dimensional Flow Case

In this section, we solve the spectral form of the global dispersive flux equation (3.3) for the three-dimensional flow case. This equation was developed for the more general case where spatial variability in medium properties is dependent on all three coordinate directions. The equation is approximate in that it is applicable only to relatively small variations in the f' process. This approximation will be discussed in more detail in a later section; in this section, we apply the inverse Fourier transform to obtain a solution to equation (3.3). In particular, evaluating the transform at zero lag, this equation can be written, after substitution of transfer functions (3.20) and (3.33),

$$\overline{q_1'c'} = -\frac{\partial \bar{c}}{\partial \xi}\,\bar{q}_1 \left\{ \iiint_{-\infty}^{\infty} \left[\frac{k_2^2+k_3^2}{k_1^2+k_2^2+k_3^2}\right]^2 \frac{\Phi_{ff}(\underset{\sim}{k})\,d\underset{\sim}{k}}{\left[\alpha_\ell k_1^2 + \alpha_t(k_1^2+k_2^2)\right]} \right.$$

$$\left. - \frac{P}{\bar{n}} \iiint_{-\infty}^{\infty} \left[\frac{k_2^2+k_3^2}{k_1^2+k_2^2+k_3^2}\right] \frac{\Phi_{ff}(\underset{\sim}{k})\,d\underset{\sim}{k}}{\left[\alpha_\ell k_1^2 + \alpha_t(k_1^2+k_2^2)\right]} \right\} + Q \qquad (3.60)$$

where

$$P = \begin{cases} M & , \text{ Archie's equation (3.25)} \\ \dfrac{\bar{n}(1-\bar{n})}{3-\bar{n}} & , \text{ Kozeny - Carmen equation (3.27)} \end{cases}$$

and

$$Q = \iiint_{-\infty}^{\infty} k_1 \left[\frac{\bar{q}_1}{\bar{n}} \bar{c}\, \Phi_{q_1 n}(\underset{\sim}{k}) + \frac{\partial \bar{c}}{\partial x_1} \Phi_{q_1 E_\ell}(\underset{\sim}{k}) \right] d\underset{\sim}{k} \ . \qquad (3.61)$$

Note that effective local longitudinal dispersivity α_ℓ and transverse dispersivity α_t of the form of equation (3.53) have been utilized to replace the local mean longitudinal and transverse coefficients in equation (3.60). If transfer functions (3.33), (3.44), and (3.50) are used to replace spectra $\Phi_{q_1 n}$ and $\Phi_{q_1 E_\ell}$ in equation (3.61), then the quantity in brackets is an even function, provided that Φ_{ff} is an even function. Since spectra are always even functions, Q adds nothing to the dispersive flux because evaluation of equation (3.61) in the k_1 direction will result in a null integral. Thus, we may express the global longitudinal dispersivity as

$$A_{\ell 3} = \iiint_{-\infty}^{\infty} \left[\frac{k_2^2 + k_3^2}{k_1^2 + k_2^2 + k_3^2} \right]^2 \frac{\Phi_{ff}(\underset{\sim}{k})\, d\underset{\sim}{k}}{\left[\alpha_\ell k_1^2 + \alpha_t (k_2^2 + k_3^2)\right]}$$

$$- \frac{P}{\bar{n}} \iiint_{-\infty}^{\infty} \left[\frac{k_2^2 + k_3^2}{k_1^2 + k_2^2 + k_3^2} \right] \frac{\Phi_{ff}(\underset{\sim}{k})\, d\underset{\sim}{k}}{\left[\alpha_\ell k_1^2 + \alpha_t (k_2^2 + k_3^2)\right]} \qquad (3.62)$$

where the first integral represents the effects of hydraulic conductivity variations. Note that the global dispersive flux (3.60) is again Fickian in nature and that it is a linear function of the mean specific discharge. Before evaluation of equation (3.62) can be contemplated, however, we are left with the difficult task of selecting a form for the spectrum of the f' process.

As in the one-dimensional flow case, selection of a spectrum Φ_{ff} is largely based on the form of its autocovariance function. A particularly well-behaved function which is widely applicable to modelling of natural phenomena is the three-dimensional negative-exponential function:

$$R_{ff}(\underset{\sim}{s}) = \sigma_f^{\,2} \exp\left[-\left(\frac{s_1^2}{\lambda_1^2} + \frac{s_2^2}{\lambda_2^2} + \frac{s_3^2}{\lambda_3^2}\right)^{1/2}\right] \tag{3.63}$$

which has the spectrum (Appendix 5)

$$\Phi_{ff}(\underset{\sim}{k}) = \frac{1}{\pi^2} \frac{\sigma_f^{\,2} \lambda_1 \lambda_2 \lambda_3}{\left[\lambda_1^2 k_1^2 + \lambda_2^2 k_2^2 + \lambda_3^2 k_3^2 + 1\right]^2} \tag{3.64}$$

where $\sigma_f^{\,2}$ is the variance of the f' process and λ_1, λ_2, and λ_3 are integral scales in the principal coordinate directions (see Appendix 1). If we allow the horizontal length scales (λ_1 and λ_2) to become inordinately large, the equation (3.63) approaches the one-dimensional negative-exponential autocovariance function. This asymptotic result plus the asymptotic approach of three-dimensional local heterogeneities to the stratified case discussed in the section entitled "Prototype " suggests a method of testing the utility of the autocovariance function (3.63). In particular, from equation (3.18) we can construct a spectral relationship between hydraulic head and the f' process. As will be demonstrated in the chapter entitled "Hydraulic Head Variance in Globally Anisotropic Media," this relationship allows us to evaluate the variance in head resulting from variations in hydraulic conductivity. However, by considering the limit where the horizontal length scales become large, the stratified case with flow parallel to bedding is approached. From our previous discussion of perturbed quantities, it is to be expected that this one-dimensional case should have zero head variance. Hence, it would also be desirable if the spectrum chosen for the solution of the global dispersivity equation would also produce this limiting case for head variance as the horizontal length scales become very large. As noted in the chapter on head variance, spectrum (3.64) does not have this limit for the asymptotic one-dimensional flow case; indeed, as λ_1 and λ_2 become large, the variance in hydraulic conductivity will increase infinitely. Admittedly, there remains a problem in that one is dealing with differing effective hydraulic conductivities between the one-dimensional and three-dimensional cases, but this disparity should not hinder attainment of the over-all limit. In general, we believe that it is desirable to use an autocovariance function which will produce this null limit for head variance in the asymptotic one-dimensional flow case.

From the discussion in the chapter concerning the variance in hydraulic head, an autocovariance function which has a spectrum that will produce a solution giving the limiting case presented in the previous paragraph is

$$R^{o}_{ff}(\underset{\sim}{s}) = \sigma_f^{\,2}\left[1 - s_3^2/(\ell_3^2\,\zeta)\right]\exp\left[-\zeta\right] \tag{3.65}$$

where

$$\zeta^2 = s_1^2/\ell_1^2 + s_2^2/\ell_2^2 + s_3^2/\ell_3^2 \quad .$$

The autocorrelation function for equation (3.65) has been plotted by contouring one quadrant of a vertical plane through the axes ($S_2 = 0$) in Figure 3.2. Clearly, it contains both elements of a simple negative-exponential function (S_1 axis) and a modified negative-exponential function (S_3 axis) similar to equation (3.55). The spectrum for this autocovariance function is (Appendix 6)

$$\Phi_{ff}^{\circ}(\underset{\sim}{k}) = \frac{4}{\pi^2} \frac{\sigma_f^2 \ell_1 \ell_2 \ell_3^3 k_3^2}{\left[\ell_1^2 k_1^2 + \ell_2^2 k_2^2 + \ell_3^2 k_3^2 + 1\right]^3} \tag{3.66}$$

In this case, ℓ_1 and ℓ_2 are integral scales while ℓ_3 is a correlation length scale.

We might also consider developing an equation for variance of tracer concentration by utilizing equation (3.1). If we were to consider, for this concentration variance equation, the same limiting case presented in preceding paragraphs, we would find that a three-dimensional autocovariance function which has an asymptotic one-dimensional form similar to equation (3.58) would be necessary to obtain a finite concentration variance in the limit. This result is only reasonable, as a spectrum which has the autocovariance function (3.58) is required to obtain a finite variance in the one-dimensional flow case. Hence, if we desired a finite concentration variance for the asymptotic one-dimensional case, it is only reasonable to expect that the asymptotic one-dimensional spectrum should remove the same order singularity as the actual one-dimensional spectrum. Clearly, the three-dimensional autocovariance function (3.65) does not have an asymptotic one-dimensional autocovariance function equivalent to (3.58) which, in turn, has the minimum spectrum to remove a fourth-order singularity at the origin.

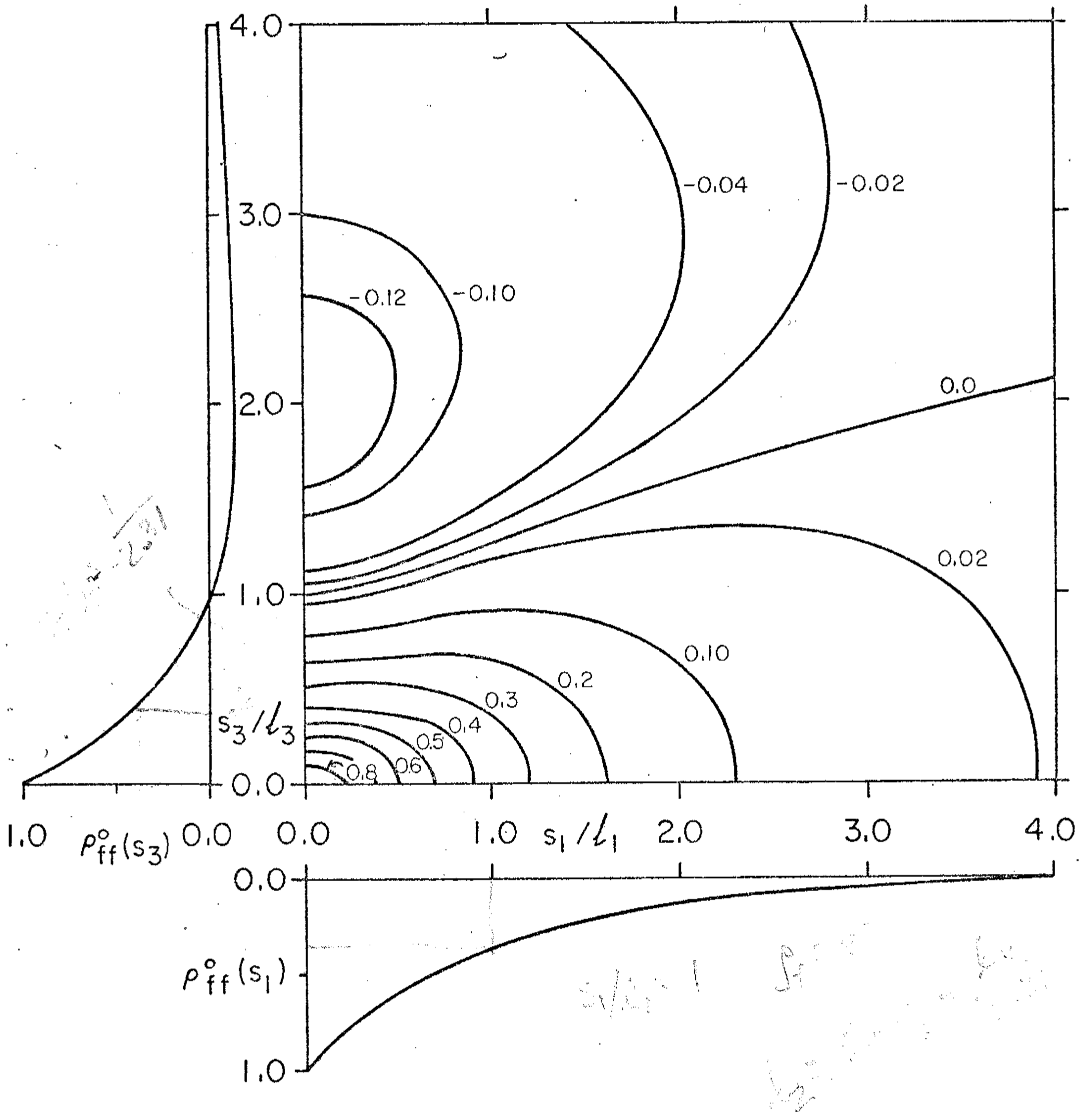

Figure 3.2. Isopleth contour of modified negative-exponential autocorrelation function in vertical plane.

We consider, however, that it is too much to expect that the autocovariance function chosen to analyze equation (3.62) should produce a finite variance for every limiting case; indeed, we have yet to show that the autocovariance function should do more than reflect the correlation structure of the medium and yet remain a viable form to solve equation (3.62). Our only fear is that one of the more complex negative-exponential forms may better reflect the correlation structure because they represent forms which allow for the solution of perfectly valid expressions. It may also happen that none of the above forms are exact estimators of the correlation structure, perhaps, because of the approximation involved in deriving the model equation and transfer functions. In summary, we close this discussion by noting that, while the simple three-dimensional negative-exponential form (3.63) is thought to be the generally preferable autocovariance function with respect to correlation structure, it will not result in a zero head variance for the asymptotic one-dimensional flow case, nor will it, for any case, produce a finite concentration variance. It can be shown that the modified negative-exponential form (3.65) will produce a result which generally gives a finite concentration variance, except for certain cases (in particular, the asymptotic one-dimensional parallel flow case), and will always produce a finite head variance.

We proceed, then, to use both spectra (3.64) and (3.66) in solving the global longitudinal dispersivity equation (3.62). Our experience has been that it is generally very difficult to completely integrate these expressions analytically, and numerical integration must be resorted to in order to obtain a complete evaluation. As a matter of simplification, the horizontal length scales have been set equal to each other ($\ell_1 = \ell_2$ and $\lambda_1 = \lambda_2$) which, we believe, does not result in a great loss in generality. Additionally, the vertical length scale is taken to be less than or equal to the horizontal length scales. In particular, for the spectrum of the simple negative-exponential autocovariance function (3.64), we obtain the expression (Appendix 7)

$$A_{\ell 3} = \frac{\lambda_3^2 \sigma_f^2}{\alpha_t} \left[F(\rho, R) - \frac{P}{\bar{n}} G(\rho, R) \right] \tag{3.67}$$

where

$$\rho = \alpha_t / \alpha_\ell \quad , \quad R = \lambda / \lambda_3 \quad , \quad \lambda = \lambda_1 = \lambda_2 \quad .$$

The factor $F(\rho,R)$ represents the solution of the first integral and is representative of the effects of variation in hydraulic conductivity, while $G(\rho,R)$ represents the second integral and is representative of porosity variations. This result indicates a dependence of the global dispersivity $A_{\ell 3}$ on a length scale, variance in the f' process, and effective local transverse dispersivity. The factors $F(\rho,R)$ and $G(\rho,R)$ are presented graphically in Figures 3.3 and 3.4, respectively, for two different values of the local dispersivity ratio ρ. For any particular ρ and R, the values of $F(\rho,R)$ and $G(\rho,R)$ are nearly identical; thus, the importance of a good estimator for the porosity factor $\bar{P}$ (equation (3.60)) is noted. Also note that as R becomes large (and therefore we approach a stratified medium condition), both $F(\rho,R)$ and $G(\rho,R)$ factors grow infinitely. The explanation for this growth is identically that of the previous paragraphs; if there is such a thing as a valid asymptotic one-dimensional equivalent of the global dispersivity equation (3.62), then

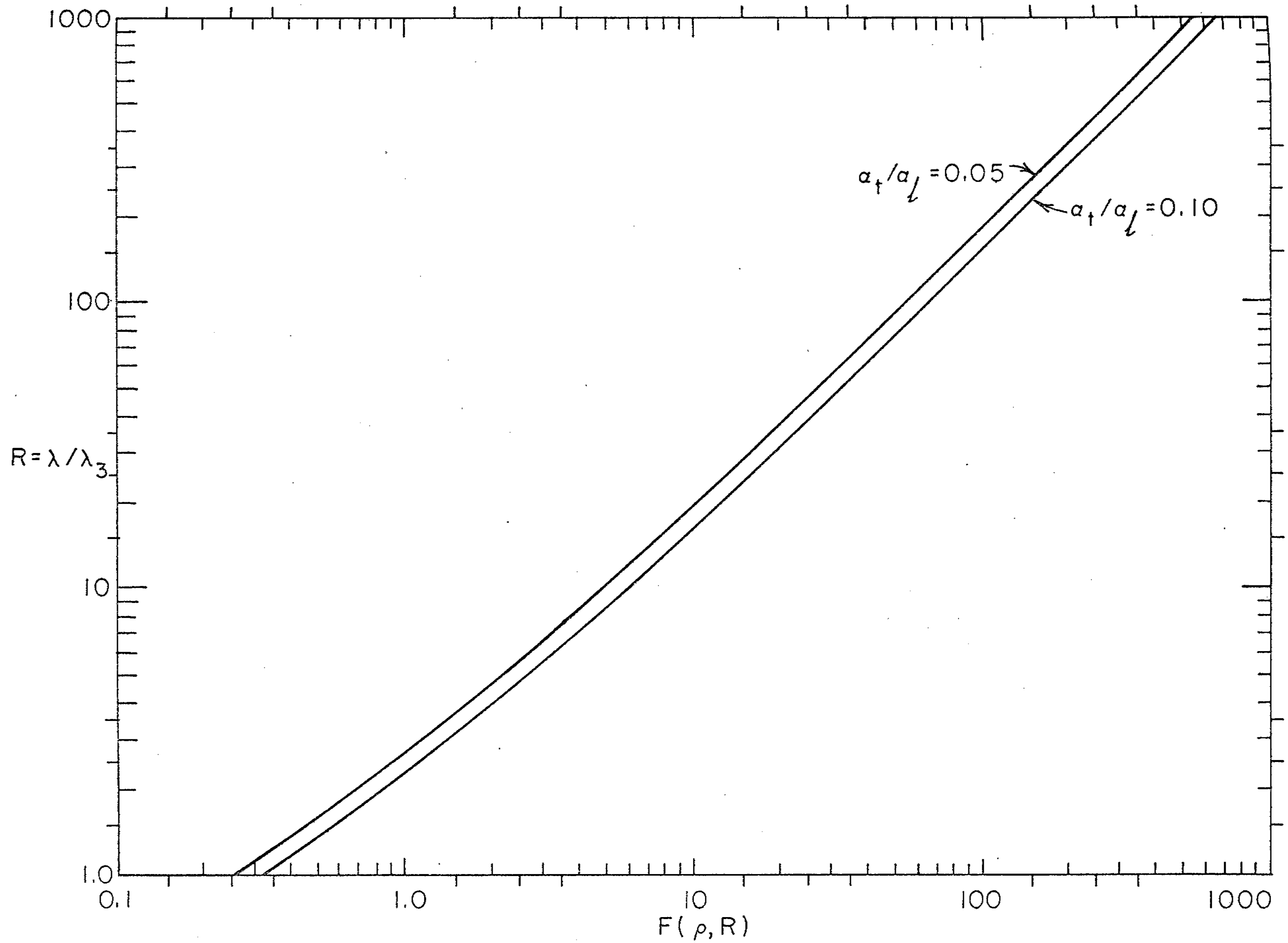

Figure 3.3. Hydraulic conductivity factor for spectrum (3.64).

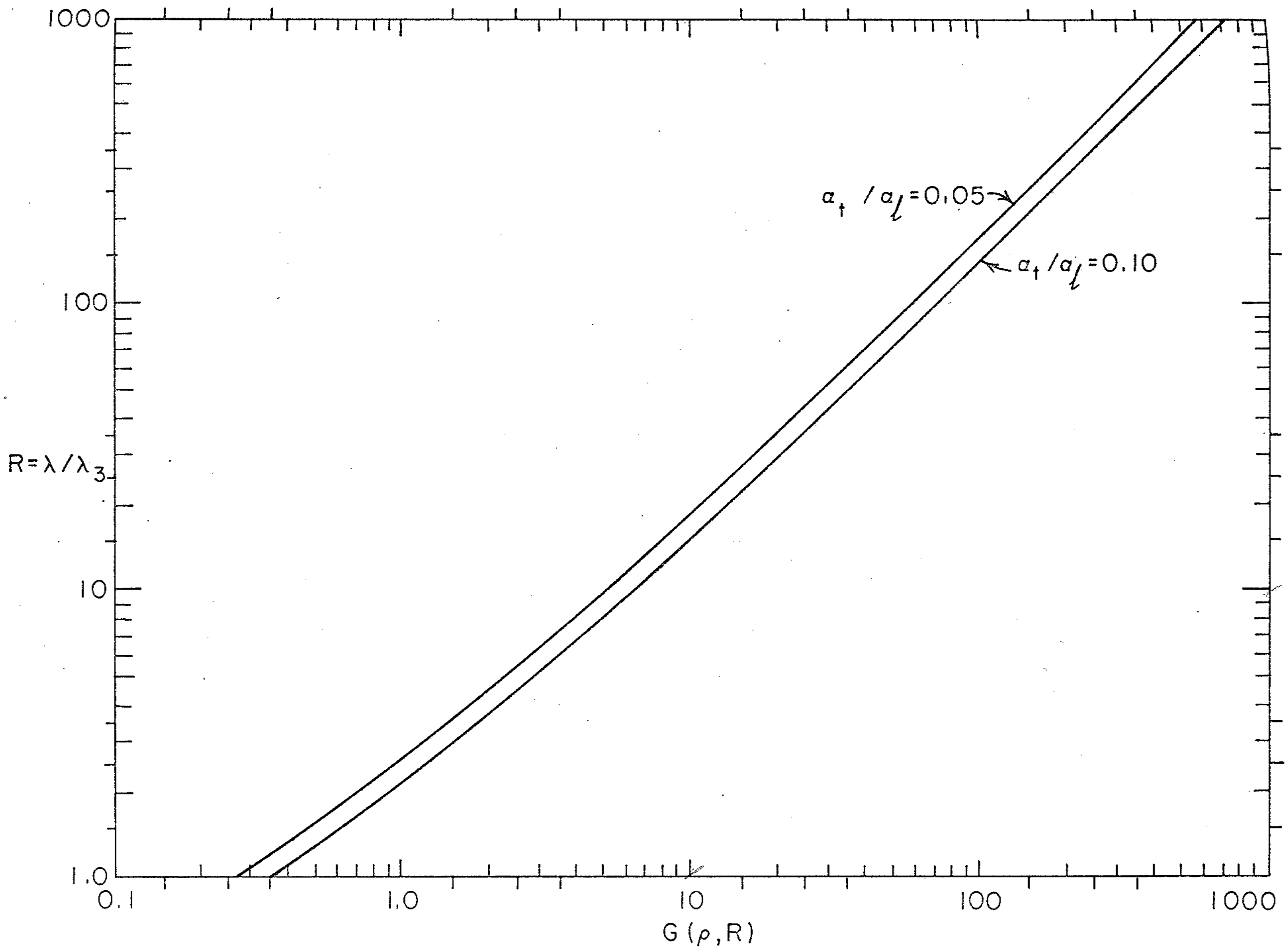

Figure 3.4. Porosity factor for spectrum (3.64).

the spectrum of the asymptotic one-dimensional autocovariance function of equation (3.63) is not sufficient to solve this expression. Indeed, at least an asymptotic autocovariance function equivalent to equation (3.56) would be necessary. Further comparisons between one-dimensional and three-dimensional results will be carried out in the next chapter: we will confine ourselves in the remainder of this chapter to the solution of the global dispersivity equation with spectrum (3.66), which does give a finite result for this limiting case.

The solution result with spectrum (3.66) is essentially identical to equation (3.67), the major difference being in the graphical representation. In particular, the solution form can be given as (Appendix 8)

$$A^{\circ}_{\ell 3} = \frac{\ell_3^2 \sigma_f^2}{\alpha_t}\left[F^{\circ}(\rho, R^{\circ}) - \frac{P}{\bar{n}} G^{\circ}(\rho, R^{\circ})\right] \tag{3.68}$$

where

$$R^{\circ} = \ell/\ell_3 \quad , \quad \ell = \ell_1 = \ell_2$$

and $F^{\circ}(\rho,R^{\circ})$ and $G^{\circ}(\rho,R^{\circ})$ are the counterparts of $F(\rho,R)$ and $G(\rho,R)$ of equation (3.67). The graphical presentation of $F^{\circ}(\rho,R^{\circ})$ and $G^{\circ}(\rho,R^{\circ})$ are to be found in Figures 3.5 and 3.6, respectively. Note that, as R° becomes large, a definite limit is reached for both cases. Again, we note the importance of adequate determination of the porosity factor P. Finally, it is to be noted that the correlation length scales λ_3 and ℓ_3 are not necessarily equal; hence, it is rather difficult to compare the graphic results from the two spectra. We will undertake such a comparison

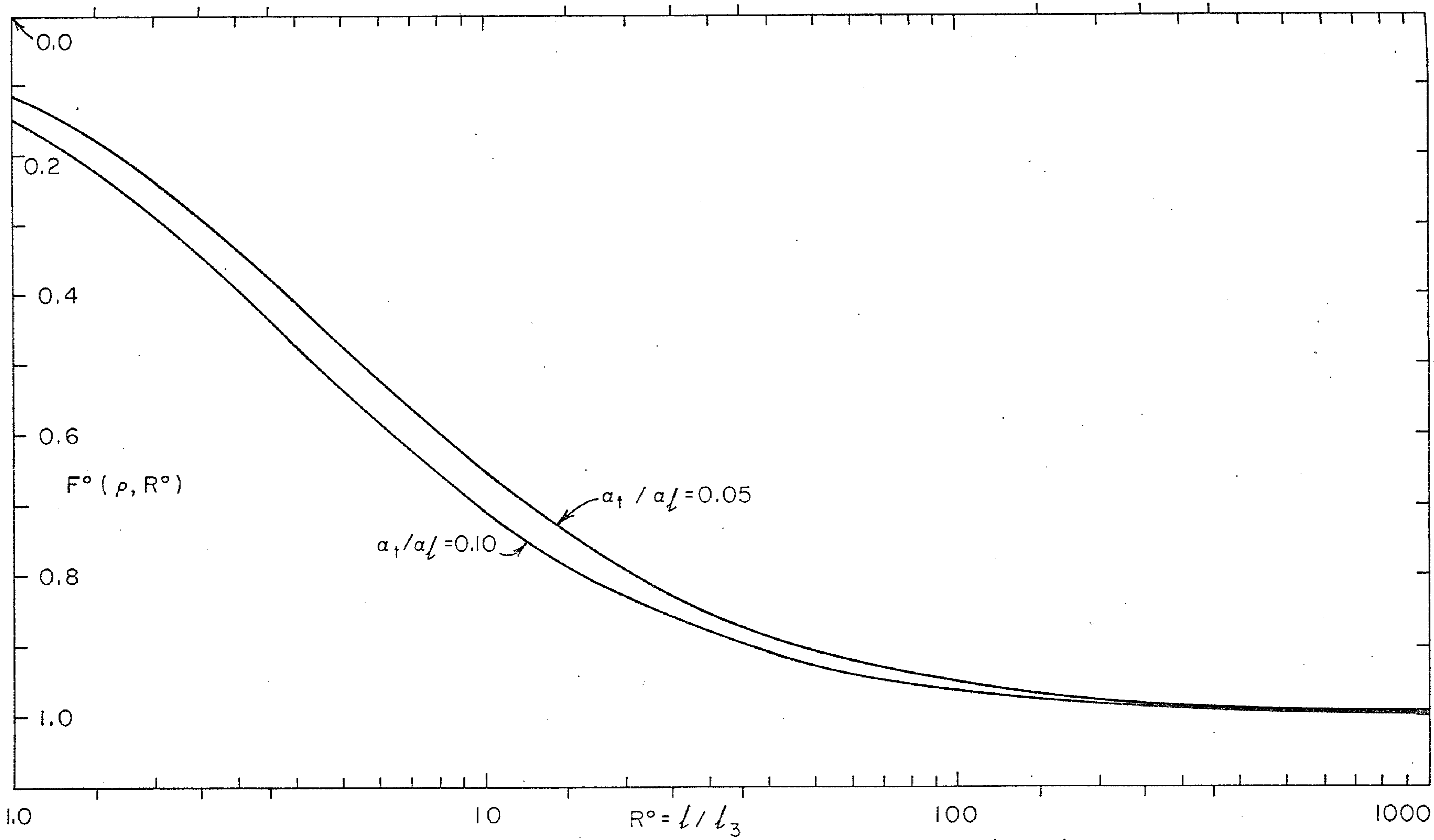

Figure 3.5. Hydraulic conductivity factor for spectrum (3.66).

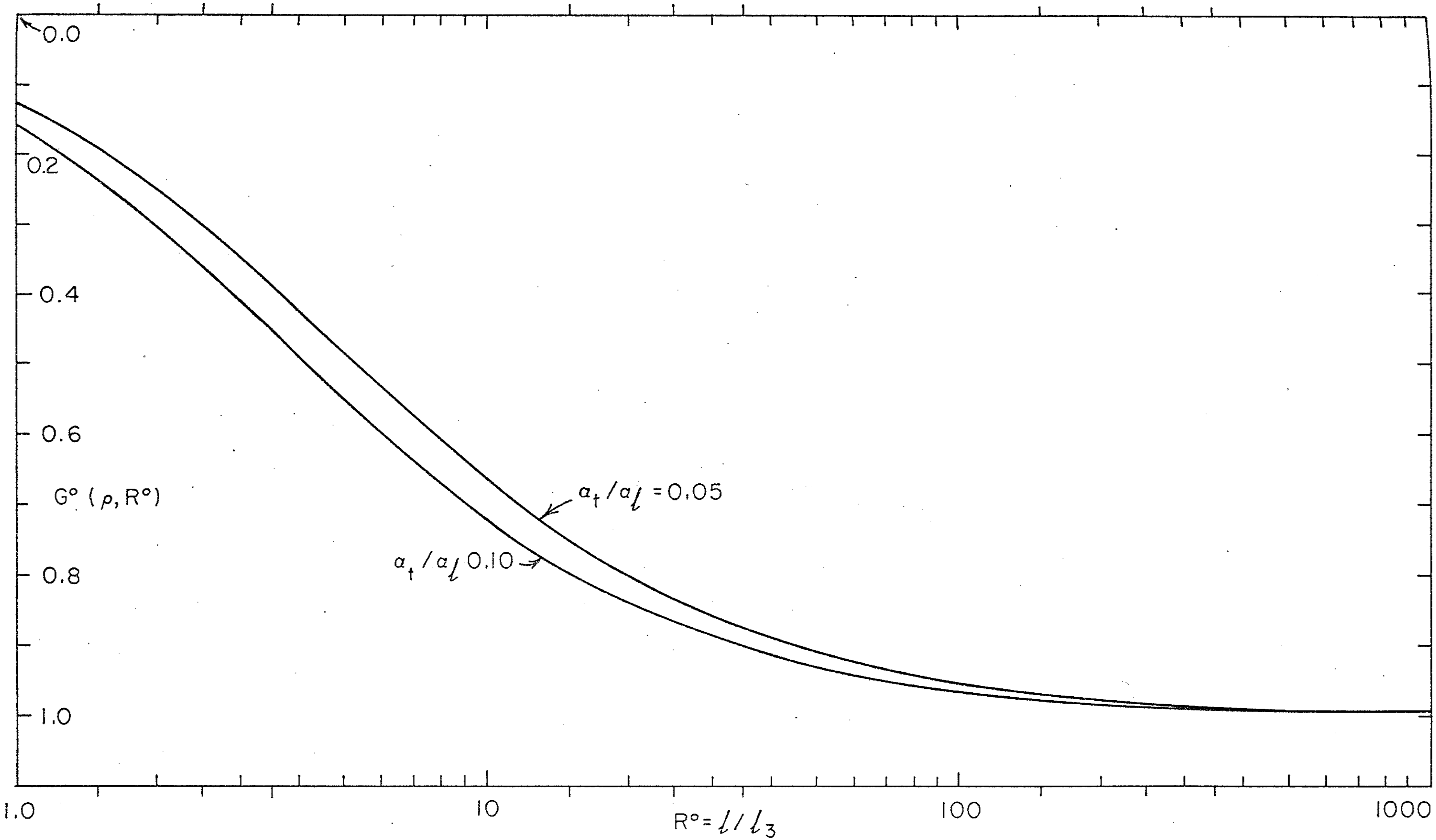

Figure 3.6. Porosity factor for spectrum (3.66).

in the next chapter: this chapter is completed with a technical note about the derivation of the global longitudinal dispersivity equation (3.62). Before leaving this section, however, we emphasize again the basic results of the three-dimensional flow case: the Fickian form of the global longitudinal dispersive flux (3.60) and its linear relationship with the mean seepage velocity.

Note to Derivation of Global Longitudinal Dispersivity Equation

In the section entitled "Prototype," it was noted that the off-diagonal bulk dispersion tensor components E_{12} and E_{13} (equation (2.7)) might be significant to the model equation. Indeed, if we had retained these terms in perturbation expression (2.14), then the model equation (2.41), resulting from a first-order analysis, would have contained the additional terms

$$\frac{\partial E_{21}'}{\partial x_2}\frac{\partial \bar{c}}{\partial x_1} + \frac{\partial E_{31}'}{\partial x_3}\frac{\partial \bar{c}}{\partial x_1} + 2\bar{E}_{21}\frac{\partial^2 c'}{\partial x_2 \partial x_1} + 2\bar{E}_{31}\frac{\partial^2 c'}{\partial x_3 \partial x_1} \tag{3.69}$$

on the right-hand side. We argue heuristically, at this point, that $\bar{E}_{21}$ and $\bar{E}_{31}$ are second order in comparison to $\bar{E}_{11}$ and $\bar{E}_{22}$. Hence, when compared to similar terms already retained in model equation (2.41), terms containing these mean off-diagonal components can be neglected. Specifically, let us assume that, in equation (2.2), we can use effective local longitudinal and transverse dispersivities $\bar{\alpha}_\ell$ and α_t. Then, to obtain an estimate of $\bar{E}_{21}$, we simply take expectations on both sides of equation (2.2), where i and j have been properly designated. This process involves evaluating the expected value of the term q_2q_1/q. This expectation can be approximated by first substituting binomial expansion (2.4b) for $1/q$ in this term. However, to a first-order approximation, this expectation is zero, causing $\bar{E}_{12}$ to also be zero. A similar analysis for the mean of diagonal tensor components would indicate the existence of a form comparable to equation (3.53). Whence, we may conclude that the mean of diagonal components must be significantly larger than either $\bar{E}_{21}$ or, for that matter, $\bar{E}_{31}$.

We are left, then, with only the first two terms in expression (3.69) to analyze. These terms can be written in spectral form as

$$\left[i k_2 \Phi_{q_1 E_{21}}(\underset{\sim}{k}) + i k_3 \Phi_{q_1 E_{31}}(\underset{\sim}{k}) \right] \frac{\partial \bar{C}}{\partial x_1} \tag{3.70}$$

after which we proceed to find appropriate transfer functions for $\Phi_{q_1 E_{21}}$ and $\Phi_{q_1 E_{31}}$. Rewriting equation (2.7a) as

$$E'_{21} \approx \beta q'_2 \quad , \quad \beta = (\alpha_I - \alpha_{II}) \tag{3.71}$$

we obtain the mean-removed equation

$$E'_{21} \approx \bar{\beta} q'_2 \tag{3.72}$$

where a first-order approximation has been made. Similarly, from equation (2.7b),

$$E'_{31} \approx \bar{\beta} q'_3 \quad . \tag{3.73}$$

Equations (3.72) and (3.73) can be written in terms of complex Fourier amplitudes as

$$dZ_{E_{21}}(\underset{\sim}{k}) = \bar{\beta}\, dZ_{q2}(\underset{\sim}{k}) \tag{3.74a}$$

and

$$dZ_{E_{31}}(\underset{\sim}{k}) = \bar{\beta}\, dZ_{q_3}(\underset{\sim}{k}) \quad . \tag{3.74b}$$

respectively. The Darcy ralationship for q_2' can be written

$$q_2' = -K_\ell \exp[f'] \frac{\partial \phi'}{\partial X_2} \tag{3.75}$$

a first-order approximation of which is

$$q_2' \approx -K_\ell \frac{\partial \phi'}{\partial X_2} \quad . \tag{3.76}$$

Similarly, for q_3',

$$q_3' \approx -K_\ell \frac{\partial \phi'}{\partial X_3} \quad . \tag{3.77}$$

Equations (3.76) and (3.77) can be written in terms of complex Fourier amplitudes as

$$dZ_{q_2}(\underset{\sim}{k}) = -i\, k_2 K_\ell\, dZ_\phi(\underset{\sim}{k}) \tag{3.78a}$$

and $$dZ_{q_3}(\underset{\sim}{k}) = -i\, k_3 K_\ell\, dZ_\phi(\underset{\sim}{k}) \quad , \tag{3.78b}$$

respectively. Finally, using equation (3.18), we obtain the following relationships for the E'_{21} and E'_{31} processes in terms of complex Fourier amplitudes:

$$dZ_{E_{21}}(\underset{\sim}{k}) = -k_1 k_2\, \bar{q}_1 \bar{\beta}\, dZ_f(\underset{\sim}{k}) \tag{3.79a}$$

and $$dZ_{E_{31}}(\underset{\sim}{k}) = -k_1 k_3 \bar{q}_1 \bar{\beta}\, dZ_f(\underset{\sim}{k}) \ . \tag{3.79b}$$

From equations (3.79a) and (3.79b), we obtain transfer functions for spectra $\Phi_{q_1E_{21}}$ and $\Phi_{q_1E_{31}}$ by properly combining their complex conjugates with equation (3.19) and taking expected values:

$$\Phi_{q_1E_{21}}(\underset{\sim}{k}) = -k_1 k_2 q_1^2 \beta \left[\frac{k_2^2 + k_3^2}{k_1^2 + k_2^2 + k_3^2}\right] \Phi_{ff}(\underset{\sim}{k}) \tag{3.80a}$$

and $$\Phi_{q_1E_{31}}(\underset{\sim}{k}) = -k_1 k_3 q_1^2 \beta \left[\frac{k_2^2 + k_3^2}{k_1^2 + k_2^2 + k_3^2}\right] \Phi_{ff}(\underset{\sim}{k}) \ . \tag{3.80b}$$

From transfer functions (3.80), and our knowledge of various forms available for Φ_{ff} we conclude that expression (3.70) is an odd function with regard to the k_1 variable. Therefore, in the final analysis of the global longitudinal dispersive flux, expression (3.70) would suffer the same fate as the Q equation (3.61) and have a null integral. Thus, we conclude that inclusion of terms in expression (3.69) in the model equation would have no effect on the final result of our three-dimensional analysis.

EVALUATION AND APPLICATION

Limitations of First-Order Analysis

Throughout much of the analysis presented to this point, it was noted that the one-dimensional flow (or completely stratified) case contains fewer approximations than the three-dimensional case. We consider, however, that the three-dimensional flow case is, in most instances, more representative of actual transport phenomena in porous media. The one-dimensional case represents an ideal model that forms a reference point with which comparisons can be made, but is seldom realized in its full idealization in actual field situations. Hence, much of the analysis in this chapter will concern itself with the three-dimensional flow case.

A moderately severe restriction to the three-dimensional flow case has already been indicated in the section entitled "Prototype," where it was noted that the population equivalent of the geometric mean would be used to estimate the effective hydraulic conductivity. Surprisingly, error resulting from use of the logarithm of hydraulic conductivity in the calculation of head variance appears to be small over most ranges of the variance of the f' process. In particular Gutjahr et al. (in press) found that, for a one-dimensional case with flow perpendicular to stratification, the error in estimation of head variance amounts to approximately 10% for a σ_f equal to one. In three-dimensional situations, where flow paths are less restricted, it is expected that even less error will be produced. Thus, with regard to variance in flow, it is generally expected that the approximate solution utilizing the logarithm of hydraulic conductivity will produce a respectable solution except when σ_f is significantly larger than one (e.g., on the order of 1.5).

Throughout the first-order analysis presented in the preceding chapters, a number of second-order terms were neglected in order to obtain a linear model equation. Perhaps the most significant of these terms is expression (2.29c), since it represents convective transport resulting from randomness in the medium. As discussed previously, this term could represent an important contributor to lateral mixing -- a phenomenon very necessary to the Taylor (1953) model. Thus, we attempt to attain a reasonable estimate of the significance of this term.

Term (2.29c) actually contains three components corresponding to the three cardinal directions. Since we are principally interested in the lateral mixing aspect of the problem, an estimate of the term

$$q_3' w' - \overline{q_3' w'} \quad , \quad w' = \partial c' / \partial x_3 \tag{4.1}$$

in comparison to the retained convective term

$$q_1' \overline{w} \quad , \quad \overline{w} = \partial \overline{c} / \partial \xi \tag{4.2}$$

would be desirable. We assume that the derivative of the c' process, w', has zero mean and is second-order stationary. As the standard deviation is a generally accepted measure of the variability of a random process, we will attempt to derive variance expressions for both of the above terms. These variance expressions will generally be evolved from transfer functions which have been developed in previous sections: If they are not available, then appropriate expressions will be developed by the same kind of first-order analysis used in the previous chapter. Thus, the expressions developed in this section for the variances of processes will themselves be approximations since second-order terms of the same type as those we wish to approximate have been deleted. Obviously, these approximations will not be valid for media which are highly variable; but as an order-of-magnitude estimate of what we wish to approximate, this iterative procedure is considered acceptable.

For expression (4.1), we shall assume that both the q_3' and w' processes are approximately jointly normal. Then we will examine their correlation coefficient $\overline{q_3'w'}/\sigma_{q_3}\sigma_w$ and determine its magnitude. If the correlation coefficient is small, we shall conclude that the product of the variances of the q_3' process and w' process is a sufficient estimate of the variance of their product (Ross, 1972, p. 41). The cross spectrum Φ_{q_3w} of these two processes is, by the representation theorem,

$$\Phi_{q_3w}(\underset{\sim}{k}) = \overline{dZ_{q_3}(\underset{\sim}{k})\, dZ_w(\underset{\sim}{k})} \quad . \tag{4.3}$$

However, since the w' process is the derivative of the c' process, it may be represented, in terms of complex Fourier amplitudes, as

$$dZ_w(\underset{\sim}{k}) = i k_3 dZ_c(\underset{\sim}{k}) \quad . \tag{4.4}$$

A first order approximation of the q_3' term is

$$q_3'(\underset{\sim}{x}) \approx -K_\ell \frac{\partial \phi'(\underset{\sim}{x})}{\partial x_3} \tag{4.5}$$

which, in terms of complex Fourier amplitudes, is

$$dZ_{q_3}(\underset{\sim}{k}) = -i k_3 K_\ell dZ_\phi(\underset{\sim}{k}) \quad . \tag{4.6}$$

By properly combining this result with transfer function (3.18), and then comparing it with transfer function (3.19), we can relate the complex amplitudes of the q_1' process and the q_3' process:

$$dZ_{q_3}(\underset{\sim}{k}) = -\frac{k_1 k_3}{k_2^2 + k_3^2}\, dZ_{q_1}(\underset{\sim}{k}) \ . \tag{4.7}$$

Finally, we use equation (3.1) to relate the c' process to the f' process. For simplicity, we drop consideration of the effect of porosity variations on the process, obtaining the equation

$$dZ_c(\underset{\sim}{k}) = -\frac{dZ_{q_1}(\underset{\sim}{k}) - i k_1 dZ_{E\ell}(\underset{\sim}{k})}{\left[\bar{E}_\ell k_1^2 + \bar{E}_t (k_2^2 + k_3^2)\right]} \frac{\partial \bar{c}}{\partial \xi} \ . \tag{4.8}$$

By proper substitution of equations (4.4), (4.7) and (4.8) into equation (4.3), the spectral relationship

$$\Phi_{q_3 w}(\underset{\sim}{k}) = \frac{k_1^2 k_3^2 \Phi_{q_1 E_\ell}(\underset{\sim}{k}) - i k_1 k_3^2 \Phi_{q_1 q_1}(\underset{\sim}{k})}{\left[k_2^2 + k_3^2\right]\left[\bar{E}_\ell k_1^2 + \bar{E}_t (k_2^2 + k_3^2)\right]} \tag{4.9}$$

is obtained. To obtain the cross covariance $\overline{q_3'w'}$ the inverse Fourier transform of equation (4.9), evaluated at zero lag, is obtained. However, since only even integrands will produce other than null integrals, we need only evaluate the expression

$$\overline{q_3' w'} = \iiint_{-\infty}^{\infty} \frac{k_1^2 k_3^2 \Phi_{q_1 E_\ell}(\underset{\sim}{k})\, d\underset{\sim}{k}}{\left[k_2^2 + k_3^2\right]\left[\bar{E}_\ell k_1^2 + \bar{E}_t (k_2^2 + k_3^2)\right]} \ . \tag{4.10}$$

Replacing $\Phi_{q_1 E_\ell}$ with transfer functions (3.20), (3.44), and (3.50), one finds the expression

$$\overline{q_3' w'} = \left[\alpha_\ell I_1 + B (K_\ell)^{1/2} I_2 / 4\right] \bar{q}_1 \frac{\partial \bar{c}}{\partial \xi} \ , \tag{4.11}$$

$$I_1 = \iiint_{-\infty}^{\infty} \frac{k_1^2 k_3^2 [k_2^2 + k_3^2] \Phi_{ff}(\underset{\sim}{k}) d\underset{\sim}{k}}{[k_1^2 + k_2^2 + k_3^2]^2 [\alpha_\ell k_1^2 + \alpha_t (k_2^2 + k_3^2)]} , \tag{4.12a}$$

and $$I_2 = \iiint_{-\infty}^{\infty} \frac{k_1^2 k_3^2 \Phi_{ff}(\underset{\sim}{k}) d\underset{\sim}{k}}{[k_1^2 + k_2^2 + k_3^2][\alpha_\ell k_1^2 + \alpha_t (k_2^2 + k_3^2)]} \tag{4.12b}$$

where we have assumed $\alpha_\ell \approx \bar{\alpha}_I$. To facilitate evaluation of integrals (4.12), we use the simplified spectrum

$$\Phi_{ff}(\underset{\sim}{k}) = \frac{4\sigma_f^2 \ell^5}{\pi^2} \frac{k_3^2}{[\ell^2 (k_1^2 + k_2^2 + k_3^2) + 1]^3} \tag{4.13}$$

which is the spectrum of the modified negative-exponential autocovariance function with all length scales set equal to ℓ. With spectrum (4.13), integrals (4.12) can be solved by straight-forward integration, after conversion to spherical coordinates, giving the results

$$I_1 = \frac{15}{8} \frac{\sigma_f^2}{\alpha_\ell - \alpha_t} \left\{ \frac{16}{35} + \frac{11}{5}\psi + \frac{8}{3}\psi^2 + \psi^3 \right.$$

$$\left. - [1+\psi]^3 \psi^{1/2} \tan^{-1}[1/\psi^{1/2}] \right\} \tag{4.14a}$$

and $$I_2 = \frac{9}{8} \frac{\sigma_f^2}{\alpha_\ell - \alpha_t} \left\{ \frac{8}{15} + \frac{5}{3}\psi + \psi^2 \right.$$

$$\left. - [1+\psi]^2 \psi^{1/2} \tan^{-1}[1/\psi^{1/2}] \right\} \tag{4.14b}$$

where

$$\Psi = \alpha_t/(\alpha_\ell - \alpha_t) \quad .$$

Thus, substituting equations (4.14) into equation (4.10), the cross co-variance becomes

$$\overline{q_3' w'} = \bar{q}_1 \sigma_f^2 \frac{\partial \bar{c}}{\partial \xi} \frac{\Psi}{\rho} \left\{ \frac{15}{8} \left[\frac{16}{35} + \frac{11}{5} \Psi + \frac{8}{3} \Psi^2 + \Psi^3 \right.\right.$$

$$\left. - (1+\Psi)^3 \Psi^{1/2} \tan^{-1}\left[1/\Psi^{1/2}\right] \right] + \frac{9/32}{1+5\sigma_f^2/8} \left[\frac{8}{15} + \frac{5}{3}\Psi + \Psi^2 \right.$$

$$\left.\left. - (1+\Psi)^2 \Psi^{1/2} \tan^{-1}\left[1/\Psi^{1/2}\right] \right] \right\} \tag{4.15}$$

where $\rho = \alpha_t/\alpha_\ell$ and, in consideration of equation (3.45), we have made the assumption

$$\alpha_\ell \approx B\,(K_\ell)^{1/2} \left(1 + 5\,\sigma_f^2/8\right) \quad . \tag{4.16}$$

If we assume that Ψ is small in equation (4.15) (α_ℓ is generally considered to be an order of magnitude larger than α_t), such that any Ψ of power one or greater can be neglected, we may, with regard to the quantity within the outer brackets use the approximation

$$\overline{q_1' w'} \sim \bar{q}_1 \sigma_f^2 \frac{\partial \bar{c}}{\partial \xi} \left\{ 1 - \frac{\pi \Psi^{1/2}}{2} \right\} \tag{4.17}$$

in place of equation (4.15). To complete our correlation coefficient, we need to obtain estimates of the variance of both the q_3' and w'

processes.

A spectral relationship for the w' process can be constructed from equation (4.4) by substitution of equations (4.8), (3.19), (3.43), and (3.49). Upon multiplication by the complex conjugate and taking expected values of the resulting equation, we obtain

$$\Phi_{ww}(\underset{\sim}{k}) = \left(\frac{\partial \bar{c}}{\partial \xi}\right)^2 \frac{k_3^2}{\gamma^2} \left\{\beta^2 + k_1^2\left[\alpha_\ell^2 \beta^2 + \frac{\alpha_\ell B (K_\ell)^{1/2} \beta}{2} + \frac{B^2 K_\ell}{16}\right]\right\} \Phi_{ff}(\underset{\sim}{k}) \quad (4.18)$$

where

$$\beta = \left[k_2^2 + k_3^2\right] / \left[k_1^2 + k_2^2 + k_3^2\right]$$

and

$$\gamma = \alpha_\ell k_1^2 + \alpha_t (k_2^2 + k_3^2) \quad .$$

Thus the variance of the w' process can be found by evaluating the integral expression

$$\sigma_w^2 = \left(\frac{\partial \bar{c}}{\partial \xi}\right)^2 \left\{ L_1 + L_2 + \frac{L_3}{2(1+5\sigma_f^2/8)} + \frac{L_4}{16(1+5\sigma_f^2/8)^2} \right\} , \quad (4.19)$$

$$L_1 = \iiint_{-\infty}^{\infty} \frac{k_3^2 \beta^2}{\gamma^2} \Phi_{ff}(\underset{\sim}{k}) d\underset{\sim}{k} \quad , \quad (4.20a)$$

$$L_2 = \alpha_\ell^2 \iiint_{-\infty}^{\infty} \frac{k_1^2 k_3^2 \beta^2}{\gamma^2} \Phi_{ff}(\underset{\sim}{k}) d\underset{\sim}{k} \quad , \quad (4.20b)$$

$$L_3 = \alpha_\ell^2 \iiint_{-\infty}^{\infty} \frac{k_1^2 k_3^2 \beta}{\gamma^2} \Phi_{ff}(\underset{\sim}{k}) d\underset{\sim}{k} \quad , \quad (4.20c)$$

and $$L_4 = \alpha_\ell^2 \iiint\limits_{-\infty}^{\infty} \frac{k_1^2 k_3^2}{\gamma^2} \Phi_{ff}(\underset{\sim}{k})\, d\underset{\sim}{k} \tag{4.20d}$$

where we have again made use of equation (4.16) and the assumption that $\alpha_\ell \approx \bar{\alpha}_I$. As in the previous paragraph, the simplified spectrum (4.13) is used to evaluate integrals (4.20) which, after conversion to spherical coordinates, gives the results

$$L_1 = \frac{3}{8} \sigma_f^2 \frac{\ell^2}{\alpha_t^2} \left\{ \frac{\rho[1+\psi]^4}{2} + \psi^2\left[\frac{73}{15} + \frac{22}{3}\psi + 3\psi^2\right] \right.$$

$$\left. + (\psi^{1/2}/2)\left[1 - 4\psi - 18\psi^2 - 20\psi^3 - 7\psi^4\right] \tan^{-1}\left[1/\psi^{1/2}\right] \right\}, \tag{4.21a}$$

$$L_2 = \frac{9}{8} \sigma_f^2 \left\{ -\frac{\psi^2}{\rho^2}\left[\frac{93}{35} + \frac{146}{15}\psi + 11\psi^2 + 4\psi^3\right] - \frac{\psi}{\rho}\frac{[1+\psi]^4}{2} \right.$$

$$\left. + \frac{\psi^{3/2}}{2\rho^2}\left[1 + 12\psi + 30\psi^2 + 28\psi^3 + 9\psi^4\right] \tan^{-1}\left[1/\psi^{1/2}\right] \right\}, \tag{4.21b}$$

$$L_3 = \frac{9}{8} \sigma_f^2 \left\{ -\frac{\psi^2}{\rho^2}\left[\frac{11}{5} + \frac{16}{3}\psi + 3\psi^2\right] - \frac{\psi}{\rho}\frac{[1+\psi]^3}{2} \right.$$

$$\left. + \frac{\psi^{3/2}}{2\rho^2}\left[1 + 9\psi + 15\psi^2 + 7\psi^3\right] \tan^{-1}\left[1/\psi^{1/2}\right] \right\}, \tag{4.21c}$$

and $$L_4 = \frac{9}{8} \sigma_f^2 \left\{ -\frac{\psi^2}{\rho^2}\left[\frac{5}{3} + 2\psi\right] - \frac{\psi}{\rho}\frac{[1+\psi]^3}{2} \right.$$

$$\left. + \frac{\psi^{3/2}}{2\rho^2}\left[1 + 6\psi + 5\psi^2\right] \tan^{-1}\left[1/\psi^{1/2}\right] \right\}. \tag{4.21d}$$

By making the same assumption leading to equation (4.17), we obtain the approximation

$$\sigma_w^2 \sim \left(\frac{\partial \bar{c}}{\partial \xi}\right)^2 \sigma_f^2 \left\{ \frac{0.3\,\ell^2 \psi^{1/2}}{\alpha_t^2} + \frac{4}{\rho^{1/2}} - 5 \right\} \tag{4.21}$$

for equation (4.19).

The variance for the q_3' process can be obtained from equation (4.6) by substituting for dZ_ϕ from equation (3.18). After multiplying this result by its complex conjugate and taking expected values, one obtains the spectral relationship

$$\Phi_{q_3 q_3}(\underset{\sim}{k}) = \frac{k_1^2 k_3^2 \bar{q}_1^2}{[k_1^2 + k_2^2 + k_3^2]^2} \Phi_{ff}(\underset{\sim}{k}) \tag{4.22}$$

where we again use the simplified form (4.13) for the spectrum of the f' process. Forming the inverse Fourier transform evaluated at zero lag, the integral form for the variance of the q_3' process is found:

$$\sigma_{q_3}^2 = \bar{q}_1^2 \iiint_{-\infty}^{\infty} \frac{k_1^2 k_3^2}{[k_1^2 + k_2^2 + k_3^2]^2} \Phi_{ff}(\underset{\sim}{k}) \, d\underset{\sim}{k} \tag{4.23}$$

which, upon evaluation, gives the result

$$\sigma_{q_3}^2 = \frac{9}{105} \bar{q}_1^2 \sigma_f^2 \quad . \tag{4.24}$$

We are now in a position to form the correlation coefficient for the q_3' process and w' process. Using approximations (4.17) and (4.21), as well as equation (4.24) we find

$$\frac{\overline{q_3' w'}}{\sigma_{q_3} \sigma_{w'}} = \frac{\frac{\partial \bar{c}}{\partial \xi} \bar{q}_1 \sigma_f^2 \left[1 - \frac{\pi \psi^{1/2}}{2}\right]}{0.3 \frac{\partial \bar{c}}{\partial \xi} \sigma_f^2 \bar{q}_1 \left[\frac{0.3 \ell^2 \psi^{1/2}}{\alpha_t^2} + \frac{4}{\rho^{1/2}} - 5\right]^{1/2}}$$

$$< \frac{6 \alpha_t}{\ell \psi^{1/4}} \quad . \tag{4.25}$$

As we suspect that in general $\ell >> \alpha_t$ (see Glahar, et al., 1977, for an estimate of ℓ), the quantity on the right-hand side of equation (4.25) should be much less than one. Thus, we can now argue that the product of the standard deviations is a valid estimator of term (4.1). Even if the w' process and the q_3' process were perfectly correlated, by assuming joint normality of the two processes, we could demonstrate, through the use of moment generating functions (Ross, 1972, p. 44), that this type of estimate for the variance of q'w' could not be in error by more than a factor of two.

Proceeding, then, to estimate term (4.1), first by disregarding $\overline{q_3'w'}$ (the variance of a constant is zero), and then by using the square root of approximation (4.17) and equation (4.24), we expect

$q_3'w'$ is on the order of

$$\sigma_{q_3}\sigma_{w'} \sim 0.3 \frac{\partial \bar{c}}{\partial \xi} \sigma_f^2 \bar{q}_1 \left[\frac{0.3\,\ell^2 \,\Psi^{1/2}}{\alpha_t^2} + \frac{4}{\rho^{1/2}} - 5\right]^{1/2} . \tag{4.26}$$

This term must be compared with retained term (4.2). We therefore must obtain a variance estimate for the q_1' process. From equation (3.19) we obtain the spectral relationship

$$\Phi_{q_1q_1}(\underset{\sim}{k}) = \bar{q}_1^2 \left[\frac{k_3^2 + k_2^2}{k_1^2 + k_2^2 + k_3^2}\right]^2 \Phi_{ff}(\underset{\sim}{k}) \quad . \tag{4.27}$$

Evaluating this equation for the variance $\sigma_{q_1}^2$, using spectrum (4.13) as before, the expression

$$\sigma_{q_1}^2 = \frac{24}{35} \bar{q}_1^2 \sigma_f^2 \tag{4.28}$$

is obtained. The standard deviation from this expression is used to extimate q_1' in the retained term (4.2). The retained term should be significantly larger than the neglected term (4.1) in order that the first-order analysis be valid. In particular, we expect

$$\frac{q_3' w' - \overline{q_3' w'}}{q_1' \overline{w}} \quad \text{is on the order of} \quad \frac{\sigma_{q_3} \sigma_w}{\sigma_{q_1} \overline{w}} < 1 . \tag{4.29}$$

A reasonable approximation of the ratio is

$$\frac{\sigma_{q_3} \sigma_w}{\sigma_{q_1} \overline{w}} \sim 0.2\, \sigma_f \, \frac{\ell \, \psi^{1/4}}{\alpha_t} . \tag{4.30}$$

If we assume values of ℓ = 1.0 meter, α_T = 0.01 meter and Ψ = 0.2 then, upon solving for σ_f, we find

$$\sigma_f < 0.075 \tag{4.31}$$

which is very restrictive (cf. Freeze, 1975). In part, the excessive nature of this restriction may be related to the first-order analysis upon which it is based. Nevertheless, for an aquifer in which the heterogeneities are completely isotropic, we doubt that the analysis pursued in this dissertation is viable. However, as the heterogeneities become more stratiform, one would expect the numerator in ratio (4.29) to become small since perturbations in specific discharge for other than the x_1 direction do not exist in stratified aquifers. Thus, for quasi-stratified aquifers we suspect that the variance in the f' process over which the first-order analysis is applicable would be larger than that indicated by (4.31). In reality, the region of applicability of the three-dimensional analysis is a function of both the correlation length scales as well as the variability of the medium. For a moderately stratified medium, the author suspects that a σ_f on the order of one-half will allow use of the three-dimensional analysis outlined in this report in order to predict global dispersivities. The region of acceptability for the three-dimensional analysis, however, is a point which warrants further invesitgation.

For the one-dimensional flow case, only a term similar to expression (2.38) was neglected. As the perturbation in concentration may change rapidly in the x_3 direction, this term could be significant if the variance in medium properties is also great. In general, however, we believe that neglecting this term is less important than neglecting term (2.29c), as it represents mass transfer which is Fickian in nature, and not convective. If one were to hazard an estimate, we suspect that neglecting this term may restrict us to media which have a coefficient of variation $[\sigma_K/\bar{K}]$ of unity or less.

Qualification of Long-Term Process

In the section entitled "First-Order Analysis," it was noted that, because of the slowly varying nature for the long-term process of the dispersion phenomenon, the time derivative (2.30) could be neglected. The deletion of this term from the model equation is effected through the assumption that changes in tracer concentration are more dependent on convective transport, when considered with respect to a moving coordinate system, than on time (provided sufficient time has elapsed). We find it desirable to estimate, roughly, what travel time or travel distance is involved before the slowly varying concept is acceptable.

To form an estimate, we consider that the neglected term (2.30) is much smaller than the convective term

$$\left[q_1' - \frac{\bar{q}_1}{\bar{n}} n' \right] \frac{\partial \bar{c}}{\partial \xi} \quad . \tag{4.32}$$

Thus, noting that medium properties are independent of time, we form the ratio

$$\left| \frac{\bar{n}\, \partial c'/\partial t}{\left[q_1' - n'\bar{q}_1/\bar{n} \right] \partial \bar{c}/\partial \xi} \right| << 1 \tag{4.33}$$

where we have taken the term $n'\partial\bar{c}/\partial t$ to be second order. As in the previous section, we form variance approximations for both numerator and denominator of ratio (4.33) in order to estimate the primed quantities. In this regard, we resort to use of the equations for the stratified or one-dimensional flow case in order to simplify the analysis.

As noted previously in the section entitled "One-Dimensional Flow Case," one can construct, for the one-dimensional flow case, a spectral relationship to predict the variance in concentration from the model equation (2.43). Writing this expression in terms of complex Fourier amplitudes, multiplying by its complex conjugate and taking expected values, we arrive at the spectral relationship:

$$\Phi_{cc}(k) = \frac{\left[\partial \bar{c}/\partial \xi\right]^2}{\bar{E}_t^2 k^4} \left\{ \Phi_{q_1 q_1}(k) - \left[2\,\Phi_{q_1 n}(k) - \Phi_{nn}(k) \right] \frac{\bar{q}_1}{\bar{n}} \right\} \tag{4.34}$$

where $k = k_3$. The spectrum $\Phi_{q_1 q_1}$ can be replaced by transfer function (3.24). We replace spectrum $\Phi_{q_1 n}$ by transfer function (3.39) and can easily construct a transfer function for Φ_{nn} from equation (3.38); however, we assume σ_n to be small in both cases. Substituting these transfer functions into equation (4.34) and then proceeding to take the inverse Fourier transform evaluated at zero lag, we obtain the integral expression

$$\sigma_c^2 = \frac{[\partial\bar{c}/\partial\xi]^2}{\bar{K}\,\alpha_t^2}\left[\frac{2}{3-\bar{n}}\right]^2 \int_{-\infty}^{\infty} \frac{\Phi_{kk}(k)}{k^4}\,dk \quad . \tag{4.35}$$

As noted previously, a spectrum of the form (3.57) is necessary to evaluate this integral. Precisely, this spectrum gives the result

$$\sigma_c^2 = \frac{[\partial\bar{c}/\partial\xi]^2}{\alpha_t^2}\left[\frac{2}{3-\bar{n}}\right]^2 a^4\left[\sigma_K/\bar{K}\right]^2 \quad . \tag{4.36}$$

Similarly, from transfer function (3.24) and a transfer function constructed from equation (3.38), we can derive variance expressions for the q_1' process and n' process, giving the results

$$\sigma_{q_1}^2 = \bar{q}_1^2\left[\sigma_K/\bar{K}\right]^2 \tag{4.37}$$

and $$\sigma_n^2 = \left[\frac{1-\bar{n}}{3-\bar{n}}\right]^2 \bar{n}^2\left[\sigma_K/\bar{K}\right]^2 \quad . \tag{4.38}$$

The standard deviations, obtained by taking the square root of variances (4.36), (4.37) and (4.38), become estimators for the primed quantities in (4.33).

With the information in the previous paragraph, an estimate of the ratio in equation (4.33) can be constructed by noting that $c'(t)$, linearized in t for small time, is approximately $t[\partial c'/\partial t]$: hence

$$\sigma_c \approx t\,\sigma_\tau \ , \ \tau = \partial c'/\partial t$$

and $\sigma_\tau \approx \partial[\sigma_c]/\partial t$. (4.39)

After substitution of appropriate estimators for primed quantities, we expect

$$\frac{\bar{n}\,\partial c'/\partial t}{[q_1' - n'\bar{q}_1/\bar{n}]\,\partial\bar{c}/\partial\xi} \quad \text{is on the order of} \quad \frac{\bar{n}a^2}{\bar{q}_1\alpha_t}\,\frac{\partial[\partial\bar{c}/\partial\xi]/\partial t}{\partial\bar{c}/\partial\xi} \ . \qquad (4.40)$$

Plainly, we will need estimates for derivatives of $\bar{c}$ before we can complete the ratio. These estimates may be obtained by considering the solution of the convective-dispersion equation for uniform flow with no sources or sinks:

$$\bar{n}\,\frac{\partial\bar{c}}{\partial t} + \bar{q}_1\,\frac{\partial\bar{c}}{\partial x_1} = D_\ell\,\frac{\partial^2\bar{c}}{\partial x_1^2} \qquad (4.41)$$

where D_ℓ is the effective global longitudinal dispersion coefficient. A solution of this equation for a pulse input is

$$\bar{c} = S\,t^{-1/2}\exp\left[-\xi^2/4D_\ell t\right] \qquad (4.42)$$

where S is a constant. Taking the appropriate derivatives of equation (4.41) and substituting into equation (4.39), we expect

$$\frac{\bar{n}\,\partial c'/\partial t}{[q_1' - n'\bar{q}_1/\bar{n}]\,\partial\bar{c}/\partial\xi} \quad \text{is on the order} \quad \frac{\bar{n}a^2}{\bar{q}_1\alpha_t}\left[\frac{2\xi^2 - 12D_\ell t}{8D_\ell t^2}\right] \ . \qquad (4.43)$$

From equation (4.41), ξ^2 must be on the order of $4D_\ell t$ in order that the solution concern itself with the principal part of the longitudinal mass transfer. Thus, we approximate the term in brackets on the right hand side as t^{-1}, allowing us to write ratio (4.33) as

$$t \gg \frac{\bar{n}\, a^2}{\bar{q}_1 \alpha_t} \; . \tag{4.44}$$

From our solution (3.59) for the global longitudinal dispersivity using spectrum (3.57), we may rewrite inequality (4.44) in terms of the distance $\bar{q}_1 t/\bar{n}$ necessary for a slowly varying process to become established:

$$\frac{\bar{q}_1 t}{\bar{n}} \gg \frac{3 A_\ell}{[2/(3-\bar{n})][\sigma_K/\bar{K}]^2}$$

or simply

$$\frac{\bar{q}_1 t}{\bar{n}} \gg \frac{A_\ell}{[\sigma_K/\bar{K}]^2} \; . \tag{4.45}$$

Thus, it is apparent that before the Taylor assumption becomes valid, it is necessary for the tracer to have traveled a distance equivalent to several global longitudinal dispersivities.

Result (4.45) is significant also from a planning point of view. To the extent that the analysis presented in this study can be ergodically applied to a single realization, longitudinal dispersivities calculated from a field situation will only be valid if the experimental apparatus meets this criterion. If this condition is not allowed for in field installations, then the dispersivity obtained from tracer recovery tests may be time dependent because the lateral component of mass transfer has not had sufficient travel time in which to establish itself.

Finally, we note that expression (4.45) could serve as an alternate definition of the global length scale mentioned in the introductory chapter. As noted therein, this scale is defined as the travel distance, in a globally heterogeneous medium, which is necessary before many medium parameters become meaningful. With respect to a field longitudinal dispersivity, inequality (4.45) is a criterion for obtaining this condition.

Comparisons Between Results

As mentioned earlier in the section entitled "Three-Dimensional Flow Case," equation (3.68) gives a global longitudinal dispersivity for the unstratified case which has an asymptotic one-dimensional limit for flow parallel to stratification. From Figures 3.5 and 3.6 we see that the factors $F^\circ(\rho,R^\circ)$ and $G^\circ(\rho,R^\circ)$ become unity as R° becomes large, which is equivalent to forcing the medium to become stratified. If the porosity term P resulting from the Kozeny-Carmen equation is used in the asymptotic equivalent of equation (3.68), then we obtain the result

$$\lim_{R^\circ \to \infty} A^\circ_{\ell 3} = \frac{\ell_3^2 \sigma_f^2}{\alpha_t} \frac{2}{3-\bar{n}} \quad . \tag{4.46}$$

On the other hand, if σ_n is taken to be small, then the global longitudinal dispersivity (3.59) for the one-dimensional flow case, using the simpler spectrum (3.56), can be written

$$A_\ell = \frac{\ell^2}{\alpha_t} \frac{\sigma_K^2}{\bar{K}^2} \frac{2}{3-\bar{n}} \quad . \tag{4.47}$$

Since the autocovariance function of spectrum (3.56) is the asymptotic one-dimensional equivalent of the function of spectrum (3.66), which was used to solve the three-dimensional equation (3.59), we may assume that length scales ℓ and ℓ_3 are equal. Thus, the principal difference between the direct and asymptotic one-dimensional results (4.46) and (4.47) is a factor concerning the variability in hydraulic conductivity of the medium.

If it is assumed that hydraulic conductivities are lognormally distributed then, with the aid of Appendix 2, we may make a comparison between the coefficient of variation $\sigma_K/\bar{K}$ and the variance σ_f. In particular, from equation (2b) in Appendix 2, we write

$$\sigma_K^2/\bar{K}^2 = \exp\left[\sigma_f^2\right] - 1 \quad . \tag{4.48}$$

Expanding the exponent in a Maclaurin series and truncating all terms with powers greater than two, the approximation

$$\sigma_K^2/\bar{K}^2 \approx \sigma_f^2 \tag{4.49}$$

is obtained. Thus the standard deviation of the normal process f is an estimate of the coefficient of variation of the lognormal K process, provided σ_f is small.

We recall that the derivation of the one-dimensional equation necessitated very few linearizing assumptions. Hence, the fact that the asymptotic and direct one-dimensional results differ by the same order-of-magnitude approximation used in the derivation of the three-dimensional case indicates the validity of this latter case. Indeed, as indicated in the section entitled "Limitations of First-Order Analysis," as the medium becomes more stratified, we expect the three-dimensional results to become more representative of the global dispersivity over a larger range of σ_f. For this extreme asymptotic case, by assuming that our direct one-dimensional result is essentially exact, we can estimate its associated error by comparing equations (4.48) and (4.49). In particular, for a σ_f of unity, this error is about 42%; for σ_f equal one-half, the error is about 12%. Thus some justification for citing σ_f of approximately one-half as an appropriate upper limit (for moderately stratified media) for the range of σ_f over which our three-dimensional results are valid is found here.

We also wish to make a comparison between the three-dimension results (3.67) and (3.68) which use spectra of the simple and modified negative-exponential autocovariance functions, respectively. We have noted, however, that the vertical profiles of these autocovariance functions have shapes which are rather different (see Figure 3.2). If actual field data were available such that either shape, due to the scatter in data points, could be fit to the data with a fair degree of confidence, then we would find that the condition

$$\ell_3 \approx 5\,\lambda_3/2 \tag{4.50}$$

must be satisfied (Bakr, 1976, p. 129). Since this is a desirable condition to approximate when making comparisons between results using different spectra, we will modify the global dispersivity $A_{\ell 3}^{\circ}$ to reflect equation (4.50). After deleting the porosity factor $G^{\circ}(\rho, R^{\circ})$ in order to simplify the comparison, equation (3.68) becomes

$$A_{\ell_3}^{\circ} = \frac{\lambda_3^2 \sigma_f^2}{\alpha_t} \hat{F}^{\circ}(\rho, R) \tag{4.51}$$

where

$$\hat{F}^{\circ}(\rho, R) = \frac{25}{4} F^{\circ}\left(\rho, \frac{2}{5} R\right)$$

which we compare to a similar porosity-deleted version of equation (3.67):

$$A_{\ell 3} = \frac{\lambda_3^2 \sigma_f^2}{\alpha_t} F(\rho, R) \quad . \tag{4.52}$$

Thus, by plotting hydraulic conductivity factors $\hat{F}^{\circ}(\rho,R)$ and $F(\rho,R)$ for the same values of ρ and R, we may compare $A_{\ell 3}{}^{\circ}$ and $A_{\ell 3}$ (note that the horizontal length scales are equal for spectra of both cases). This procedure has been followed in Figure 4.1 for $\rho = 0.1$. It is seen that the hydraulic conductivity factors are reasonably similar in the region of R equal unity, but when the ratio of horizontal to vertical length scales become larger than a factor of 10.0, their difference grows rapidly. These results, plus the restrictive σ_f limitations discussed previously for R equal to unity and the natural one-dimensional limit for $A_{\ell 3}{}^{\circ}$ lead us to favor the spectrum of the modified nagative-exponential autocovariance function for the solution of the three-dimensional flow case. However, until comparisons have been made between experimental results at field sites and spectral analyses of continuous hydraulic conductivity data from these same sites, no potential spectrum should be ruled out.

As a final comparison in this section, we do a sample calculation using what we consider to be typical parameter values that might be encountered in a field situation. Additionally, we make use of approximation (4.50), as we wish to assume that all data, including our spectral estimates, are equivalent. Thus, we base our analysis around equation (3.67) and adjust equation (3.68) (as was done for equation (4.51))

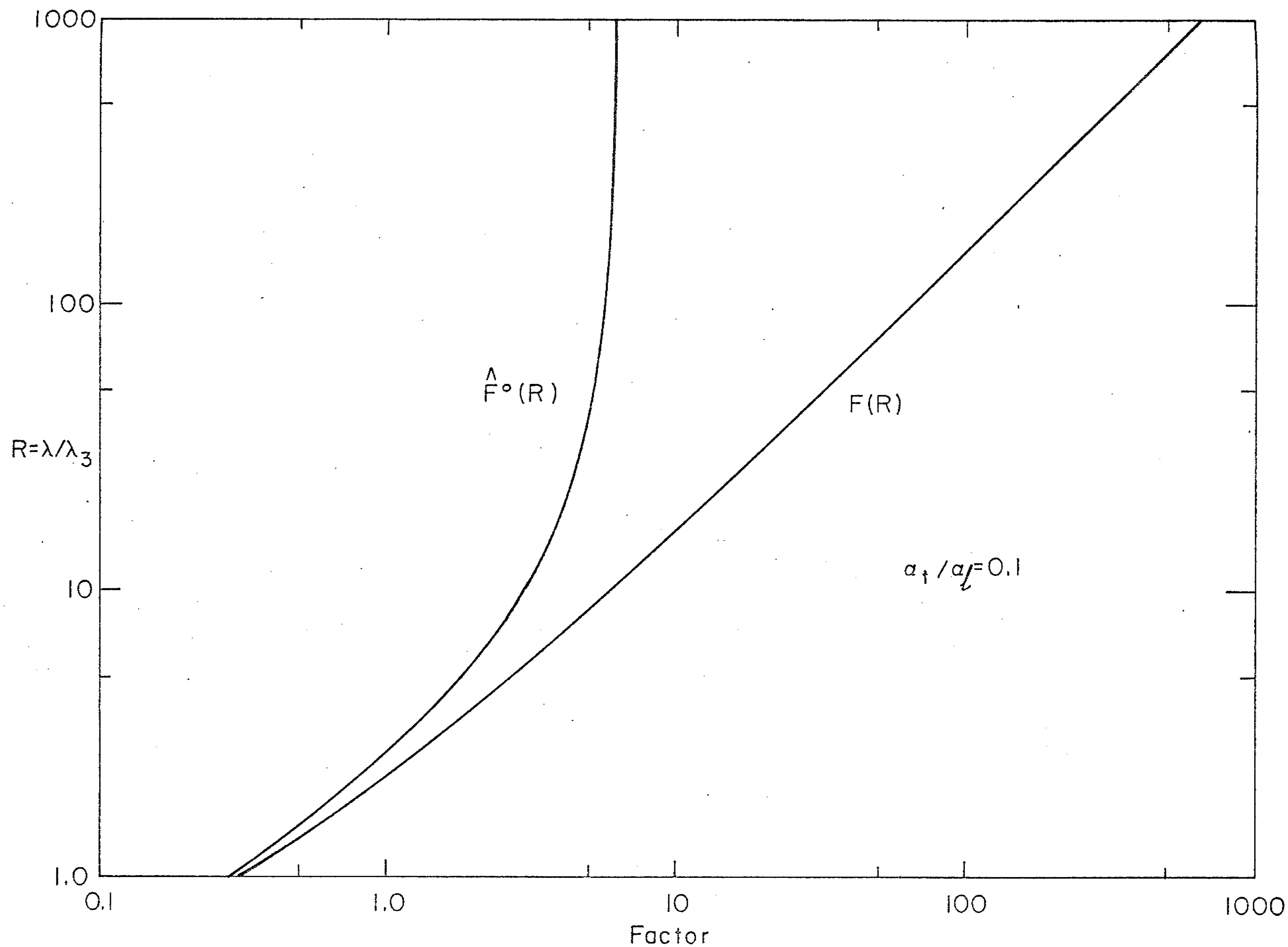

Figure 4.1. Comparison of hydaulic conductivity factors for three-dimensional flow case.

so that all calculations have a common correlation length scale ratio $R = \lambda/\lambda_3$. We also use equation (4.50) to adjust the one-dimensional case (3.59), solved with spectrum (3.56), to the same data base. These results are noted in Table 4.1, along with actual values used in the solution process. We have intentionally chosen, for the three-dimensional flow case, an aquifer in which the medium is moderately stratified ($R = 10.0$) and have selected a maximum standard deviation for the logarithm of conductivity ($\sigma_f = 0.5$) in order that a comparison can be made between the one-dimensional case and the three-dimensional cases. We note immediately the two-fold difference between the three-dimensional cases using spectra of modified and simple autocovariance functions. However, the result $A_{\ell 3}$ for the spectrum of the simpler function is rather close to the one-dimensional case. These sample calculations tend to reinforce the conclusion of the previous paragraph: even for this moderately stratified case, which the author suspects to be in an acceptable region of application, the spectrum of the modified autocovariance function gives results which are significantly different from and, in light of the previous discussion, probably more acceptable than the results from spectrum of the simple function. However, for a simple order-of-magnitude estimate of the global dispersivity, the one-dimensional result (3.59) may be sufficient. This last subject shall constitute part of the discussion of the next section.

Sensitivity of Results

In this section, we wish to explore the effects of variations in ρ and R (or $R°$) on our results. In particular, as our solution mode has provided for continuous variation in R, we desire to examine the effect of other values of the effective local dispersivity ratio ρ. Again, in

Table 4.1. Sample Calculation Comparison between Various Dispersivity Equations.

equation	spectrum	$F(\rho,R)$ or $\hat{F}^{\circ}(\rho,R)$	$G(\rho,R)$ or $\hat{G}^{\circ}(\rho,R)$	global dispersivity (meters)
(3.67) $A_{\ell 3}$	(3.64)	5.96	6.46	99
(3.68) $A_{\ell 3}{}^{\circ}$	(3.66)	2.96	3.07	50
(3.59) A_{ℓ}	(3.56)	1.0	1.0	122

$P = \dfrac{1-\bar{n}}{3-\bar{n}}$, σ_n taken small ,

$\sigma_f = 0.50$, $\rho = 0.1$, $\lambda_3 = 1.0$ meters ,

$\alpha_t = 0.01$ meters , $\bar{n} = 0.1$, $R = 10.0$.

order to simplify the analytical procedure, we assume all length scales to be equal (R = 1.0) and will neglect the porosity factor $G(\rho,R)$. Then using the spectrum of the simple negative-exponential autocovariance function (3.64), we write the global dispersivity equation (3.67) for the above conditions:

$$A_{\ell 3} = \frac{\lambda^3 \sigma_f^2}{\pi^2} \iiint_{-\infty}^{\infty} \left[\frac{k_2^2 + k_3^2}{k_1^2 + k_2^2 + k_3^2}\right]^2 \frac{1}{\left[\alpha_\ell k_1^2 + \alpha_t (k_2^2 + k_3^2)\right]} \cdot \frac{d\underset{\sim}{k}}{\left[\lambda^2 (k_1^2 + k_2^2 + k_3^2) + 1\right]^2} \qquad (4.53)$$

The solution of equation (4.53) can be obtained by transforming to spherical coordinates, after which the expression

$$A_{\ell 3} = \frac{\lambda^2 \sigma_f^2}{\alpha_t} F(\rho) \qquad (4.54)$$

where

$$F(\rho) \begin{cases} \dfrac{[1+\psi]^2}{2} [-\psi]^{1/2} \ln \left[\dfrac{(-\psi)^{1/2} + 1}{(-\psi)^{1/2} - 1}\right] - \psi \left[\dfrac{5}{3} + \psi\right], & \rho > 1 \\ \dfrac{8}{15}, & \rho = 1 \\ [1+\psi]^2 [\psi]^{1/2} \tan^{-1}\left[\psi^{-1/2}\right] - \psi\left[\dfrac{5}{3} + \psi\right], & \rho < 1 \end{cases}$$

and $\Psi = \rho/[1-\rho]$

is obtained. The hydraulic conductivity factor $F(\rho)$ has been plotted in Figure 4.2. From theoretical (Haring and Greenkorn, 1970) and experimental (Blackwell, 1962; Harleman and Rumer, 1963) results, we suggest that the local effective dispersivity ratio could range from about 0.03 to 0.3. In this range, the largest change in $F(\rho)$ occurs; however, because of the logarithmic nature of the change, $F(\rho)$ only varies by a factor of about 2.0 over this entire range. Thus, we conclude that $A_{\ell 3}$ is not extremely sensitive to ρ and that a sufficient estimate of the hydraulic conductivity factor for values of ρ at other than those values given in Figures 3.3, 3.4, 3.5, and 3.6 can be obtained from interpolation between these figures and Figure 4.2.

Finally, we wish to ascertain what the relative error would be if the global dispersivity (3.59) with spectrum (3.56) from the one-dimensional flow case were used in place of $A_{\ell 3}{}^{\circ}$ (equation (3.68)) uniformly, for all R°. In order to construct this comparison, we have used the parameter values from Table 4.1 in the previous section, with the exception that we have taken ℓ_3 equal to one meter, and have calculated $A_{\ell 3}{}^{\circ}$ for multiple values of R°. These results are plotted in Figure 4.3, showing $A_{\ell 3}{}^{\circ}$ versus R° (some error has been introduced by using a maximum value of σ_f over the entire range of R°). Additionally, by using the same parameters for A_{ℓ}, we have calculated the relative error involved in using A_{ℓ} instead of $A_{\ell 3}{}^{\circ}$, placing this result on the same figure. For R° greater than 20, the error is generally less than 20%; however, for R° equal to two, the error is approximately 250%. Thus, to the extent that the spectrum of the modified negative-exponential autocovariance function can be used to solve the three-dimensional flow case, we can conclude that, for most obviously stratified aquifers, the one-dimensional equation (3.59) using the simpler spectrum (3.56) will

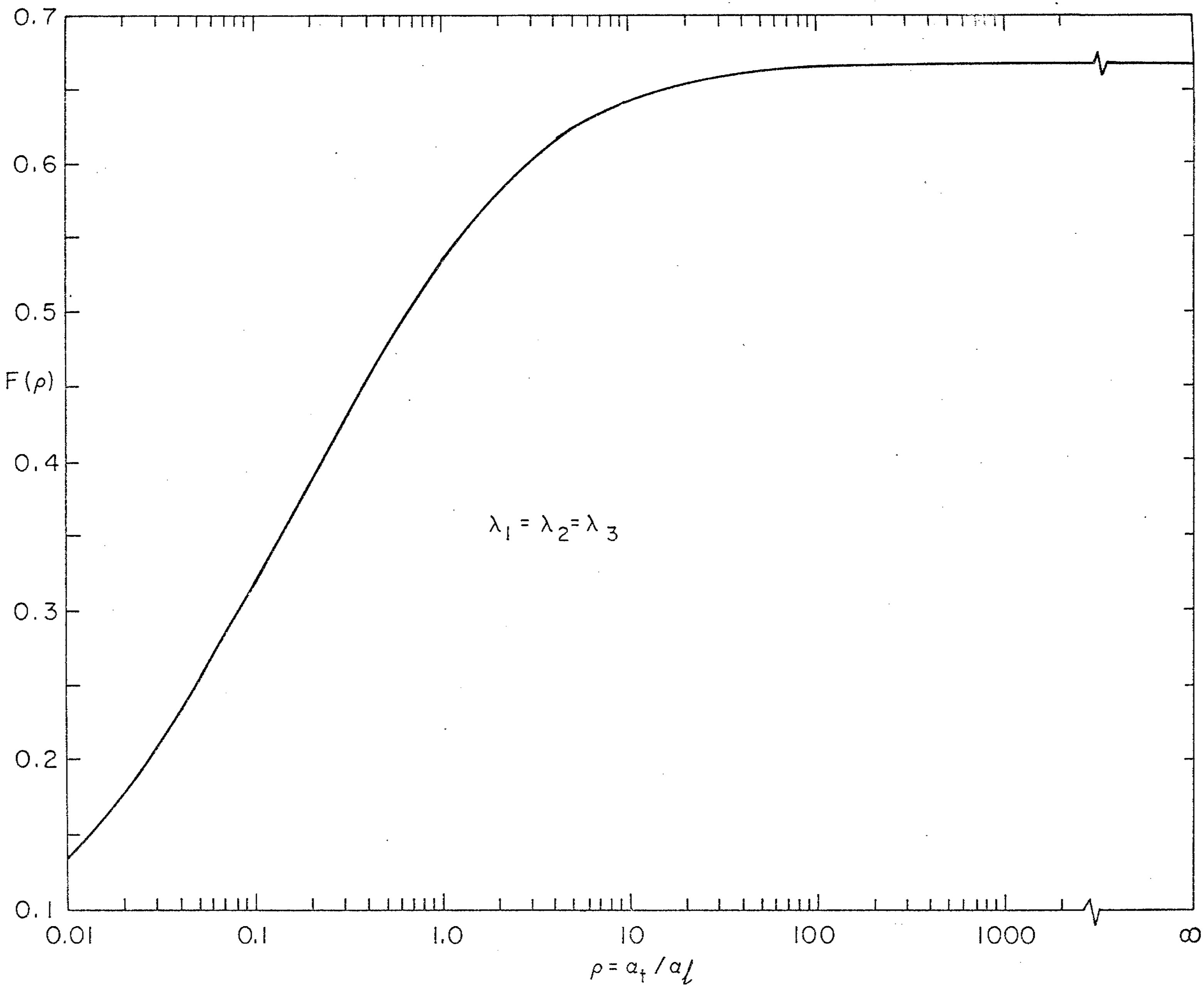

Figure 4.2. Hydraulic conductivity factor as function of local dispersivity ratio.

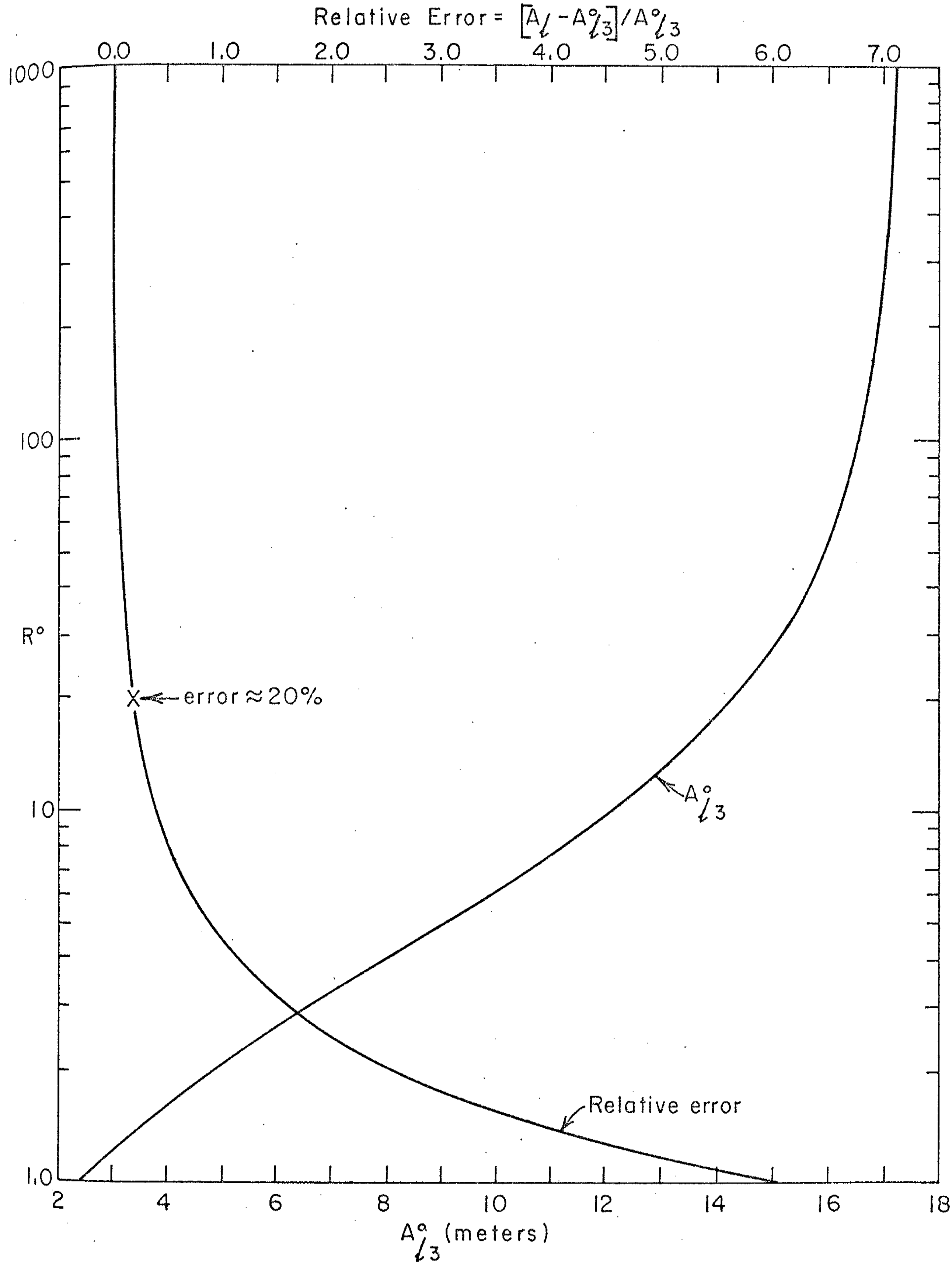

Figure 4.3. Comparison between one-dimensional and three-dimensional results.

give a sufficient estimate of the global longitudinal dispersivity. For aquifers which fall into the nebulous region around $R°$ equal to ten, an estimate of the horizontal correlation length scale should be obtained. This subject will be pursued further in the next section.

Application of Results

Throughout much of the discussion in this section, we make liberal use of the concept of ergodicity (Appendix 1). We simply do not have data from, nor are we interested in, multiple realizations of tracer experiments in probabilistically similar media. Typically, we are concerned with the spreading of a pollutant in a particular aquifer. Ergodicity allows us to assume that statistical parameters obtained from intensively sampling a single realization are equivalent to ensemble parameters. Thus, in the following paragraphs, we will concern ourselves with data obtained from a single realization, keeping the concept of ergodicity in the back of our minds.

In the section entitled "One-Dimensional Flow Case," it was assumed from equation (3.53) that a quantity α_t exists such that

$$\alpha_t = \overline{E}_t / \overline{q}_1 \quad . \tag{4.55}$$

The quantity α_t was referred to as the effective local transverse dispersivity and represents the average local transfer of mass resulting from local dispersion. As the global longitudinal dispersivity is inversely proportional to this quantity, it is imperative to have a good estimator of α_t. We will suggest a number of possible means by which this quantity could be estimated; however, we feel that this is a point which merits further investigation if the method is to obtain acceptance.

An obvious method of obtaining transverse dispersivities is to make laboratory measurements on cores. This suggestion is fraught with difficulties as it is usually necessary to inject two fluids at the same time in order that a steady-state distribution of tracer concentration be obtained. A device which may be adaptable for undisturbed cores has been developed by Hassinger and Rosenberg (1968), provided that the grain-size distribution is such that the boundary conditions of the solution are not exceeded. Assuming that it is indeed possible to obtain cores and measure transverse dispersivity at this scale, then yet another question remains concerning the method of averaging necessary to produce an "effective" local dispersivity necessary to sustain equation (4.55). (We assume throughout this discussion that measurements at a core scale are representative of the local phenomenon.) In particular, from equation (4.55), we note that

$$\alpha_t = \overline{\alpha_{II} q_1} / \bar{q}_1 = \left[\overline{\alpha_{II}}\, \bar{q}_1 + \overline{\alpha'_{II} q'_1} \right] / \bar{q}_1 \tag{4.56}$$

after the appropriate perturbation expressions have been substituted for α_{II} and q_1. If we assume that the covariance between α_{II} and q_1 is small, then the appropriate estimator for α_t is simply the arithmetic mean of $\bar{\alpha}_{II}$ (note that a similar approximation was made in the formulation of equation (4.12): $\alpha_\ell \approx \bar{\alpha}_I$). We suspect that this assumption is a reasonable approximation when variability in medium properties is small; however, it may be advisable for future investigators to examine this covariance in detail.

As undisturbed cores are frequently difficult to obtain, we also look at other methods of predicting α_t. Frequent attempts have been made to relate both lateral and longitudinal dispersivities to the median (50%) grain size, d_{50}, which could be determined from sieve analysis of material obtained from the medium. In particular, because of the frequently proposed linear relationship between α_I and d_{50}, we propose that a similar relationship

$$\alpha_{II} = B_1 d_{50} \quad , \tag{4.57}$$

where B_1 is a material constant, could be used for the transverse dispersivity. Harleman and Rumer (1963), from results of laboratory experiments have indicated that the relationship between α_{II} and d_{50} may be other than linear. However, because of the limited number and type of data points used, their results cannot be considered conclusive.

Another frequently noted relationship in the literature is

$$K = A\left[d_{50}\right]^2 \tag{4.58}$$

(Bear, 1972, p. 133). For the one-dimensional case, using equation (2.6b), we may estimate the mean transverse coefficient $\bar{E}_t$ as

$$\bar{E}_t = AB_1 J\overline{\left[(d_{50})^3\right]} \quad . \tag{4.59}$$

If we assume a perturbation expression for d_{50} similar to equation (2.8), then upon expanding expression (4.59) and truncating the cubic term, we obtain

$$\bar{E}_t \approx \bar{q}_1 B_1 \overline{d_{50}}\left[1 + 3\left(\sigma_{d_{50}}/\overline{d_{50}}\right)^2\right] \quad . \tag{4.60}$$

Thus, the effective dispersivity α_t can be expressed as

$$\alpha_t = B_1 \overline{d_{50}} \left[1 + 3 \left(\sigma_{d_{50}} / \overline{d_{50}} \right)^2 \right] . \tag{4.61}$$

Equation (4.61) indicates the importance of not assuming a direct relationship between the effective parameter α_t and the mean of the median grain size $\bar{d}_{50}$. For the three-dimensional case, a similar expression can be developed using the logarithm of the K process; however, the analysis would entail finding an expression for the covariance of the d_{50}' and $\partial\phi'/\partial x_1$ processes.

Before the above method could be applied to a particular aquifer, it would be necessary to determine the material constant B_1 for the medium in question. This may be a rather tedious process until a sufficient body of literature is built up. Indeed, it may even be futile, as Klotz (1973) also notes a strong influence of the uniformity coefficient μ ("Ungleichförmigkeitsgrad") on the longitudinal coefficient. We suspect the existence of a similar influence of μ on the transverse coefficient. In fact, it may be more profitable to investigate the possibility of the form

$$\alpha_{II} = B_1 d_{50} + B_2 \mu \tag{4.62}$$

in an effort to incorporate this additional factor.

Another method, which might be more utile, would be the development of an expression for the transverse dispersivity similar to equation (3.45):

$$\alpha_{II} = B_3 (K)^{1/2} \tag{4.63}$$

(the intrinsic permeability rather than hydraulic conductivity could also be used). This equation is particularly attractive as we must collect some hydraulic conductivity information for the medium in any case. In particular, for the one-dimensional flow case, we note that

$$\bar{E}_t = \overline{\alpha_{II} q_1} = B_3 J \overline{[K^{3/2}]} \tag{4.64}$$

after substituting equation (3.7) and (4.63) into equation (2.6b) and taking expected values. By substituting perturbation expression (2.13) for the quantity in brackets on the right-hand side, and then expanding this result in a binomial series and truncating after the third term, we obtain

$$\bar{E}_t \approx B_3 \bar{q}_1 \bar{K}^{1/2} \left[1 + (3/8)(\sigma_K / \bar{K})^2 \right] \quad . \tag{4.65}$$

An estimate for α_t, then, is

$$\alpha_t = B_3 \bar{K}^{1/2} \left[1 + (3/8)(\sigma_K / \bar{K})^2 \right] \quad . \tag{4.66}$$

A similar expression can be developed for the three-dimensional case by using the logarithm of the K process; however, the analysis would also entail finding an expression for the covariance of f' and $\partial\phi'/\partial x_1$ processes.

Finally, we note that if a sufficiently accurate estimator for the effective dispersivity ratio ρ were developed, then the mass of data already in the literature for logitudinal dispersivities could be used to estimate an effective local longitudinal dispersivity α_ℓ, which could then be transformed into α_t. Indeed, if an accurate estimate of ρ were available, then one could use the simpler laboratory methods and obtain α_I directly from cores, averaging these values to obtain α_ℓ, and use ρ to obtain α_t. It appears to us that, for any particular uniformity coefficient μ, estimators such as (4.57) and (4.63), and their alternate forms for α_I, should be consistent. Thus, ρ is probably more a function of μ than of some average medium parameter. In any case, for a few particular values of μ, there is already sufficient data in the literature to estimate ρ (e.g., Harleman and Rumer, 1963; Blackwell, 1962); then, we have a fair idea of what to expect for typical values of ρ and have used these values in the construction of Figures 3.3, 3.4, 3.5 and 3.6. However, before even the single decimal-point accuracy required for the prediction of global longitudinal dispersivities can be obtained, more work will be required in this area.

For the most part, we have recommended the estimator developed from the Kozeny-Carmen equation (3.30) to estimate the porosity term P in either three-dimensional global dispersivity equation. This recommendation is based mostly on ease of use and not on accuracy. The slope term M in Archie's equation (3.25) may, in reality, be a more satisfactory estimator of this factor. Archie (1950) cites a slope factor of 3% on a $\log_{10}$ scale; this slope translates into a slope M of about 0.013 for a natural logarithmic scale. On the other hand, P is approximately equal to 0.3 $\bar{n}$ from the Kozeny-Carmen equation. Thus, a considerable reduction in the significance of the porosity factor $G(\rho,R)$ (or $G°(\rho,R°)$) results if the slope M is used for P. This estimator (M) for P is also more sensitive to the value choosen for $\bar{n}$. If the mean porosity for the medium is high (i.e., $\bar{n} \approx 0.25$), then we might conclude that we could neglect the porosity term $G(\rho,R)$ altogether. Only in cases where mean porosities are low (i.e., $\bar{n} \approx 0.1$) does the porosity term, when M is an estimator of P, significantly decrease the global longitudinal dispersivity. The choice of an estimator for the factor P will probably evolve from the experience of the investigator while using the method.

The global dispersivity equations require the estimate of at least a vertical correlation length scale, and possibly an estimate of the ratio R (or R°) of horizontal to vertical length scales. The province of estimation of length scales is largely found in the theory of spectral estimation, which has been dealt with extensively by Bakr (1976). Suffice it to say that, given a sufficient array of evenly spaced data from a single realization of an experiment, methods exist to extract an estimate of the spectrum and autocovariance function of the process in question. Then, by a process of curve fitting, a length scale can be extracted from these estimates for a particular autocovariance function or spectrum. Thus, we need not concern ourselves with the actual mechanics; the knowledge that it can be done is adequate. Instead, we turn to questions more directly related to the problem at hand.

In most field situations, a single vertical array of data as obtained from a well will be available to the investigator. This array will enable him to determine a vertical length scale; however, his manner of dealing with the horizontal length scale will largely depend on his geologic knowledge of the aquifer. For instance, this knowledge, perhaps drawn from the mode of deposition, will enable him to decide whether he can neglect the horizontal length scale altogether and rely on a global dispersivity from the stratified case for his predictor.

On the other hand, if he must use one of the three-dimensional cases, something in the depositional record may enable him to obtain a rough estimate of what the ratio of horizontal to vertical length scales should be. For example, he may decide that a particular bar or channel deposit may be indicative of this ratio. If all else fails, the investigator may find it necessary to drill additional observation wells (which may be available to him in any case) and attempt to statistically correlate data as, for instance, obtained from geophysical logs between the various wells. If a reasonable correlation is obtained, he may decide that the horizontal length scale is greater than the separation distance of these wells. On the other hand, if a poor correlation is obtained, he may decide that the length scale is less than this separation distance. Admittedly, all of the above suggestions for estimating the horizontal correlation length scale, or the ratio R, are only quasi-analytic; however, we feel that few alternatives exist in this matter as it would be prohibitively expensive to drill the necessary array of wells to estimate both of these length scales via spectral analysis. Indeed, the above suggestions certainly are not the only possible schemes to obtain this information. Electrical resistivity measurements, taken over a gridded area of the aquifer, provided that there are no extraneous influences, may also give an idea of the horizontal scale, or could be subject to spectral analysis themselves. Thus, we do not consider the lack of a ready-made horizontal length scale as an impediment to the application of the equations developed in this study.

To obtain our estimate of the vertical length scale, and therefore an estimate of the spectrum, it is preferable to have a vertical array of hydraulic conductivity measurements, or at least estimates thereof. Data of this nature are also necessary to predict the variance in hydraulic conductivity (or its logarithm) which is another necessary input into the global dispersivity equation. These data can be obtained directly from permeameter analysis of cores, which would also enable one to measure other parameters such as porosity. If core data is not available, then goephysical logs have a large potential for providing both estimates of hydraulic conductivity and porosity. In particular. some companies can computer process certain suites of geophysical logs and obtain an estimate of hydraulic conductivity (Schlumberger, 1974). If these services are not available, it may be possible, with a minimal number of hydraulic conductivities obtained from cores, to calibrate a particular log, or suite of logs, of one's choosing. Rabe (1957) has reported some success in this regard with respect to gamma ray logs of argillaceous petroleum reservoirs. Thus, we suspect that geophysical logs may develop into a useful tool in the estimation of hydraulic conductivity spectra and deserve further consideration as a method of obtaining the necessary data for making these estimates.

One direct application noted in the section entitled "Qualification of Long-Term Process" is the travel distance criterion expressed in equation (4.45). This criterion is of practical concern in the design of any field installation to obtain tracer information for the purpose of calculating global dispersion coefficients. Another related design problem is the sampling interval over which an observation well will extract tracer from the medium. If the travel-distance criterion has been satisfied, then we should expect that the tracer mass will be well mixed vertically in the flow system. However, as we are in reality dealing with a single realization, if we were to sample only at a single point in the medium, we would, in effect, also be sampling the consequence of some local heterogeneity on the tracer distribution. In order to avoid this problem, we suggest that observation wells should be designed with sampling intervals equivalent to three or four vertical correlation length scales.

HYDRAULIC HEAD VARIANCE IN GLOBALLY ANISOTROPIC MEDIA

Background

Although not of direct interest to this report, we cover this topic for two reasons: First, it has direct application in clarifying the choice of spectra used in the section entitled "Three-Dimensional Flow Case." Second, it is of interest as an important aspect of inverse problems and parameter estimation. Bakr (1976) and Bakr et al. (in press) have studied this aspect of flow phenomena in porous media, using both one-dimensional and three-dimensional flow cases; however their three-dimension solution was obtained by using an isotropic spectrum similar to equation (3.64) (i.e., all length scales were taken to be equal). We propose to solve the three-dimensional flow case with a spectrum which has variable length scales in all directions. For his isotropic spectrum, Bakr found that head variance σ_ϕ^2 is proportional to the variance of f process σ_f^2, to the square of the mean gradient J and to the square of the length scale λ; that is

$$\sigma_\phi^2 \propto J^2 \sigma_f^2 \lambda^2 \quad . \tag{5.1}$$

This result, however, gives us little indication if a reasonable limit can be reached for the asymptotic one-dimensional flow case. We realize, from previous discussion, that the variance in head should be zero for this asymptotic case. This condition will form the principal criterion for selection of a spectrum in this analysis.

Derivation and Choice of Spectrum

From equation (3.18), and our (by now) intimate familiarity with the representation theorem, we can immediately write the spectral relationship between hydraulic head and hydraulic conductivity:

$$\Phi_{\phi\phi}(\underset{\sim}{k}) = J^2 \frac{k_1^2}{[k_1^2 + k_2^2 + k_3^2]^2} \Phi_{ff}(\underset{\sim}{k}) \ . \tag{5.2}$$

We note that this relationship applied to three-dimensional flow and is suitable in the range of $\sigma_f < 1.0$ (Gutjahr et al., in press). Putting equation (5.2) in variance form, then, we obtain

$$\sigma_\phi^2 = J^2 \iiint_{-\infty}^{\infty} \frac{k_1^2}{[k_1^2 + k_2^2 + k_3^2]^2} \Phi_{ff}(\underset{\sim}{k}) d\underset{\sim}{k} \tag{5.3}$$

which puts us in a position to investigate various forms for spectrum Φ_{ff}.

The spectrum of the negative-exponential autocovariance function (3.64) will be investigated first. Putting the horizontal length scales equal ($\lambda = \lambda_1 = \lambda_2$), equation (5.3) in terms of spectrum (3.64) can be written

$$\sigma_\phi^2 = \frac{J^2 \sigma_f^2}{\pi^2} \lambda^2 \lambda_3 \iiint_{-\infty}^{\infty} \frac{k_1^2}{[k_1^2 + k_2^2 + k_3^2]^2}$$

$$\cdot \frac{d\underset{\sim}{k}}{[\lambda^2(k_1^2 + k_2^2) + \lambda_3^2 k_3^2 + 1]^2} \ . \tag{5.4}$$

Now, in order to simulate the one-dimensional case of flow parallel to stratification, we take λ_3 small in comparison to λ in the denominator of equation (5.4). Then, upon transforming to cylindrical coordinates

$$k_1 = r \cos\theta \quad ,$$

$$k_2 = r \sin\theta \quad ,$$

and $k_3 = k$

equation (5.4) can be written

$$\sigma_\phi^2 = \frac{J^2\sigma_f^2}{\pi^2}\lambda^2\lambda_3 4\int_0^\infty\int_0^\pi\int_0^\infty \frac{r^2\cos^2\theta}{(r^2+k^2)^2}\cdot\frac{r\,dr\,d\theta\,dk}{(\lambda^2 r^2+1)^2} \tag{5.5}$$

which, after evaluation, gives the result

$$\sigma_\phi^2 = \frac{\pi}{8}\lambda_3^2\sigma_f^2 J^2\frac{\lambda}{\lambda_3} \quad . \tag{5.6}$$

To obtain the asymptotic one-dimensional case, we examine the ratio λ/λ_3 as it becomes large; however, this quantity has no bounds and σ_ϕ^2 can become infinitely large. This is not a desirable limiting result.

Using a procedure similar to that outlined in the previous paragraph, it can be demonstrated that the spectrum of the modified negative-exponential function (3.66) will give a zero limit for the asymptotic one-dimensional case with flow parallel to stratification. However, as the modified negative-exponential autocovariance functions contains both elements of one-dimensional function (3.55) and the simple, one-dimensional negative-exponential function, its length scales are not equal to each other when we take $\ell_1 = \ell_2 = \ell_3$. This is essentially the same phenomenon discussed in the section entitled "Comparisons of Results." A spectrum which would produce an autocovariance function with equal length scales is

$$\Phi_{ff}(\underset{\sim}{k}) = \frac{4}{\pi^2}\sigma_f^2 \gamma_1\gamma_2\gamma_3 \frac{\gamma_1^2 k_1^2 + \gamma_2^2 k_2^2 + \gamma_3^2 k_3^2}{\left[\gamma_1^2 k_1^2 + \gamma_2^2 k_2^2 + \gamma_3^2 k_3^2 + 1\right]^3} \tag{5.7}$$

where γ_1, γ_2, and γ_3 represent equivalent correlation length scales. This spectrum will, by an analysis similar to that presented in the preceding paragraph, produce zero head variance for the asymptotic case with flow parallel to stratification and finite head variance for flow perpendicular to stratification. However, it will not produce the equivalent one-dimensional result for flow parallel to stratification for the global longitudinal dispersive flux equation (3.62) that spectrum (3.66) does. To demonstrate this conclusion, we examine a generalized form of the integral expressions in equation (3.62):

$$I_3 = \frac{4}{\pi^2}\sigma_f^2\gamma_1\gamma_2\gamma_3 \iiint_{-\infty}^{\infty} \left[\frac{k_2^2 + k_3^2}{k_1^2 + k_2^2 + k_3^2}\right]^n \frac{1}{\left[\alpha_\ell k_1^2 + \alpha_t (k_2^2 + k_3^2)\right]}$$

$$\cdot \frac{\gamma_1^2 k_1^2 + \gamma_2^2 k_2^2 + \gamma_3^2 k_3^2}{\left[\gamma_1^2 k_1^2 + \gamma_2^2 k_2^2 + \gamma_3^2 k_3^2 + 1\right]^3} \, d\underset{\sim}{k} \quad . \tag{5.8}$$

Transforming to coordinates

$$x_1 = \gamma_1 k_1 \quad , \quad x_2 = \gamma_2 k_2 \quad \text{and} \quad x_3 = \gamma_3 k_3 \tag{5.9}$$

one obtains

$$I_3 = \frac{4}{\pi^2}\sigma_f^2 \iiint_{-\infty}^{\infty} \left[\frac{R_1^2 R_3^2 x_2^2 + R_1^2 x_3^2}{R_3^2 x_1^2 + R_1^2 R_3^2 x_2^2 + R_1^2 x_3^2}\right]^n$$

$$\cdot \frac{a_3^2 R_1^2}{\left[\alpha_\ell R_3^2 X_1^2 + \alpha_t \left(R_1^2 R_3^2 X_2^2 + R_1^2 X_3^2\right)\right]}$$

$$\cdot \frac{X_1^2 + X_2^2 + X_3^2}{\left[X_1^2 + X_2^2 + X_3^2 + 1\right]^3} \, d\underset{\sim}{X} \tag{5.10}$$

where $R_1 = a_1/a_2$ and $R_3 = a_3/a_2$. We now take the limit of this expression as R_1 goes to unity and R_3 goes to zero, giving us the result

$$I_3 = \frac{4}{\pi^2} \sigma_f^2 \iiint_{-\infty}^{\infty} \frac{a_3^2}{\alpha_t X_3^2} \frac{X_1^2 + X_2^2 + X_3^2}{\left[X_1^2 + X_2^2 + X_3^2 + 1\right]^3} d\underset{\sim}{X} \ . \tag{5.11}$$

Equation (5.11) is, in effect, an integral form of the asymptotic one-dimensional result. This equation is transformed into spherical coordinates

$$X_1 = r \operatorname{Sin}\phi \operatorname{Sin}\theta \quad ,$$

$$X_2 = r \operatorname{Sin}\phi \operatorname{Cos}\theta \quad ,$$

and $$X_3 = r \operatorname{Cos}\phi \quad , \tag{5.12}$$

giving the result

$$I_3 = \frac{4}{\pi^2} \frac{a_3^2}{\alpha_t} \sigma_f^2 \int_0^{2\pi} \int_0^{\pi} \int_0^{\infty} \frac{r^2 \operatorname{Sin}\phi \, dr \, d\phi \, d\theta}{\left[r^2 + 1\right]^3 \operatorname{Cos}^2\phi}$$

$$= \frac{1}{2} \frac{a_3^2}{\alpha_t} \sigma_f^2 \int_0^{\pi} \frac{\operatorname{Sin}\phi}{\operatorname{Cos}^2\phi} \, d\phi = \infty \tag{5.13}$$

as we are integrating across a singularity at $\Pi/2$. Thus, spectrum (3.66) is the only spectrum we have found in our investigation which produces the proper limits for the asymptotic case of flow parallel to stratification in both head and dispersion applications. Since we consider that the limiting case of flow parallel to stratification is a reasonable condition to place on both applications, we will proceed to solve equation (5.3) with spectrum (3.66). However, for future investigations where head variance in three-dimensional flow is the primary concern, because of its more symmetric form, we recommend that spectrum (5.7) be seriously considered.

Solution of Head Variance Equation and Discussion

The actual mechanics of solving hydraulic head variance equation (5.3) with spectrum (3.66) are to be found in Appendix 9. We need concern ourselves merely with the general form of the solution, noting only that, in order to completely evaluate the triple integral, numerical integration was again used. The general form of the solution is

$$\sigma_\phi^2 = \ell_3^2 J^2 \sigma_f^2 H(R_1^\circ, R_3^\circ) \tag{5.14}$$

where $R_1^\circ = \ell_1/\ell_2$ and $R_3^\circ = \ell_2/\ell_3$. The head variance factor $H(R_1^\circ, R_3^\circ)$ is plotted on Figure 5.1 for continuous values of R_3° and for three discrete values of R_1°. Note the consistent approach of $H(R_1^\circ, R_3^\circ)$ to zero as R_3° increases in value. This consistent approach to zero variance as R_3° increases is in agreement with our concept of the one-dimensional parallel flow case. Surprisingly, the highest variance of those cases plotted occur when the length scales ℓ_1 and ℓ_3 are equal and ℓ_2 is ten-fold greater than either of these scales. Thus, if flow

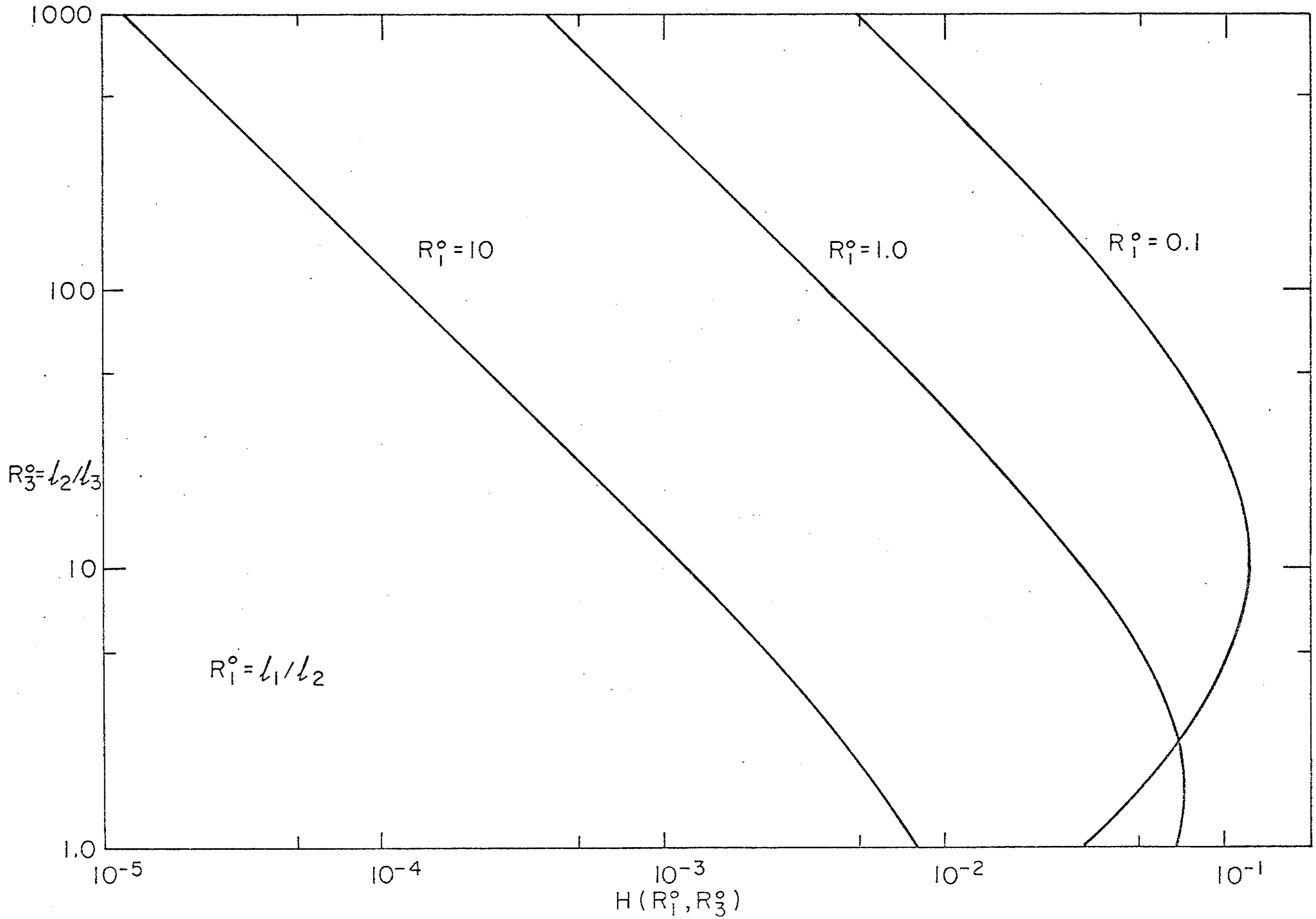

Figure 5.1. Variance factor for hydraulic head.

can be visualized as being perpendicular to the major axis of ellipsoidal-shaped local heterogeneities, equation (5.14) indicates that the variance in head will be greater for this configuration than for any other orientation of flow with respect to this medium. This configuration of flow and local heterogeneities may occur, for instance, for flow in a medium containing numerous bar or channel deposits. We also note that for values of $R_1^\circ = 0.1$ and $R_3^\circ = 1.0$, we are beginning to simulate a case of flow perpendicular to stratification. We would expect that flow perpendicular to stratification would be associated with the greatest head variance in porous media. That we should find the greatest variance associated with another case suggests that the spectrum we have chosen for this solution is not general enough for a complete study of head variance in three-dimensional flow. Thus, we end with a recommendation that, for the three-dimensional flow case, future investigators may wish to solve equation (5.3) with spectrum (5.7).

CONCLUSIONS AND RECOMMENDATIONS

Conclusions

Our principal conclusions concern the forms of global longitudinal dispersivity equations (3.59), (3.67) and (3.68). Within the limits of the first-order analysis leading up to these equations, their derivation indicates that global longitudinal dispersion is Fickian in nature. This result is of advantage to the modeller of transport phenomena in porous media, as it means that he can continue to use the convective-dispersion equation, provided certain travel-time restrictions are satisfied. In relation to this basic result, we note the solution of the global dispersive flux equation (2.21) indicates that the global longitudinal dispersion coefficient D_ℓ is a simple product of the mean specific discharge $\bar{q}_1$ and a global dispersivity A_ℓ; that is,

$$D_\ell = A_\ell \bar{q}_1 \quad . \tag{6.1}$$

With regard to the actual form of the global longitudinal dispersivity, we note that the first-order analysis and properties of stationary processes generally give us a form that is dependent on the variance in hydraulic conductivity σ^2, a correlation length scale ℓ and a local effective dispersivity α_t such that

$$A_\ell \propto \ell^2 \sigma^2 / \alpha_t \quad . \tag{6.2}$$

In addition while the effect of porosity variations on the global dispersivity is generally small, it acts to reduce the size of the coefficient by as much as 30%.

The spectrum of the modified negative-exponential autocovariance function (3.66) appears to give a preferable solution (3.68) to the three-dimensional global dispersivity equation (3.62). This conclusion is largely based on the existence of asymptotic one-dimensional equivalents for the solution, with this spectrum, of both the global dispersivity equation (3.62) and the head variance equation (5.3). However, we do recognize the greater utility of the simple negative-exponential autocovariance function in spectral estimation.

For many stratified aquifers, the one-dimensional equation (3.59) with spectrum (3.56) is suggested for use in estimation of global dispersivities. Otherwise, for less stratified cases, equation (3.68) is suggested, provided that the variance of the logarithm is not great ($\sigma_f \approx 0.5$). This latter case will necessitate estimation of horizontal correlation length scale, which may call upon the ingenuity of the investigator. Additionally, there remains to be resolved the question of the Fourier-Stieltjes representation of random variables for the three-dimensional flow case.

Perhaps the greatest obstacle to the application of the global dispersivity equation to prediction is the estimation of the effective local transverse dispersivity α_t. Several suggestions have been advanced as to how this problem can be approached; however, it will probably take more experimental work of the nature performed by Klotz (1973), but expressly oriented at prediction of the local transverse parameter α_{II}, before this problem can be resolved. Other parameters, such as vertical correlation length scales, hydraulic conductivity variance and porosity, can be adequately estimated from core analysis or geophysical logs.

Another inference we can deduce from these results is that, because of the complicity of erogodicity, there exists a travel distance, equivalent to expression (4.45), which must be satisfied before the dispersion process in natural aquifers is classically Fickian. If this distance criterion is not satisfied, then the global dispersivity, with which we would model the process, is not independent of time. Thus, a travel distance equivalent to several dispersivities should be considered in any design of field apparatus to measure global dispersivities. This travel distance is necessary for sufficient lateral transfer of tracer to occur, after which Taylor's (1953) assumption becomes valid.

Recommendations

One of the major restrictions on the use of these results for unstratified media is that they can be applied only in cases where σ_f is relatively small. This restriction arises from the first-order analysis used in derivation of the three-dimensional model equation. We suspect, however, that the approach of Buyevich et al. (1969), with appropriate modifications to their first-order analysis, may produce better results for cases where σ_f is large (i.e., $\sigma_f \approx 1$). In particular, if the Lagrangian autocorrelation function were used to derive the variance in particle position (Taylor, 1954), then the function itself might be deduced from the continuity equation. However, we suggest that the logarithm of hydraulic conductivity be used in the first-order analysis of this equation which, we believe, will produce a superior result than that obtained by Buyevich et al. In any case, it should be noted that this suggested analysis is not simple.

With regard to the results presented in this report, we strongly recommend that they be subject to rigorous scrutiny in a field situation.

In particular, if a site is available where field determinations of global dispersivities have been realized, and where sufficient hydraulic conductivity or geophysical log data are available from a well bore, we suggest that these equations be applied and comparisons be made. Even if no estimate of the effective local transverse dispersivity α_t is available, then this parameter can be backed out of the equations and compared to the few values available in the literature.

Finally, as we have noted extensively, the effective local dispersivity parameter α_t should be examined more closely. Several suggestions have been put forth for its evaluation already; however, it might be advisable to pursue equation (4.56) in order to analyze its structure in more detail. Additionally, the laboratory work to quantify the empirical equations relating local dispersivities to medium properties should not be neglected.

REFERENCES

Abramowitz, M., and Stegun, I. A., eds., 1965, Handbook of Mathematical Functions: New York, Dover Publications, 1045 p.

Aitchison, J., and Brown, J. A. C., 1957. The Lognormal Distribution: Cambridge, Cambridge Univ. Press, 176 p.

Alpay, O. A., 1972, A practical approach to defining reservoir heterogeneity: Jour. Petr. Tech., v. 24, p. 841-848.

Archie, G. E., 1950, Introduction to petrophysics of reservoir rocks: Am. Assoc. Petr. Geologists Bull., v. 34, no. 5, p. 943-961.

Aris, R., 1956, On the dispersion of a solute in a fluid flowing through a tube: Proc. Royal Soc. [London], Series A, v. 235, p. 67-77.

Bakr, A. A. M., 1976, Stochastic analysis of the effect of spatial variations of hydraulic conductivity of groundwater flow:, Ph.D. dissertation, New Mexico Institute of Mining and Technology, 244 p.

Bakr, A. A. M., Gelhar, L. W., Gutjahr, A. L., and MacMillan, J. R., in press, Stochastic analysis of a spatial variability in subsurface flows: WRR.

Bear, J., 1972, Dynamics of Fluids in Porous Media: New York, Elsevier, 764 p.

Blackwell, R., 1962, Laboratory studies of microscopic dispersion phenomena: Soc. Petr. Engrs. Jour., v. 2, no. 1, p. 1-8.

Boreli, M., Radojković, M., Jović, S., Vuković, M., and Matić, B., in press, Identification of dispersion characteristics of porous media by means of piezometric data, in Hydrodynamic Diffusion and Dispersion in Porous Media: Proc. Symp. (IAHR), April 20th - 22nd, 1977, Univ. of Pavia, Italy.

Bredehoeft, J. D., 1964, Variation of permeability in the Tensleep

Sandstone in the Bighorn Basin, Wyoming, as interpreted from core analysis and geophysical logs: U. S. Geol. Survey Prof. Paper 501-D, p. D166-D170.

Buyevich, Yu. A., Leonov, A. I., and Safrai, V. M., 1969, Variations in filtration velocity due to random large-scale fluctuations of porosity: Jour. Fluid Mech., vol. 37, part 2, p. 371-381.

Byrd, P. F., and Friedman, M. D., 1954, Handbook of Elliptic Integrals for Engineers and Physicists: Berlin, Springer-Verlag, 355 p.

Claridge, E. L., 1972, Discussion of the use of capillary tube networks in reservoir performance studies: Soc. Petr. Engrs. Jour., v. 11, no. 3, p. 352-361.

Corompt, P., Gaillard, B., Guizerix, J., Margrita, R., Molinari, J., Corda, R., Crampon, N., and Olivier, D., 1974, Methode pour la determination de caracteristiques de transfert de substances pollutants dans les nappes aquiferes, in Isotope Techniques in Groundwater Hydrology: Proc. Symp. (IAEA), Vienna, Austria, v. 2, p. 406-424.

de Josselin de Jong, G., 1958, Longitudinal and transverse diffusion in granular deposits: Trans. Amer. Geophy. Union, v. 39, no. 1, p. 67-74.

Erdélyi, A., ed., 1954, Tables of Integral Transforms, Volume I: New York, McGraw-Hill, 391 p.

__________, 1954a, Tables of Integral Transforms, Volume II: New York, McGraw-Hill, 451 p.

Freeze, R. A., 1975, A stochastic-conceptual analysis of one-dimensional groundwater flow in nonuniform homogeneous media: WRR, v. 11, no. 5, p. 725-741.

Fried, J. J., and Combarnous, M. A., 1971, Dispersion in porous media, in Advances in Hydroscience, Vol. 7: New York, Academic Press, p. 116-282.

Fried, J. J., 1972, Some recent applications of the theory of dispersion in porous media, in Fundamentals of Transport Phenomena in Porous Media: Proc. 2nd Int. Symp. (IAHR-ISSS), August 7th - 11th, 1972, Univ. of Guelph, Ontario, Canada, v. 1, p. 722-731.

__________, 1975, Groundwater pollution, in Developments in Water Science, Vol. 4: Amsterdam, Elsevier, 330 p.

Gelhar, L. W., 1976, Stochastic analysis of flow in aquifers, in Advances in Groundwater Hydrology: Proc. Symp. (AWRA), September 22nd - 23rd, 1976, Chicago, Illinois.

__________, 1976a, Effect of hydraulic conductivity variations on groundwater flows, in Stochastic Hydrology: Proc. 2nd Int. Symp. (IAHR), August 2nd - 4th, 1976, Univ. of Lund, Sweden, p. 27-1 - 27-16.

Gelhar, L. W., Bakr, A. A., Gutjahr, A. L., and MacMillan, J. R., 1977, Comments on 'a stochastic-conceptual analysis of one-dimensional groundwater flow in nonuniform homogeneous media' by R. Allen Freeze: WRR, v. 13, no. 2, p. 477-479.

Gradshteyn, and Ryzhik, 1965, Table of Integrals Series and Products: New York, Academic Press, 1086 p.

Greenkorn, R. A., and Kessler, D. P., 1969, Dispersion in homogeneous nonuniform anisotropic porous media: Industrial and Engineering Chemistry, v. 61, no. 9, p. 14-32.

Groult, J., Reiss, L. H., and Montadert, L., 1966, Reservoir inhomogeneities deduced from outcrop observations and production logging:

Jour. Petr. Tech., v. 18, p. 883-891.

Gutjahr, A. L., Gelhar, L. W., Bakr, A. A., and MacMillan, J. R., in press, Stochastic analysis of spatial variation in subsurface flows, part II, evaluation and application: WRR.

Haring, R. E., and Greenkorn, R. A., 1970, A statistical model of a porous medium with nonuniform pores: AIChE Jour., v. 16, no. 3, p. 477-483.

Harleman, D. R. F., Melhorn, P. F., and Rumer, R. R., 1963, Dispersion-permeability correlation in porous media: Proc. ASCE, Jour. Hyd. Div., v. 89, part 1, HY2, p. 67-85.

Harleman, D. R. F., and Rumer, R. R., 1963, Longitudinal and lateral dispersion in an isotropic porous medium: Jour. Fluid Mech., v. 16, part 3, p. 385-394.

Hassinger, R. and von Rosenberg, D., 1968, A mathematical and experimental examination of transverse dispersion coefficients: Soc. Petr. Engrs. Jour., v. 8, no. 2, p. 195-204.

Heller, J. P., 1972, Observations of mixing and diffusion in porous media, in Fundamentals of Transport Phenomena in Porous Media: Proc. 2nd Int. Symp. (IAHR-ISSS), August 7th - 11th, 1972, Univ. of Guelph, Ontario, Canada, p. 1-26.

Klotz, D., 1973, Untersuchungen zur Dispersion in poroesen Medien: Z. Deutsch. Geol. Ges., v. 124, p. 521-533.

Koval, E. J., 1963, A method for predicting the performance of unstable miscible displacement in heterogeneous media: Soc. Petr. Engrs. Jour., v. 3, no. 2, p. 145-154.

Law, J., 1944, A statistical approach to the interstitial heterogeneity of sand reservoirs: Trans. AIME, Petr. Div., v. 155, p. 202-222.

Lumley, J. L., and Panofsky, H. A., 1964, The Structure of Atmospheric Turbulence: New York, John Wiley and Sons, 239 p.

Marle, C., Simandoux, P., Pacsirzky, J., and Gaulier, C., 1967, Etude du dé placement de fluides miscibles en milieu poreux stratifié: Revue de l'Institute Francais du Pétrole, v. 22, no. 2, p. 272-294.

Mercado, A., 1967, The spreading pattern of injected water in a permeable stratified aquifer, in Artificial Recharge and Management of Aquifers: Symp. of Haifa (IASH), March 19th-26th, 1967, Pub. 72, p. 23-36.

Oakes, D. B., and Edworthy, K. J., 1977, Field measurements of dispersion coefficients in the United Kingdom, in Groundwater Quality, Measurement, Prediction and Protection: Papers and Proc. Water Research Centre Conference, September 6th-8th, 1976, Univ. of Reading, Berkshire, England, p. 274-297.

Oberhettinger, Fritz, 1973, Fourier Transforms of Distributions and their Inverses: New York, Academic Press, 167 p.

Pettijohn, F. J., Potter, P. E., and Siever, R., 1973, Sand and Sandstone: New York, Springer-Verlag, 618 p.

Rabe, C. L., 1957, A relation between gamma radiation and permeability, Denver-Julesburg Basin: Trans. AIME, Soc. Petr. Engrs., v. 210, p. 358-360.

Renault, D., Numtzer, P., Zilliox, L., and Hirtz, J., 1975, Propogation d'un front de pollution dans un aquifère: Contribution expérimentale à l'étude da la dispersion en milieu poreux stratifié: T.S.M. L'Eau, 70^{e} annee, no. 4, p. 153-157.

Ross, S. M., 1972, Introduction to Probability Models: New York, Academic Press, 272 p.

Saffman, P. G., 1959, A theory of dispersion in a porous medium: Jour. Fluid Mech., v. 6, p. 321-349.

Scheidegger, A. E., 1954, Statistical hydrodynamics in porous media: Jour. Applied Physics, v. 25, no. 8, p. 994-1001.

Schlumberger, 1974, Log Interpretation: Volume 2 -- Applications: New York, Schlumberger Ltd., 116 p.

Schwartz, F. W., 1977, Macroscopic dispersion in porous media: the controlling factors: WRR, v. 13, no. 4, p. 743-752.

Skibitzke, H. E., and Robinson, G. M., 1963, Dispersion in ground water flowing through heterogeneous materials: U. S. Geol. Survey Prof. Paper 386-B, 3 p.

Slobod, R. L., and Thomas, R. A., 1963, Effect of transverse diffusion on fingering in miscible-phase displacement: Soc. Petr. Engrs. Jour., v. 3, no. 1, p. 9-13.

Starr, J. L., and Parlange, J. -Y., 1976, Solute dispersion in saturated soil columns: Soil Science, v. 121, no. 6, p. 364-372.

Taylor, G. I., 1953, Dispersion of soluble matter in solvent flowing slowly through a tube: Proc. Royal Soc. [London], Series A, v. 219, p. 186-203.

__________, 1954, The dispersion of matter in turbulent flow through a pipe: Proc. Royal Soc. [London], Series A, v. 223, p. 446-468.

Tennekes, H., and Lumley, J. L., 1974, A First Course in Turbulence: Cambridge, Mass., M.I.T. Press, 300 p.

Titchmarsh, E. C., 1948, Theory of Fourier Integrals, 2nd ed.: London, Oxford Univ. Press, 394 p.

Warren, J. E., and Price, H. S., 1961, Flow in heterogeneous porous media: Soc. Petr. Engrs. Jour., v. 1, no. 3, p. 153-169.

Warren, J. E., and Skiba, F. F., 1964, Macroscopic dispersion: Trans. AIME, Soc. Petr. Engrs., v. 231, p. 215-230.

Wilson, J. L., and Gelhar, L. W., 1974, Dispersive mixing in a partially saturated porous medium: MIT, Ralph M. Parsons Laboratory for Water Resources and Hydrodynamics, report no. 191, 353 p.

Zilliox, L., and Muntzer, P., 1975, Effect of hydrodynamic processes on the development of groundwater pollution: studies on physical models in a saturated porous medium: Prog. in Water Tech., v. 7, p. 561-568.

Appendix 1

SOME PROPERTIES OF STATIONARY RANDOM FIELDS

Much of the notation for this appendix (and report) was drawn from a book by Lumley and Panofsky (1964), which also serves as a basic reference for many of the concepts of random-fields processes. It is suggested that the reader may wish to review the first chapter of this reference before proceeding further. In this appendix, properties of three-dimensional processes (m = 3) will be reviewed, realizing that the one-dimensional case (m = 1) can be obtained by elimination of two dimensions in lag space and frequency space.

Equations which repute to model natural phenomenon frequently contain random coefficients or variables. These random differential equations can often by analyzed by means of the representation theorem if they are linear, or at least are amenable to some linearizing assumptions. Our primary objective, then, is to introduce enough concepts from random-field processes so that we may state this theorem without proof.

A variable $f'(\underset{\sim}{x})$ is called a stochastic process on $\underset{\sim}{X}$ if it is a random variable for every $\underset{\sim}{x}$ contained in $\underset{\sim}{X}$. When $\underset{\sim}{x}$ is a spatial variable in some region $\underset{\sim}{X}$, then $f'(\underset{\sim}{x})$ is a random field. The stochastic process is considered to be statistically homogeneous or spatially second-order stationary if the autocovariance function

$$\mathrm{Cov}\left[f'(\underset{\sim}{x}),\, f'(\underset{\sim}{x}+\underset{\sim}{s})\right] = R_{ff}(\underset{\sim}{s}), \quad \underset{\sim}{s} = (s_1, s_2, s_3) \tag{1}$$

is a function only of the separation vector $\underset{\sim}{s}$ and if the expected values of $f'(\underset{\sim}{x})$,

$$\overline{f'(\underset{\sim}{x})} = \mu , \tag{2}$$

is independent of $\underset{\sim}{x}$. The autocovariance function is frequently normalized by the variance σ_f^2 of the process to form the autocorrelation function

$$\rho_{ff}(\underset{\sim}{s}) = R_{ff}(\underset{\sim}{s})/\sigma_f^2 . \tag{3}$$

When the autocovariance function is transferred from lag space to frequency space by means of the Fourier transform, it is commonly referred to as the power spectrum Φ_{ff}:

$$\Phi_{ff}(\underset{\sim}{k}) = (2\pi)^{-m} \iiint_{-\infty}^{\infty} e^{-i\underset{\sim}{k}\cdot\underset{\sim}{s}} R_{ff}(\underset{\sim}{s})\, d\underset{\sim}{s} \; , \; \underset{\sim}{k} = (k_1, k_2, k_3) \tag{4}$$

where $\underset{\sim}{k}$ is the wave number vector. While the autocovariance function is a measure of correlation at any particular lag, the power of a spectrum is a measure of how variability of the process is spread over frequency space. If the power of Φ_{ff} is spread over a large portion of the frequency space, then the process is highly correlated at small spacings. On the other hand, if the power is concentrated about the origin, then the process tends to be uniformly correlated in lag space. Note that the inverse Fourier transform of Φ_{ff} evaluated at zero lag ($\underset{\sim}{s} = 0$) is equivalent to the variance of the process.

A similar set of definitions exists for the cross correlation and cross spectrum of two processes; that is, the correlation function and spectrum calculated for two different stationary random variables $f'(\underset{\sim}{x})$ and $g'(\underset{\sim}{x})$ are given by

$$\rho_{fg}(\underset{\sim}{\xi}) = \mathrm{Cov}\left[f'(\underset{\sim}{x}), g'(\underset{\sim}{x}+\underset{\sim}{\xi})\right] \Big/ \overline{f'g'} = R_{fg}(\underset{\sim}{\xi}) \Big/ \overline{f'g'} \tag{5}$$

and

$$\Phi_{fg}(\underset{\sim}{k}) = (2\pi)^{-m} \iiint_{-\infty}^{\infty} e^{-i\underset{\sim}{k}\cdot\underset{\sim}{\xi}} R_{fg}(\underset{\sim}{\xi})\, d\underset{\sim}{\xi} \quad . \tag{6}$$

With the above definitions in mind, we state the representations theorem without proof: If $f'(\underset{\sim}{x})$ is a zero-mean statistically homogeneous random field, then there exists a distribution function $F(\underset{\sim}{k})$ such that

$$R_{ff}(\underset{\sim}{\xi}) = \iiint_{-\infty}^{\infty} e^{-i\underset{\sim}{k}\cdot\underset{\sim}{\xi}}\, dF(\underset{\sim}{k}) \quad . \tag{7}$$

In addition, there exists a complex, three-dimensional random distribution, $Z_f(\underset{\sim}{k})$, such that

$$f'(\underset{\sim}{x}) = \iiint_{-\infty}^{\infty} e^{-i\underset{\sim}{k}\cdot\underset{\sim}{x}}\, dF_f(\underset{\sim}{k}) \tag{8}$$

where $dZ_f(\underset{\sim}{k})$ are complex Fourier amplitudes. The spectrum Φ_{ff} is related to the complex Fourier amplitudes by

$$\overline{dZ_f(\underset{\sim}{k})\, dZ_f^*(\underset{\sim}{k}^\circ)} = \begin{cases} 0 & \underset{\sim}{k} \neq \underset{\sim}{k}^\circ \\ \Phi_{ff}(\underset{\sim}{k})\, d\underset{\sim}{k} & \underset{\sim}{k} = \underset{\sim}{k}^\circ \end{cases} \tag{9}$$

where the star and bar indicate a complex conjugate and expectation, respectively. The integrals in equation (8) are Fourier-Stieltjes integrals. A similar result holds for cross spectra of two different processes; that is

$$\overline{dZ_f(\underset{\sim}{k})\,dZ_g(k^\circ)} = \begin{cases} 0 & \underset{\sim}{k} \neq \underset{\sim}{k}^\circ \\ \Phi_{fg}(\underset{\sim}{k})\,d\underset{\sim}{k} & \underset{\sim}{k} = \underset{\sim}{k}^\circ \end{cases} \quad (10)$$

Manipulation of many random differential equations by means of relations (9) and (10) allows for the determination of transfer functions between spectra and/or cross spectra.

In the three-dimensional case, it is logical to explore the relative amount of correlation along each of the major axes. A measure of this correlation is the integral scale, which for three dimensions may be defined

$$\lambda_i = \int_0^\infty \rho_{ff}(\underset{\sim}{s})\,ds_i \quad , \quad i = 1, 2, 3 \quad (11)$$

where the separation vector $\underset{\sim}{s}$ contains only the i^{th} component, the others having been set equal to zero. This expression gives us the average volume over which correlation occurs and is related to the correlation length scale in the i^{th} direction. It should be noted that integral scales do not always exist along every principal axis of all autocorrelation functions.

Correlation-scale parameters are contained in every spectrum and autocovariance function. If an integral scale exists, then correlation scales are some constant multiple of the integral scale. That is

$$a_i = c\lambda_i \quad , \quad i = 1, 2, 3 \quad (12)$$

where a_i is the correlation length scale and c is a constant (when c is equal to unity, the integral scale λ_i will generally be used to connote the correlation scale). If an integral scale does not exist, then the correlation scale is usually equivalent to that lag distance over which the autocorrelation function is positive. That is, if $\rho_{ff}(\underset{\sim}{s})$ has no integral scale, but $\rho_{ff}(s_i)$ is equal to zero on the x_i axis, then a_i is taken to equal s_i, provided that s_i is unique. Correlation length scales determine isotropy of the correlation structure of the process. If a_i is not equal to a_j $(i \neq j)$, the process is considered to be statistically anisotropic in space.

As a final note to this appendix, it should be acknowledged that the probabilistic basis for the above formulae is an ensemble of realizations of the experiment in question. An ensemble is the collection of all possible realizations of the process over the entire space. An ensemble average (or probability average) at a fixed point would be the average of all observations taken at that point -- not duplicated measurements but results from a new experiment or ensemble member taken repetitively. As an ensemble, in this sense, is seldom available to us in hydrology, a question arises as to our ability to transfer information to and from a single realization of the experiment. As it happens, spatial averages are asymptotically equivalent to ensemble averages, provided that the spatial sampling domain is sufficiently large. The concept of interchangeability of spatial and ensemble averages is generally referred to as ergodicity, and will be used extensively in this report to explain the transfer of information.

Appendix 2

GEOMETRIC MEAN AND LOGNORMAL DISTRIBUTION

In this appendix, the primary objective is to point out the relation between the geometric mean and the lognormal distribution. For a more detailed analysis of the lognormal distribution, the reader may find the book by Aitchison and Brown (1957) to be helpful.

The moments of a lognormally distributed random variable X can be most easily determined by utilizing the transformation

$$Y = \ell n\left[X\right] \tag{1}$$

where Y is a normal random variable. The mean μ_x and standard deviation σ_x of the lognormal distribution follow directly from the law of the unconscious statistician (Ross, 1972, p. 35):

$$\mu_X = \exp\left[\mu_Y + \sigma_Y^2/2\right] \tag{2a}$$

and $$\sigma_X = \mu_X \left\{\exp\left[\sigma_Y^2\right] - 1\right\}^{1/2} \tag{2b}$$

where μ_y and σ_y are the mean and standard deviation of the normal random variable Y, respectively.

The geometric mean is commonly defined as

$$X_g = \left[\prod_{i=1}^{n} X_i\right]^{\frac{1}{n}} . \tag{3}$$

This expression can be equivalently written in terms of logarithms as

$$X_g = \exp\left[G\right] \quad , \quad G = \sum_{i=1}^{n} \frac{\ell n X_i}{n} . \tag{4}$$

However, if X_1, X_2, ... are independent, identically distributed random variables, all greater than zero, with mean μ_x and standard deviation σ_x then, by the central limit theorem (Ross, 1972, p. 53), G is an approximately normally distributed random variable with mean μ_y and standard deviation σ_y/n. In turn, X_g must then be a lognormally distributed with the approximate mean

$$\overline{X}_g \approx \exp\left[\mu_Y + \sigma_Y^2/2n^2\right] . \tag{5}$$

As n becomes large, the expected value of the geometric mean is simply the exponent of μ_y, or

$$\overline{X}_g = \exp\left[\mu_Y\right] \quad , \quad n \to \infty . \tag{6}$$

Thus $\bar{X}_g$ is the population equivalent of the geometric mean. Note that the above derivation is not dependent on the underlying distribution of X_i. However, if X_i is lognormally distributed, then $\bar{X}_g$ is equivalent to the median of this distribution.

Appendix 3

CONVECTIVE-DISPERSION EQUATION

A rather nice derivation of the convective-dispersion equation for flow through porous media is to be found in Wilson and Gelhar (1974). The following derivation is largely excerpted from this source.

Consider a fixed elementary volume V, defined as the interior surface S, containing a solute c in a porous medium with porosity n. The liquid-solid matrix is regarded as a continuum. A balance for the solute mass in V may be written

$$\frac{\partial}{\partial t}\int_V nc\,dV = -\int_S \underset{\sim}{q}c\cdot\underset{\sim}{n}\,dS - \int_S \underset{\sim}{N}\cdot\underset{\sim}{n}\,dS + \int_V r\,dV \qquad (1)$$

where

$\underset{\sim}{q}$ specific discharge vector;

$\underset{\sim}{n}$ unit normal to surface;

n porosity;

r source or sink of solute in V;

and $\underset{\sim}{N}$ local dispersive flux of solute.

By applying the divergence theorem to the surface integrals, and by assuming that V is not time dependent, we may write equation (1) as

$$\int_V \frac{\partial}{\partial t}\left[nc\right]dV = -\int_V \nabla\cdot(\underset{\sim}{q}c + \underset{\sim}{N})\,dV + \int_V r\,dV \quad . \qquad (2)$$

Since the volume V is arbitrary, equation (2) yields

$$\frac{\partial}{\partial t}\left[nc\right] + \nabla\cdot\left[c\underset{\sim}{q} + \underset{\sim}{N}\right] - r = 0 \quad . \qquad (3)$$

Most commonly, a Fickian model is chosen for the local dispersive flux vector, in which case

$$\underset{\sim}{N} = -\bar{\bar{E}} . \nabla c = -n \bar{\bar{D}} . \nabla c \quad (4)$$

where

$\bar{\bar{E}}$ local bulk dispersion tensor;

and $\bar{\bar{D}}$ mechanical dispersion tensor.

Note that the local bulk dispersion tensor $\bar{\bar{E}}$ is reduced from the mechanical dispersion tensor $\bar{\bar{D}}$ by a factor of the porosity. The mechanical dispersion tensor is considered to represent the total dispersion in the fluid phase due to a Fickian process. Equations (3) and (4) represent the principal vehicles for the analysis presented in the text.

Appendix 4

MOVING COORDINATES

For steady state, mean uniform flow in the x_1 direction, the moving coordinate ξ can be defined as

$$\xi = x_1 - t\bar{q}_1/\bar{n} \tag{1}$$

where

	x_1	Eulerian coordinate;
	$\bar{q}_1$	mean seepage velocity in x_1 direction;
	$\bar{n}$	mean porosity;
and	t	travel time.

The moving coordinate ξ represents the location x_1 with respect to the average particle position after some specified time t. (To obtain the entire effect of this coordinate, consider ξ to be constant. Since $\bar{q}_1$ and $\bar{n}$ are flow system constants and time t continues to operate under any circumstances, x_1 must increase at a rate equivalent to $t\bar{q}_1/\bar{n}$. Thus, ξ is a moving coordinate in the sense that it "moves" with the mean velocity.)

If $f(\xi,t)$ is a function of both time and position, then its total derivative is

$$df(\xi,t) = \frac{\partial f(\xi,t)}{\partial \xi} d\xi + \frac{\partial f}{\partial t} dt \ . \tag{2}$$

Hence, the partial derivatives of $f(\xi,t)$ with respect to time and space in Eulerian coordinates are

$$\left.\frac{\partial f(\xi,t)}{\partial t}\right|_{x_1} = \frac{\partial f(\xi,t)}{\partial \xi}\cdot\left.\frac{\partial \xi}{\partial t}\right|_{\xi} + \left.\frac{\partial f}{\partial t}\right|_{\xi} \tag{3}$$

or

$$\left.\frac{\partial f(\xi,t)}{\partial t}\right|_{x_1} = \left.\frac{\partial f}{\partial t}\right|_{\xi} - \frac{q_1}{n}\left.\frac{\partial f(\xi,t)}{\partial \xi}\right|_{t} \tag{4}$$

and

$$\left.\frac{\partial f(\xi,t)}{\partial x_1}\right|_{t} = \left.\frac{\partial f(\xi,t)}{\partial \xi}\right|_{t} . \tag{5}$$

Transformations of this type are frequently employed to reduce the number of variables in first-order partial differential equations.

Appendix 5

NEGATIVE-EXPONENTIAL AUTOCOVARIANCE FUNCTION

To derive the negative-exponential autocovariance function in three dimensions, we first assume the spectral form

$$\Phi(\underset{\sim}{k}) = \frac{N}{\left[a_1^2 k_1^2 + a_2^2 k_2^2 + a_3^2 k_3^2 + 1\right]^2} \tag{1}$$

where N is some normalizing constant, and then take its Fourier transform

$$R(\underset{\sim}{s}) = N \iiint_{-\infty}^{\infty} \frac{\exp[i\underset{\sim}{k} \cdot \underset{\sim}{s}]\, d\underset{\sim}{k}}{\left[a_1^2 k_1^2 + a_2^2 k_2^2 + a_3^2 k_3^2 + 1\right]^2} \, . \tag{2}$$

The three-dimensional transformation

$$x_1 = a_1 k_1 \;, \quad x_2 = a_2 k_2 \;, \quad \text{and} \quad x_3 = a_3 k_3 \tag{3}$$

is adopted, from which equation (2) can be rewritten as

$$R(\underset{\sim}{s}) = \frac{N}{a_1 a_2 a_3} \iiint_{-\infty}^{\infty} \frac{\exp\left[i(x_1\lambda_1 + x_2\lambda_2 + x_3\lambda_3)\right]}{\left[x_1^2 + x_2^2 + x_3^2 + 1\right]^2} \, d\underset{\sim}{x} \tag{4}$$

where

$$\lambda_1 = \frac{s_1}{a_1} \;, \quad \lambda_2 = \frac{s_2}{a_2} \;, \quad \text{and} \quad \lambda_3 = \frac{s_3}{a_3} \, .$$

A transformation to spherical coordinates

$$\rho^2 = \lambda_1^2 + \lambda_2^2 + \lambda_3^2$$

$$\lambda_1 = \rho \operatorname{Cos} \phi$$

$$\lambda_2 = \rho \operatorname{Sin} \phi \operatorname{Cos} \theta$$

$$\lambda_3 = \rho \operatorname{Sin} \phi \operatorname{Sin} \theta \tag{5}$$

and

$$r^2 = x_1^2 + x_2^2 + x_3^2$$

$$x_1 = r \operatorname{Cos} \alpha$$

$$x_2 = r \operatorname{Sin} \alpha \operatorname{Cos} \beta$$

$$x_3 = r \operatorname{Sin} \alpha \operatorname{Sin} \beta \tag{6}$$

is adopted. The argument of the exponent can be written

$$\underset{\sim}{\lambda} \cdot \underset{\sim}{x} = \frac{\rho r}{2} \Big\{ \operatorname{Cos}(\phi - \alpha) + \operatorname{Cos}(\phi + \alpha) + \operatorname{Cos}(\theta - \beta) \Big[\operatorname{Cos}(\phi - \alpha) - \operatorname{Cos}(\phi + \alpha) \Big] \Big\} . \tag{7}$$

Because of the symmetric nature of the function being transformed, we may choose the radius vector ρ to occupy any position we please. In particular, we let ρ lie along the λ_1 axis and choose θ equal to β. This causes the simplified form

$$\underset{\sim}{\lambda} \cdot \underset{\sim}{x} = \rho r \operatorname{Cos} \alpha \tag{8}$$

to appear in the argument of the exponent. Equation (4), in spherical coordinates, then becomes

$$R(\underset{\sim}{s}) = \frac{N}{a_1 a_2 a_3} \int_0^\infty \int_0^\pi \int_0^{2\pi} \frac{\exp\left[i \rho r \operatorname{Cos} \alpha\right] r^2 \operatorname{Sin} \alpha \, d\beta \, d\alpha \, dr}{\left[r^2 + 1\right]^2} . \tag{9}$$

Integration of the first integral is obvious. Integration of the second yields

$$\int_0^{\pi} \sin\alpha \exp\left[i\rho r \cos\alpha\right] d\alpha = \frac{2}{\rho r} \sin\rho r \quad . \tag{10}$$

Thus,

$$R(\underset{\sim}{s}) = \frac{4\pi N}{a_1 a_2 a_3 \rho} \int_0^{\infty} \frac{r}{[r^2+1]^2} \sin\rho r \, dr \tag{11}$$

which is the Fourier sine transform of the function $r[r^2 + 1]^{-2}$. Erdélyi (1954, p. 67, no. 2.2 (35)) gives this transform as

$$R(\underset{\sim}{s}) = \frac{N\pi^2}{a_1 a_2 a_3} \exp\left[-\left(\frac{s_1}{a_1} + \frac{s_2}{a_2} + \frac{s_3}{a_3}\right)^{1/2}\right] \quad . \tag{12}$$

The normalizing constant can be obtained from the variance σ^2 of the process (i.e., when the autocovariance function is evaluated at zero lag) and is found to be

$$N = \sigma^2 \frac{a_1 a_2 a_3}{\pi^2} \quad . \tag{13}$$

Substitution of equation (13) into equations (1) and (12) gives the proper form of the spectrum and autocovariance function.

Appendix 6

MODIFIED NEGATIVE-EZPONENTIAL AUTOCOVARIANCE FUNCTION

To derive the modified negative-exponential autocovariance function, we first assume the spectral form

$$\phi(\underset{\sim}{k}) = \frac{N a_3^2 k_3^2}{\left[a_1^2 k_1^2 + a_2^2 k_2^2 + a_3^2 k_3^2 + 1\right]^3} \tag{1}$$

where N is a normalizing constant, and then take its Fourier transform:

$$R(\underset{\sim}{s}) = N \iiint_{-\infty}^{\infty} \frac{a_3^2 k_3^2 \exp[i \underset{\sim}{k} \cdot \underset{\sim}{s}] d\underset{\sim}{k}}{\left[a_1^2 k_1^2 + a_2^2 k_2^2 + a_3^2 k_3^2 + 1\right]^3} \quad . \tag{2}$$

The three-dimensional transformation

$$x_1 = a_1 k_1 \quad , \quad x_2 = a_2 k_2 \quad , \text{ and } \quad x_3 = a_3 k_3 \tag{3}$$

is adopted, from which equation (2) can be rewritten as

$$R(\underset{\sim}{s}) = \frac{N}{a_1 a_2 a_3} \iiint_{-\infty}^{\infty} \frac{x_3^2 \exp[i(x_1\lambda_1 + x_2\lambda_2 + x_3\lambda_3)]}{\left[x_1^2 + x_2^2 + x_3^2 + 1\right]^3} d\underset{\sim}{x} \tag{4}$$

where

$$\lambda_1 = \frac{s_1}{a_1} \quad , \quad \lambda_2 = \frac{s_2}{a_2} \quad , \text{ and } \quad \lambda_3 = \frac{s_3}{a_3} \quad .$$

Equation (4) can be written

$$R(\underset{\sim}{s}) = \frac{N}{a_1 a_2 a_3} \int_{-\infty}^{\infty} x_3^2 \, I(x_3) \exp[i\lambda_3 x_3] \, dx_3 \tag{5}$$

where

$$I(x_3) = \iint_{-\infty}^{\infty} \frac{\exp[i(\lambda_1 x_1 + \lambda_2 x_2)]}{[x_1^2 + x_2^2 + A^2]^3} dx_1 dx_2$$

and $A^2 = x_3^2 + 1$.

The integral $I(x_3)$ can be solved by using the polar coordinate transformation

$$r^2 = x_1^2 + x_2^2$$

$$\rho^2 = \lambda_1^2 + \lambda_2^2 \tag{6}$$

which gives the equivalent integral

$$I(x_3) = \int_0^{\infty} \int_0^{2\pi} \frac{\exp[ir\rho \cos\theta] r \, d\theta \, dr}{[r^2 + A^2]^3} \tag{7}$$

where θ is the relative angle between ρ and r. Integration with respect to θ results in a zero-order Bessel function $J_0(\rho r)$ (Abramowitz and Stegun, 1965, p. 360, no. 9.1.21), allowing equation (7) to be written

$$I(x_3) = \frac{2\pi}{\rho^{1/2}} \int_0^{\infty} \frac{r^{1/2} (r\rho)^{1/2}}{[r^2 + A^2]^3} J_0(\rho r) \, dr \ . \tag{8}$$

Equation (8) is a zero-order Hankel transform which, when evaluated, gives (Erdélyi, 1954a, p. 360, no. 8.5(2))

$$I(x_3) = \frac{\pi \rho^2}{4} \frac{K_2(A\rho)}{x_3^2 + 1} \tag{9}$$

where $K_2(A\rho)$ is a second-order modified Bessel function. Thus, equation (5) can be written

$$R(\underset{\sim}{s}) = \frac{\pi\rho^2 N}{4a_1a_2a_3}\int_{-\infty}^{\infty}\frac{x_3^2 K_2(A\rho)\exp[i\lambda_3x_3]\,dx_3}{x_3^2+1} \tag{10}$$

or

$$R(\underset{\sim}{s}) = \frac{\pi\rho^2 N}{4a_1a_2a_3}\left\{\int_{-\infty}^{\infty}K_2(A\rho)\exp[i\lambda_3x_3]\,dx_3 - \int_{-\infty}^{\infty}\frac{K_2(A\rho)\exp[i\lambda_3x_3]\,dx_3}{x_3^2+1}\right\} \tag{11}$$

The recurrence relationship (Abramowitz and Stegun, 1965, p. 376, no. 9.6.26)

$$K_2(z) = \frac{2}{z}K_1(z) + K_0(z) \tag{12}$$

is used to rewrite equation (11) as

$$R(\underset{\sim}{s}) = \frac{\pi\rho^2 N}{4a_1a_2a_3}\left\{\frac{2}{\rho}\int_{-\infty}^{\infty}\frac{K_1(A\rho)\exp[i\lambda_3x_3]\,dx_3}{[x_3^2+1]^{1/2}} + \int_{-\infty}^{\infty}K_0(A\rho)\exp[i\lambda_3x_3]\,dx_3 - \int_{-\infty}^{\infty}\frac{K_2(A\rho)\exp[i\lambda_3x_3]\,dx_3}{x_3^2+1}\right\} \tag{13}$$

which is the Fourier transform of three different modified Bessel functions. These transforms are available in Erdélyi (1954, p. 56, nos. 1.13 (43, 44, and 45)), allowing equation (13) to be written

$$R(\underset{\sim}{s}) = \frac{\pi \rho^2 N}{4 a_1 a_2 a_3} \left\{ \frac{\pi}{\rho^2} \exp\left[-(\lambda_3^2 + \rho^2)^{1/2} \right] \right.$$

$$+ \frac{\pi}{2} \left[\lambda_3^2 + \rho^2 \right]^{-1/2} \exp\left[-(\lambda_3^2 + \rho^2)^{1/2} \right]$$

$$\left. - \left(\frac{\pi}{2}\right)^{1/2} \frac{1}{\rho^2} \left(\lambda_3^2 + \rho^2\right)^{3/4} K_{3/2}\left[(\lambda_3^2 + \rho^2)^{1/2} \right] \right\} . \tag{14}$$

Using the identity (Abramowitz and Stegun, 1965, p. 444, no. 10.2.17)

$$K_{3/2}(z) = \left(\frac{1}{2}\,\frac{\pi}{z}\right)^{1/2} \left(1 + \frac{1}{z}\right) \exp[-z] \tag{15}$$

equation (14) can be written

$$R(\underset{\sim}{s}) = \frac{N \pi^2}{4 a_1 a_2 a_3} \left\{ 1 + \frac{(\rho^2 - \zeta^2)}{\zeta} \right\} \exp\left[-\zeta \right] \tag{16}$$

where

$$\zeta^2 = s_1^2/a_1^2 + s_2^2/a_2^2 + s_3^2/a_3^2$$

and $\rho^2 = s_1^2/a_1^2 + s_2^2/a_2^2$.

The factor N can be found by evaluating $R(\underset{\sim}{s})$ at zero lag. In particular,

$$N = \frac{4}{\pi^2} a_1 a_2 a_3 \sigma^2 \tag{17}$$

which, when substituted into equations (1) and (16), gives the proper form for the spectrum and autocovariance function.

Appendix 7

EVALUATION OF INTEGRALS WITH SPECTRUM OF SIMPLE NEGATIVE-EXPONENTIAL AUTOCOVARIANCE FUNCTION

In this appendix, integrals of the form

$$I_1 = N \iiint_{-\infty}^{\infty} \frac{\left[k_2^2 + k_3^2\right]^2}{\left[k_1^2 + k_2^2 + k_3^2\right]^2 \left[\alpha_\ell k_1^2 + \alpha_t (k_2^2 + k_3)^2\right]}$$

$$\cdot \frac{d\underset{\sim}{k}}{\left[a_1^2 k_1^2 + a_2^2 k_2^2 + a_3^2 k_3^2 + 1\right]^2} \tag{1}$$

and

$$I_2 = N \iiint_{-\infty}^{\infty} \frac{k_2^2 + k_3^2}{\left[k_1^2 + k_2^2 + k_3^2\right]\left[\alpha_\ell k_1^2 + \alpha_t (k_2^2 + k_3^2)\right]}$$

$$\cdot \frac{d\underset{\sim}{k}}{\left[a_1^2 k_1^2 + a_2^2 k_2^2 + a_3^2 k_3^2 + 1\right]^2} , \tag{2}$$

where N is the normalization constant from Appendix 5, are evaluated. Throughout the evaluation process, a_3 is assumed to be smaller than or equal to either a_1 or a_2. Transforming to spherical coordinates

$$k_1 = r \operatorname{Cos} \phi$$

$$k_2 = r \operatorname{Sin} \phi \operatorname{Cos} \theta$$

$$k_3 = r \operatorname{Sin} \phi \operatorname{Sin} \theta \tag{3}$$

equation (1) can be written

$$\frac{I_1}{N} = \int_0^{\pi} \frac{\sin^5\phi \, d\phi}{\left[\alpha_\ell \cos^2\phi + \alpha_t \sin^2\phi\right]} \int_0^{\infty} dr$$

$$\cdot \int_0^{2\pi} \frac{d\theta}{\left[r^2 a_1^2 \cos^2\phi + r^2 \sin^2\phi \left(a_2^2 \cos^2\theta + a_3^2 \sin^2\theta\right) + 1\right]^2} \quad . \tag{4}$$

Letting J(ϕ,r) equal the last integral on the right-hand side, this integral is rewritten as

$$J(\phi, r) = 4 \int_0^{\pi/2} \frac{d\theta}{\left[A^2 + B^2 \cos^2\theta\right]^2} \tag{5}$$

where

$$A^2 = r^2\left[a_1^2 \cos^2\phi + a_3^2 \sin^2\phi\right] + 1$$

and $B^2 = r^2\left[a_2^2 - a_3^2\right] \sin^2\phi \quad .$

Although simple in appearance, the integral is not simple in solution. To solve, one applies the transform

$$B \cos\theta = A \tan u \tag{6}$$

which allows equation (5) to be written as

$$J(\phi, r) = \frac{4}{A^3} \int_0^{\alpha} \frac{du}{\sec^2 u \left[B^2 - A^2 \tan^2 u\right]^{1/2}} \tag{7}$$

where

$$\alpha = \tan^{-1}[B/A] \quad .$$

After further adjustments, equation (7) becomes

$$J(\emptyset, r) = \frac{4}{A^3} \int_0^{\alpha} \frac{\cos^3 u \, du}{\left[B^2(1-\sin^2 u) - A^2 \sin^2 u\right]^{1/2}} \quad . \tag{8}$$

Yet another transformation

$$V = \sin u \tag{9}$$

is applied to equation (8) to obtain

$$J(\emptyset, r) = \frac{4}{A^3} \int_0^{\gamma} \frac{(1-V^2)\, dV}{\left[B^2 - (A^2 + B^2)V^2\right]^{1/2}} \tag{10}$$

where

$$\gamma = \frac{B/A}{\left[1 + B^2/A^2\right]^{1/2}} \quad .$$

Equation (10) is split into two integrals

$$J(\emptyset, r) = \frac{4}{A^3} \left\{ \int_0^{\gamma} \frac{dV}{\left[B^2 - (A^2+B^2)V^2\right]^{1/2}} - \int_0^{\gamma} \frac{V^2\, dV}{\left[B^2 - (A^2+B^2)V^2\right]^{1/2}} \right\} \tag{11}$$

which can be solved by straight-forward integration:

$$J(\emptyset, r) = \frac{\pi}{A^3} \left\{ \frac{2A^2 + B^2}{\left[A^2 + B^2\right]^{3/2}} \right\} \quad . \tag{12}$$

Putting $L(\phi)$ equal to the penultimate integral on the right-hand side of equation (4), one obtains, after proper substitution for A and B,

$$L(\phi) = \pi \int_0^\infty \frac{[d^2 r^2 + 2]\, dr}{[(b^2 r^2 + 1)(c^2 r^2 + 1)]^{3/2}} \tag{13}$$

where

$$b^2 = a_1^2 \cos^2\phi + a_3^2 \sin^2\phi$$

$$c^2 = a_1^2 \cos^2\phi + a_2^2 \sin^2\phi$$

and $d^2 = b^2 + c^2$.

Splitting equation (13) into the two integrals

$$L(\phi) = \pi \left\{ d^2 \int_0^\infty \frac{r^2\, dr}{[(b^2 r^2 + 1)(c^2 r^2 + 1)]^{3/2}} + 2 \int_0^\infty \frac{dr}{[(b^2 r^2 + 1)(c^2 r^2 + 1)]^{3/2}} \right\} \tag{14}$$

two Mellin transforms are obtained. From a book of Mellin transforms (Erdélyi, 1954, p. 312, no. 6.2(35)), one obtains the solution (after substitution for b, c, and d)

$$L(\phi) = \frac{\pi^2}{8a} \left\{ \left[1 - \frac{a^2 - a_3^2}{2a^2} \sin^2\phi \right] \cdot {}_2F_1\left(\frac{3}{2}, \frac{1}{2}; 3; \frac{a^2 - a_3^2}{2a^2} \sin^2\phi \right) \right.$$

$$+ 3\,{}_2F_1\left(\tfrac{3}{2}, \tfrac{1}{2}; 3; \frac{a^2 - a_3^2}{2a^2} \sin^2 \phi\right)\Bigg\} \tag{15}$$

where

$$a = a_1 = a_2$$

and ${}_2F_1(a,b;c;z)$ is Gauss' hypergeometric function. The solution could also have been obtained in terms of unequal length scales a_1 and a_2; however, setting these scales equal simplified the final integration. In particular, this integral can be written

$$\frac{I_1}{N} = 2\int_0^{\pi/2} \frac{[L(\phi)] \sin^5\phi \, d\phi}{[\alpha_\ell \cos^2\phi + \alpha_t \sin^2\phi]} \tag{16}$$

to which the transformation

$$u = \sin^2\phi \tag{17}$$

is applied, obtaining

$$\frac{I_1}{N} = \frac{1}{\alpha_\ell}\int_0^1 \frac{[L(\sin^{-1}\sqrt{u})]\, u^2}{\left[1 - \frac{\alpha_\ell - \alpha_t}{\alpha_\ell} u\right]} \cdot \frac{du}{(1-u)^{1/2}} \; . \tag{18}$$

We allow

$$C = \frac{\alpha_\ell - \alpha_t}{\alpha_\ell} = 1 - \rho \tag{19a}$$

and $D = \dfrac{a^2 - a_3^2}{a^2} = 1 - \dfrac{1}{R^2}$. (19b)

where $\rho = \alpha_t / \alpha_\ell$ and $R = a/a_3$.

Expanding equation (18) in terms of equations (15) and (19) and equation (13), Appendix 5, one obtains

$$I_1 = \frac{a_3^2 \sigma^2}{\alpha_t} F(\rho, R) \tag{20}$$

where

$$F(\rho,R) = \frac{1}{8} \frac{\rho}{R} \left\{ \int_0^1 \frac{(1 - Du/2)\, u^2}{[1 - Cu][1-u]^{1/2}} \right.$$

$$\cdot {}_2F_1(3/2, 3/2; 3; Du)\, du$$

$$\left. + 3 \int_0^1 \frac{u^2}{[1 - Cu][1-u]^{1/2}} {}_2F_1(3/2, 1/2; 3; Du)\, du \right\} . \tag{21}$$

Equation (21) was integrated numerically with a standard program package. Values for Gauss' hypergeometric function were obtained by summation of Gauss' hypergoemetric series (Abramowitz and Stegun, 1965, p. 556, no. 15.1.1). Results were checked against the case $\rho = 1$ and $R = 1$, which has a simple analytic solution.

Integral (2) was similarly converted to spherical coordinates (3), giving the result

$$\frac{I_2}{N} = \int_0^{\pi} \frac{\sin^3\phi \, d\phi}{\left[\alpha_\ell \cos^2\phi + \alpha_t \sin^2\phi\right]} \int_0^{\infty} dr$$

$$\cdot \int_0^{2\pi} \frac{d\theta}{\left[a_1^2 r^2 \cos^2\phi + r^2 \sin^2\phi \left(a_2^2 \cos^2\theta + a_3^2 \sin^2\theta\right) + 1\right]^2} \quad . \tag{22}$$

The last two integrals on the right-hand side are the same as the last two in equation (4). Therefore, evaluation of these integrals will give precisely the same result as equation (15). Hence only the solution form for the final integration is noted:

$$\frac{I_2}{N} = 2 \int_0^{\pi/2} \frac{\left[L(\phi)\right] \sin^3\phi \, d\phi}{\left[\alpha_\ell \cos^2\phi + \alpha_t \sin^2\phi\right]} \quad . \tag{23}$$

Using transformation (17), the form

$$\frac{I_2}{N} = \frac{1}{\alpha_\ell} \int_0^1 \frac{\left[L(\sin^{-1}\sqrt{u})\right] u}{\left[1 - \left(\frac{\alpha_\ell - \alpha_t}{\alpha_\ell}\right) u\right]} \cdot \frac{du}{\left[1 - u\right]^{1/2}} \tag{24}$$

is obtained. From equation (19) and other results of the previous integration, a solution of the form

$$I_2 = \frac{a_3^2 \sigma^{-2}}{\alpha_t} \, G(\rho, R) \tag{25}$$

where

$$G(\rho, R) = \frac{1}{8}\,\frac{\rho}{R}\left\{\int_0^1 \frac{(1 - Du/2)\,u}{\left[1 - Cu\right]\left[1 - u\right]^{1/2}}\right.$$

$$\cdot\ {}_2F_1\,(3/2, 3/2\,;\, 3\,;\, Du)\,du$$

$$\left. + 3\int_0^1 \frac{u}{\left[1 - Cu\right]\left[1 - u\right]^{1/2}}\ {}_2F_1\,(3/2, 1/2\,;\, 3\,;\, Du)\,du\right\} \qquad (26)$$

is obtained. Integration of this expression was carried out numerically in a fashion similar to integral (21).

Appendix 8

EVALUATION OF INTEGRALS WITH SPECTRUM OF MODIFIED NEGATIVE-EXPONENTIAL AUTOCOVARIANCE FUNCTION

In this appendix, integrals of the form

$$I_1 = N \iiint_{-\infty}^{\infty} \frac{\left[k_2^2 + k_3^2\right]^2}{\left[k_1^2 + k_2^2 + k_3^2\right]^2 \left[\alpha_\ell k_1^2 + \alpha_t (k_2^2 + k_3^2)\right]}$$

$$\cdot \frac{a_3^2 k_3^2 \, d\underset{\sim}{k}}{\left[a_1^2 k_1^2 + a_2^2 k_2^2 + a_3^2 k_3^2 + 1\right]^3} \qquad (1)$$

and

$$I_2 = N \iiint_{-\infty}^{\infty} \frac{k_2^2 + k_3^2}{\left[k_1^2 + k_2^2 + k_3^2\right]\left[\alpha_\ell k_1^2 + \alpha_t (k_2^2 + k_3^2)\right]}$$

$$\cdot \frac{a_3^2 k_3^2 \, d\underset{\sim}{k}}{\left[a_1^2 k_1^2 + a_2^2 k_2^2 + a_3^2 k_3^2 + 1\right]^3} \qquad (2)$$

where N is the normalizing constant from Appendix 6, are evaluated. Throughout the evaluation process, a_3 is assumed to be smaller than or equal to either a_1 or a_2. Transforming to spherical coordinates

$$k_1 = r \operatorname{Cos} \phi$$

$$k_2 = r \operatorname{Sin} \phi \operatorname{Cos} \theta$$

$$k_3 = r \operatorname{Sin} \phi \operatorname{Sin} \theta \qquad (3)$$

equation (1) can be written .

$$I_1 = N a_3^2 \int_0^{\pi} \frac{\sin^7\phi \, d\phi}{\left[\alpha_\ell \cos^2\phi + \alpha_t \sin^2\phi\right]} \int_0^{2\pi} \sin^2\theta \, d\theta$$

$$\cdot \int_0^{\infty} \frac{r^2 \, dr}{\left[\left(a_1^2 \cos^2\phi + \sin^2\phi \left(a_2^2 \cos^2\theta + a_3^2 \sin^2\theta\right)\right) r^2 + 1\right]^3} \quad . \tag{4}$$

Letting $J(\phi,\theta)$ equal the last integral on the right-hand side, this integral is rewritten as

$$J(\phi,\theta) = \int_0^{\infty} \frac{r^2 \, dr}{\left[E r^2 + 1\right]^3} \tag{5}$$

where

$$E = a_1^2 \cos^2\phi + \sin^2\phi \left[a_2^2 \cos^2\theta + a_3^2 \sin^2\theta\right]$$

which has the solution

$$J(\phi,\theta) = \pi / \left[16 E^{3/2}\right] \quad . \tag{6}$$

Putting $L(\phi)$ equal to the penultimate integral on the right-hand side, one obtains

$$L(\phi) = \frac{\pi}{4} \int_0^{\pi/2} \frac{\sin^2\theta \, d\theta}{\left[A^2 + B^2 \cos^2\theta\right]^{3/2}} \tag{7}$$

where

$$A^2 = a_1^2 \cos^2\phi + a_3^2 \sin^2\phi$$

and $B^2 = \left[a_2^2 - a_3^2\right] \mathrm{Sin}^2 \phi$

after proper substitution of equation (6). To solve equation (7), the transformation

$$B \cos\theta = A \tan u \tag{8}$$

is applied, which allows equation (8) to be written

$$L(\phi) = \frac{\pi}{4A^2B^2} \int_0^{\alpha} \left[B^2 \cos^2 u - A^2 \sin^2 u\right]^{1/2} du \tag{9}$$

where

$$\alpha = \tan^{-1}\left[B/A\right] \quad .$$

A further transformation of this type

$$V = \sin u \tag{10}$$

allows equation (9) to be written as

$$L(\phi) = \frac{\pi\left[A^2 + B^2\right]^{1/2}}{4A^2B^2} \int_0^{\gamma} \left[\frac{\gamma^2 - V^2}{1 - V^2}\right]^{1/2} dV \tag{11}$$

where

$$\gamma = B/\left[A^2 + B^2\right]^{1/2} \quad .$$

The solution to this integral, as given by Gradshteyn and Ryzhik (1965, p. 276, no. 3.169.9), is

$$L(\phi) = \frac{\pi (A^2 + B^2)^{1/2}}{4 A^2 B^2} \left\{ E(\gamma) - \frac{A^2}{A^2 + B^2} K(\gamma) \right\} \tag{12}$$

where $E(\gamma)$ and $K(\gamma)$ are complete elliptic integrals (Byrd and Friedman, 1954, p. 9). Setting length scales a_1 and a_2 equal, this result can be written in the form (after substitution for A and B)

$$L(\phi) = \frac{\pi}{4\left[a^2 - a_3^2\right] \sin^2\phi} \left\{ \frac{a\, E(t)}{\left[a^2 \cos^2\phi + a_3^2 \sin^2\phi\right]} - \frac{K(t)}{a} \right\} \tag{13}$$

where

$$t = \left[1 - a_3^2/a^2\right]^{1/2} \sin\phi \quad .$$

Thus, equation (4) can be written

$$I_1 = 2 N a_3 \int_0^{\pi/2} \frac{L(\phi) \sin^7\phi \, d\phi}{\left[\alpha_\ell \cos^2\phi + \alpha_t \sin^2\phi\right]} \tag{14}$$

to which the transform

$$u = \cos\phi \tag{15}$$

is applied, obtaining

$$I_1 = \frac{2 N a_3}{\alpha_\ell} \int_0^1 \frac{\left[1 - u^2\right]^3 L(\cos^{-1} u)\, du}{\left[u^2 (1 - \alpha_t/\alpha_\ell) + \alpha_t/\alpha_\ell\right]} \quad . \tag{16}$$

We allow

$$C = 1 - \alpha_t / \alpha_\ell = 1 - \rho \tag{17a}$$

and $$D = 1 - a_3^2 / a^2 = 1 - 1/R^2 \tag{17b}$$

where

$$\rho = \alpha_t / \alpha_\ell \text{ and } R = a/a_3 \; .$$

Expanding equation (16) in terms of equations (13) and (17) and equation (17), Appendix 6, one obtains

$$I_1 = \frac{a_3^2 \sigma^2}{\alpha_t} F(\rho, R) \tag{18}$$

where

$$F(\rho, R) = \frac{2}{\pi} \frac{\rho}{DR} \int_0^1 \frac{[1 - u^2]^2}{[Cu + \rho]} \left\{ \frac{E(t)}{[Du^2 + 1/R^2]} - K(t) \right\} du \tag{19}$$

and $t = \left[D(1 - u^2)\right]^{1/2}$.

Equation (19) was integrated numerically with a standard program package. Values for complete elliptic integrals E(t) and K(t) were obtained from very accurate polynomial approximations (Abramowitz and Stegun, 1965, p. 591, no. 17.3.34 and p. 592, no. 17.3.36). Results were checked against the case $\rho = 1$ and $R = 1$, which has a simple analytic solution.

Integral (2) was similarly converted to spherical coordinates (3), giving the result

$$I_2 = N a_3^2 \int_0^{\pi} \frac{\sin^5 \phi \, d\phi}{\left[\alpha_\ell \cos^2 \phi + \alpha_t \sin^2 \phi\right]} \int_0^{2\pi} \sin^2 \theta \, d\theta$$

$$\cdot \int_0^{\infty} \frac{r^2 \, dr}{\left[\left(a_1^2 \cos^2 \phi + \sin^2 \phi \left(a_2^2 \cos^2 \theta + a_3^2 \sin^2 \theta\right)\right) r^2 + 1\right]^3} \, . \qquad (20)$$

The last two integrals on the right-hand side are the same as the last two integrals in equation (4). Therefore, evaluation of this integral will give precisely the same result as equation (13). Hence, only the solution form for the final integration is noted:

$$I_2 = 2 N a_3^2 \int_0^{\pi/2} \frac{L(\phi) \sin^5 \phi \, d\phi}{\left[\alpha_\ell \cos^2 \phi + \alpha_t \sin^2 \phi\right]} \, . \qquad (21)$$

Using transformation (15), the form

$$I_2 = \frac{2 N a_3^2}{\alpha_\ell} \int_0^{1} \frac{\left[1 - u^2\right]^2 L(\cos^{-1} u) \, du}{\left[u^2 (1 - \alpha_t/\alpha_\ell) + \alpha_t/\alpha_\ell\right]} \qquad (22)$$

is obtained. From equation (17) and other results of the previous integration, the solution is of the form

$$I_2 = \frac{a_3^2 \sigma^2}{\alpha_t} G(\rho, R) \qquad (23)$$

where

$$G(\rho, R) = \frac{2}{\pi} \frac{\rho}{DR} \int_0^1 \frac{1 - u^2}{\left[Cu^2 + \rho\right]} \left\{ \frac{E(t)}{\left[Du^2 + 1/R^2\right]} - K(t) \right\} du. \tag{24}$$

Integration of this expression was carried out in a fashion similar to integral (19).

Appendix 9

SOLUTION OF VARIANCE EQUATION FOR HYDRAULIC HEAD

In this appendix, an integral of the form

$$I = \iiint_{-\infty}^{\infty} \frac{k_1^2}{\left[k_1^2 + k_2^2 + k_3^2\right]^2} \Phi(\underset{\sim}{k}) d\underset{\sim}{k} \tag{1}$$

is evaluated where the spectrum from Appendix 6 is chosen to represent $\Phi(\underset{\sim}{k})$. Substituting for $\Phi(\underset{\sim}{k})$, then, one obtains

$$I = \frac{4}{\pi^2} a_1 a_2 a_3 \sigma^2 \iiint_{-\infty}^{\infty} \frac{k_1^2}{\left[k_1^2 + k_2^2 + k_3^2\right]^2}$$

$$\cdot \frac{a_3^2 k_3^2}{\left[a_1^2 k_1^2 + a_2^2 k_2^2 + a_3^2 k_3^2 + 1\right]^3} d\underset{\sim}{k} \quad . \tag{2}$$

A transformation into spherical coordinates

$$\begin{aligned} a_1 k_1 &= r \operatorname{Cos} \phi \\ a_2 k_2 &= r \operatorname{Sin} \phi \operatorname{Cos} \theta \\ a_3 k_3 &= r \operatorname{Sin} \phi \operatorname{Sin} \theta \end{aligned} \tag{3}$$

gives the result

$$I = \frac{4}{\pi^2} \frac{(a_1 a_2 a_3)^4}{a_1^2} \sigma^2 \int_0^{\pi} \operatorname{Cos}^2 \phi \operatorname{Sin}^3 \phi \, d\phi$$

$$\cdot \int_0^{2\pi} \frac{\operatorname{Sin}^2 \theta \, d\theta}{\left[a_2^2 a_3^2 \operatorname{Cos}^2 \phi + a_1^2 a_3^2 \operatorname{Sin}^2 \phi \operatorname{Cos}^2 \theta + a_1^2 a_2^2 \operatorname{Sin}^2 \phi \operatorname{Sin}^2 \theta\right]^2} \int_0^{\infty} \frac{r^2 dr}{[r^2+1]^3} . \tag{4}$$

The last integral on the right-hand side is easily solved, giving the numerical result $\pi/16$. The penultimate integral can be written

$$J(\phi) = 4\int_0^{\pi/2} \frac{\sin^2\theta \, d\theta}{\left[A^2\sin^2\theta + B^2\right]^2} \tag{5}$$

where

$$A^2 = a_1^2 \sin^2\phi \, (a_2^2 - a_3^2)$$

and $B^2 = a_2^2 a_3^2 \cos^2\phi + a_1^2 a_3^2 \sin^2\phi$.

The transformation

$$A \sin\theta = B \tan u \tag{6}$$

is applied to equation (6). This transformation gives the result

$$J(\phi) = \frac{4}{BA^2}\int_0^{\alpha} \frac{\cos u \sin^2 u \, du}{\left[A^2\cos^2 u - B^2\sin^2 u\right]^{1/2}} \tag{7}$$

where

$$\alpha = \tan^{-1}\left[A/B\right] .$$

Integral (7) can be further simplified by applying the transformation

$$A\left[A^2 + B^2\right]^{-1/2} \sin x = \sin u \tag{8}$$

which gives the much reduced integral

$$J(\phi) = \frac{4}{B}\left[A^2 + B^2\right]^{-3/2} \int_0^{\pi/2} \operatorname{Sin}^2 x \, dx \quad . \tag{9}$$

Evaluation of integral (9) gives the form

$$J(\phi) = \pi/\left[B\,(A^2 + B^2)^{3/2}\right] \quad . \tag{10}$$

Substitution of this results into equation (4) produces the rather complex expression (after substitution for A and B)

$$I = \frac{1}{4}\,\frac{(a_1 a_2 a_3)^4}{a_1^2}\,\sigma^{-2}$$

$$\cdot \int_0^{\pi} \frac{\operatorname{Cos}^2\phi \operatorname{Sin}^3\phi \, d\phi}{\left[a_2^2 a_3^2 \operatorname{Cos}^2\phi + a_1^2 a_3^2 \operatorname{Cos}^2\phi\right]^{1/2}\left[a_1^2 a_2^2 \operatorname{Sin}^2\phi + a_2^2 a_3^2 \operatorname{Cos}^2\phi\right]^{3/2}} \tag{11}$$

Finally, making the additional transformation

$$u = \operatorname{Cos}\phi \tag{12}$$

one obtains the form

$$I = a_3^2 \, \sigma^{-2} H(R_1, R_3) \tag{13}$$

where

$$H(R_1, R_3) = \frac{1}{2} \frac{1}{R_3^5 R_1^2} \int_0^1 \frac{u^2 - u^4}{\left[R_1^2 + (1 - R_1^2) u^2\right]^{1/2}}$$

$$\cdot \frac{du}{\left[R_1^2 - (R_1^2 - 1/R_3^2) u^2\right]^{3/2}} \tag{14}$$

and $R_1 = a_1/a_2$ and $R_3 = a_2/a_3$. This last expression was evaluated numerically using a standard program package. The results were checked against the values $R_1 = 1.0$ and $R_3 = 1.0$, which is easily evaluated analytically.

This dissertation is accepted on behalf of the faculty of the Institute by the following committee:

Allan R. Gutjahr — for Lynn Gelhar —
Adviser

Allan R. Gutjahr

Rufus T. Getzen

John R. McMillan

Feb 3, 1978 —
Date